



GRADUATE EDUCATION  
(301) 295-3913  
FAX: (301) 295-6772

# UNIFORMED SERVICES UNIVERSITY OF THE HEALTH SCIENCES

4301 JONES BRIDGE ROAD  
BETHESDA, MARYLAND 20814-4799



## APPROVAL SHEET

Title of Dissertation: "Cataracts in the Fat Sand Rat: An Ocular Complication of Diabetes"

Name of Candidate: LTC Cheryl DiCarlo  
Doctor of Philosophy Degree  
29 March 2001

Dissertation and Abstract Approved:

M. R. Adelman

Mark Adelman, Ph.D.  
Department of Anatomy, Physiology & Genetics  
Chairperson

3/29/01  
Date

Diane Borst

Diane Borst, Ph.D.  
Department of Anatomy, Physiology & Genetics  
Major Advisor

29 March 01  
Date

Terez Shea-Donohue

Terez Shea-Donohue, Ph.D.  
Department of Medicine  
Member

032901  
Date

Harvey Pollard

Harvey Pollard, MD, Ph.D.  
Department of Anatomy, Physiology & Genetics  
Member

0329.01  
Date

David Mears

David Mears, Ph.D.  
Department of Anatomy, Physiology & Genetics  
Member

3/29/01  
Date

Michelle Chenault

Michelle Chenault, Ph.D.  
Department of Anatomy, Physiology & Genetics  
Member

3/29/01  
Date

Gerald Robison

Gerald Robison, Ph.D.  
National Eye Institutes, NIH  
Member

3/29/01  
Date



## **COPYRIGHT PAGE**

**The author hereby certifies that the use of any copyrighted material in the dissertation manuscript entitled:**

**“Cataracts in the Fat Sand Rat: An Ocular Complication of Diabetes”**

**is appropriately acknowledged and, beyond brief excerpts, is within the permission of the copyright owner.**

**Cheryl D. DiCarlo**

**LTC, VC, USA**

**Department of Anatomy, Physiology & Genetics**

**Uniformed Services University of the Health Sciences**

## ABSTRACT

**Purpose:** The fat sand rat, *Psammomys obesus*, a spontaneous model for Type 2 diabetes, develops cataracts within days of the onset of clinical diabetes. The purpose of this research was to determine the crystallin composition of the normal sand rat lens and determine the changes that occur during diabetic cataract formation.

**Materials and Methods:** Slit-lamp biomicroscopy was used for ocular examinations. Blood glucose, glycated hemoglobin (HbA1c), aqueous glucose, vitreous glucose, vitreous glycated protein and lens extract glycated protein and protein values were determined using standard techniques and colorimetric test kits. Location of glucose transporter (GLUT) transcripts was determined using reverse transcriptase polymerase chain reaction (rtPCR). Lens extracts were prepared then separated by gel filtration chromatography to study the crystallin classes by SDS-PAGE. Western blotting and mass spectrometry were used to verify the crystallin composition.

**Results:** Blood glucose, aqueous glucose, vitreous glucose and glycated hemoglobin (HbA1c) levels were all significantly elevated in the diabetic sand rats. Water-soluble protein levels were higher in the control sand rats. No significant differences were seen among glycated protein levels of the lens extracts. GLUT1, GLUT3 and GLUT4 transcripts were present in the anterior epithelial cells of the lens but only the GLUT4 transcript was present in the lens

fiber cells. SDS-PAGE of the diabetic animals revealed an increased banding pattern at 35 – 42 kDa and a band shift from 22.5 to 23.5 kDa. Western blotting and mass spectrometry confirmed  $\alpha$ -A crystallin aggregates and  $\beta$ B2/ $\beta$ B3 crystallin band shifts, respectively.

Discussion: This is the first report of characterization of the normal and cataractous lens in the fat sand rat. The elevated glucose and HbA1c values in the blood of diabetic sand rats result in high levels of glucose within the eye. In the diabetics, there are  $\alpha$ A crystallin aggregates and  $\beta$ B2/ $\beta$ B3 crystallin ratio shifts with cataracts. The diabetic cataracts seen on the slit-lamp exam are similar to those seen in humans. The data reported here provides the groundwork for medical therapies aimed at reversal or prevention of diabetic cataracts instead of surgical alleviation of this common cause of blindness. The sand rat is an excellent choice for such diabetes research.

**TITLE PAGE**

**CATARACTS IN THE FAT SAND RAT:  
AN OCULAR COMPLICATION OF DIABETES**

**by**

**Cheryl D. DiCarlo, D.V.M.**

**Lieutenant Colonel, Veterinary Corps, U.S. Army**

**Dissertation submitted to the Faculty of the Department of Anatomy, Physiology  
and Genetics Graduate Program of the Uniformed Services University of the  
Health Sciences in partial fulfillment of the requirements for the degree of Doctor  
of Philosophy 2001.**

## DEDICATION AND ACKNOWLEDGEMENTS

This dissertation is dedicated to my husband, Dr. W. Patrick Roach, my research advisor Dr. Diane Borst, and a dear family friend, Mrs. M. Frazier for their love, support and friendship. I would not have been able to accomplish this work without them. To Patrick, “the love of my life,” I thank him for his ability to provide unwavering love and emotional support during the entirety of our marriage and especially during these last three years. To Diane, I thank you for being “the best mentor a graduate student could possibly have” by providing a positive and challenging research environment. Lastly, to my dear friend, Marge, I thank you for your friendship and counsel over the last twenty years.

There are several people that I am also compelled to acknowledge. The first of which is my research committee including Dr. Mark Adelman, Chairman; Dr. Diane Borst; Dr. Harvey Pollard; Dr. Terez Shea-Donohue; Dr. David Mears; Dr. W. Gerald Robison and Dr. Michelle Chenault. I thank them all for their guidance, support and spirited discussions during numerous committee meetings. In addition to my committee, I must acknowledge Dr. Linda Cork, Chairman, Department of Comparative Medicine, Stanford University, for her mentorship over the course of my entire undergraduate and graduate education. To Linda, I thank you for being a role model and friend, and for setting the standards for what a woman can achieve. I additionally want to thank the U.S. Army Veterinary Corps for giving me this educational opportunity and acknowledge all the support

I received from the Uniformed Services University. I extend my dearest thanks to all of you!

## TABLE OF CONTENTS

Approval Sheet .....	i
Copyright page .....	ii
Abstract .....	iii
Title Page .....	v
Dedication and Acknowledgements.....	vi
Table of Contents .....	viii
List of Tables .....	xi
List of Figures .....	xii
Chapter One .....	1
Introduction.....	1
Insulin and Normal Glucose Homeostasis.....	1
Classification of Diabetes .....	3
Pathogenesis of Diabetes.....	5
Normal Lens Biology .....	8
Diabetic Cataract Formation .....	13
Hyperglycemia, Glucose Entry into the Lens and Cataract Formation .....	14
Hyperglycemia and Glycated Proteins in the Eye.....	15
The Fat Sand Rat and Other Common Rodent Models for Diabetes.....	17
U.S. Populations at Risk for Type 2 diabetes .....	19
Significance .....	21
Hypothesis.....	22
Specific Aim #1 .....	23

Specific Aim #2.....	24
Specific Aim #3.....	25
Specific Aim #4.....	26
Chapter 2.....	30
Abstract .....	30
Introduction.....	32
Materials and Methods .....	36
Results.....	41
Discussion .....	44
Acknowledgments .....	51
Chapter 3.....	63
Sand Rat Body Weights .....	63
Slit-lamp Examinations and Photography.....	64
Diabetic Blood Glucose Levels .....	67
Glycated Protein Determination using the Fructosamine Test Kit.....	68
rtPCR for GLUT-3 Transporter Transcript.....	70
Summary .....	71
Chapter 4.....	93
Abstract .....	93
Introduction.....	95
Materials and Methods .....	98
Results.....	103
Discussion .....	105

Acknowledgments .....	111
Chapter 5.....	125
Chromatography Set-up and Column Calibration .....	125
Chromatography Curves .....	126
Isoelectric Focusing and 2-Dimensional Gels.....	127
Enzymes or Taxon-Specific Crystallins?.....	130
Special Staining of the Water-soluble and Pellet Fractions of Lens extracts .	132
Summary .....	134
Chapter 6.....	150
Discussion .....	150
References .....	160

## LIST OF TABLES

Table 1.01 .....	29
Table 2.01 .....	53
Table 2.02 .....	55
Table 2.03 .....	56
Table 4.01 .....	113
Table 4.02 .....	114

## LIST OF FIGURES

Figure 2.01 .....	57
Figure 2.02 .....	58
Figure 2.03 Through 2.07 .....	59
Figure 2.08 .....	61
Figure 2.09 .....	62
Figure 3.01 .....	73
Figure 3.02 .....	74
Figure 3.03 .....	75
Figure 3.04 .....	76
Figure 3.05 .....	77
Figures 3.06 through 3.09 .....	79
Figures 3.10 through 3.12 .....	80
Figures 3.13 through 3.16 .....	81
Figures 3.17 through 3.19 .....	82
Figure 3.20 .....	83
Figures 3.21 and 3.22.....	84
Figures 3.23 and 3.24.....	85
Figures 3.25 and 3.26.....	87
Figures 3.27 and 3.28.....	88
Figure 3.29 .....	90
Figure 3.30 .....	92
Figure 4.01 .....	115

Figure 4.02 .....	116
Figures 4.03 and 4.04.....	117
Figures 4.05 and 4.06.....	118
Figures 4.07 and 4.08.....	119
Figures 4.09 and 4.10.....	120
Figure 4.11 .....	123
Figure 4.12 .....	124
Figure 5.01 .....	136
Figure 5.02 .....	137
Figure 5.03 .....	140
Figure 5.04 .....	141
Figure 5.05 .....	142
Figure 5.06 .....	143
Figure 5.07 .....	144
Figure 5.08 .....	145
Figure 5.09 .....	146
Figure 5.10 .....	147
Figure 5.11 .....	147
Figure 5.12 .....	149

## CHAPTER ONE

### Introduction

This dissertation is divided into six chapters, the first of which discusses background information on Type 2 diabetes and the effects of this disease on the lens of the eye. Chapter Two is a copy of a paper that will be submitted to *Comparative Medicine*; it discusses development of this Type 2 diabetic model along with how the glucose levels affect the lens of the eye. Chapter Three contains additional research data gathered but not submitted for publication, related to topics contained in Chapter Two. Chapter Four is a copy of a paper that will be submitted to *Experimental Eye Research* discussing the normal crystallin protein structure of the sand rat lens and the effects of diabetic cataracts on these lens proteins. Chapter Five contains additional research data not submitted for publication on topics related to those in Chapter Four. Chapter Six summarizes and discusses the research contained in Chapters Two through Five.

### Insulin and Normal Glucose Homeostasis

Insulin is an anabolic hormone produced and released from Beta cells in the pancreatic Islet of Langerhans in response to elevated blood glucose levels.

Insulin has several functions but its major function is to increase the rate of glucose transport into certain cells in the body. Insulin mRNA is translated into preproinsulin. The “pre” piece is an endoplasmic reticulum signal peptide, which is cleaved off to yield proinsulin. Proinsulin is stored in vesicles with C-peptide.

The “pro” piece is cleaved off in the immature secretory granules and insulin is secreted from the granules as needed (Alberts et al. 1994).

The influx of glucose into the Beta cell stimulates immediate release of the insulin stored in granules. If the glucose stimulus continues, the Beta cell is stimulated to synthesize more insulin. Other compounds such as intestinal hormones, some amino acids, sulfonylureas, calcium influx, alpha-adrenergics, cAMP and glucagon-like peptide stimulate the release of insulin. But, of these, only glucose stimulates insulin synthesis. Since sugars cannot diffuse through a cell membrane lipid bilayer, glucose is transported into the Beta cell by the insulin-independent transporting protein-2 (GLUT-2). The GLUT proteins are a group of transmembrane proteins that transport glucose by facilitated diffusion (Shepard and Kahn 1999). There are several types of GLUT proteins with varying distribution and affinity for glucose. Of these, GLUT-4 is the major insulin responsive glucose transporter. GLUT-4 is located in muscle and adipose tissue. It is recycled between the cell membrane and the intracellular storage vesicles. Stimuli such as insulin and exercise increase the translocation of the protein to the membrane for increased movement of glucose into the muscle cells (Shepard and Kahn 1999). Defects in any of these regulatory areas of glucose homeostasis, such as insulin production, insulin secretion or glucose transport and utilization, could potentially cause diabetes.

Insulin first acts on a cell by binding to the insulin receptor. The insulin receptor is a transmembrane receptor tyrosine kinase. The receptors are tetramers with two glycoprotein subunits,  $\alpha$  and  $\beta$ . Insulin binding to the receptor tyrosine kinase triggers a number of intracellular responses including mitochondrial enzyme synthesis, protein synthesis, DNA synthesis and translocation of GLUT proteins allowing glucose entry into the cell (Cotran et al. 1999).

### Classification of Diabetes

Diabetes mellitus is a metabolic disorder of impaired glucose utilization. It is classified into Type 1 (Insulin-Dependent Diabetes Mellitus = IDDM) and Type 2 (Non-Insulin Dependent Diabetes Mellitus = NIDDM) diabetes. This classification is based on clinical signs and age of onset, genetics, insulin responses and origin. Type 1 diabetes results from an absolute lack of insulin caused by a decreased number of functioning Beta cells in the pancreas. Type 1 is initially diagnosed in children (less than 20 years of age) of normal weight with a reduction in functioning Beta cells and subsequent insulin depletion due to an immunopathologic event affecting the pancreas. In some Type 1 diabetic patients, there is a disorder in the genes encoding class II antigens of the major histocompatibility region of chromosome 6 (HLA-D)(Cotran et al. 1999).

Eighty to ninety percent of diabetic patients have Type 2 diabetes or NIDDM. Initially, in Type 2 diabetes there is an insulin resistance rather than an absence of insulin as seen in Type 1. Type 2 diabetes is further subdivided into Obese,

Non-obese types and Maturity-Onset Diabetes of the Young (MODY) categories. There is evidence for a genetic basis since some non-diabetic relatives of Type 2 diabetic patients have insulin resistance (Shepard and Kahn 1999) and genetic evidence has been reported in studies involving specific ethnic groups. The San Antonio Heart Study reported that the prevalence of Type 2 diabetes was twice as great among Mexican-Americans with first-degree relatives with diabetes compared to those with no family history (Stern et al. 1983). African-Americans and Pima Indians (native North Americans from the Southwestern U.S. and Mexico) are believed to have inherited a "thrifty gene." In 1962, geneticist James Neel proposed this theory (Neel 1962). Neel's theory applied to populations that relied on farming, hunting and fishing for food. These populations would go through periods of feast and famine and the "thrifty gene" would allow them to gain weight during the plentiful times. This same gene may be responsible for an increased susceptibility to developing Type 2 diabetes. To date, there is no known association of this gene with a defect of chromosome 6 (HLA-D) as there is in Type 1 diabetic patients. In the rare MODY cases, there is an autosomal dominant defect in chromosomes 7, 12 and 20. These individuals present with diabetes at 25 years of age or earlier and have an abnormal pattern of glucose-stimulated insulin secretion (Yamagata et al. 1996). But by far, the most common type of diabetes is the Obese Type 2. In general, Type 2 diabetes presents in overweight adults greater than 30 years of age that have normal or increased levels of insulin resulting from insulin resistance (Cotran et al. 1999).

## **Pathogenesis of Diabetes**

**As previously mentioned, Type 1 diabetes may result from an induced autoimmune defect (virally induced) or a genetic component relating to a defect in the major histocompatibility gene on chromosome 6. Antibodies are produced against pancreatic islet cell proteins. This results in a deficiency of insulin, thus the name, insulin-dependent diabetes. The pathogenesis of Type 2 diabetes is less clearly defined. There are three possible mechanisms that may result in diabetes, the first two of which are target cell defects and the third of which is a Beta cell defect. The first mechanism is related to a decreased number of insulin receptors on the target cells. This decreased number of receptors leads to decreased glucose transportation into the target cell. The second mechanism is a post-receptor defect causing a reduction in GLUT transporters in the target cells. This defect prevents glucose from moving into the cell by transmembrane facilitated diffusion. The third mechanism is inadequate insulin secretion by the Beta cells of the pancreas. This also results in decreased glucose transportation into the target cell. All three of these mechanisms result in insulin resistance, chronic hyperglycemia and glucose toxicity (Cotran et al. 1999).**

**In addition to the three mechanisms described above for Type 2 diabetes, there is also the theory that an abnormal insulin product is produced. This was reported by Kaiser, et al, (Kaiser et al. 1997) and was described to be a possible mechanism for Type 2 diabetes in the fat sand rat. An abnormal insulin product would be similar to the Beta cell defect of inadequate insulin secretion. It would**

result in hyperglycemia by preventing glucose from entering the insulin-dependent cell.

Regardless of the type of diabetes, the chronic complications responsible for significant morbidity are related to the resultant hyperglycemia. Diabetic hyperglycemia causes elevated glucose concentrations outside the cells that require insulin for glucose transport (i.e. adipocytes and myocytes). It also causes elevated intracellular glucose concentrations in cells that do not require insulin for glucose transport (i.e. neurons and erythrocytes). Both intracellular and extracellular elevations of glucose may result in nonenzymatic glycosylation (glycation). This is the chemical attachment of glucose to the amino group of proteins without the requirement for an enzyme. Non-reversible glycation of proteins in the blood is directly related to the level of blood glucose. Glycated hemoglobin (HbA1c) is an example of this irreversible process occurring inside the red blood cell. HbA1c is commonly used clinically for assessment of the glycemic state. It yields information on the diabetic patient for a longer period of time than a single blood glucose value. In humans, the HbA1c value represents the mean blood glucose picture for the past 120 days (since 120 days is the average life span of a human erythrocyte). In some rodents, HbA1c represents the mean blood glucose concentration for approximately the last 60 days (personal communication with Dr. Chenault). The use of the HbA1c value in animal models is an important tool. It is important since the stress of animal handling alone may result in a falsely elevated blood glucose value.

The non-reversible products of glycation are produced by protein cross-linking and are called advanced glycation end products (AGE). There are two factors determining the extent of protein glycation by this process. The first is the half-life of the protein and the second is the duration and extent of the hyperglycemia (Lundquist and Osterlin 1994). AGE products are produced extracellularly in interstitial tissues and surrounding blood vessels. This has been proposed to result in increased basement membrane thickening. AGEs can also bind to receptors on endothelial cells, monocytes, macrophages, lymphocytes and mesangial cells. The binding stimulates a cascade of cytokine and growth factor release, monocyte emigration, proliferation and synthesis of extracellular matrix and stimulates increased endothelial cell permeability. As already described with the HbA1c values, intracellular protein glycation also occurs. Protein glycation is responsible for many complications seen in diabetes including neuropathy and retinopathy. Current medical therapies include aminoguanidine, which potentially binds to precursors of AGE products and prevent the irreversible cross-linking to proteins (Degenhardt et al. 1999).

Insulin is not required for glucose transport in some tissues and organs such as the lens of the eye. In the hyperglycemic state, an increased amount of glucose moves into the cells of these tissues and is metabolized by aldose reductase to sorbitol (a polyol). An increased flux through this pathway leads to an increased intracellular osmolarity and a concurrent decrease in myo-inositol content. The

decreased myo-inositol is responsible for decreases in phosphoinositide, diacylglycerol, protein kinase C and  $\text{Na}^+$ ,  $\text{K}^+$  - ATPase activity. This mechanism is believed to be responsible for the Schwann cell damage in peripheral neuropathy, the pericyte death associated with diabetic retinopathy, and the anterior epithelial cell and fiber cell swelling of the lens. Aldose reductase inhibitors are being tested for amelioration of the effects of this increased flux through the polyol pathway (Robison et al. 1995), (Jacot et al. 1997), (Robison et al. 1998).

### Normal Lens Biology

The lens of the eye is formed in the embryo from the surface ectoderm of the head. The surface ectoderm thickens, invaginates and then pinches off inside the optic cup. On day 33 in the human embryo, the cells of the posterior aspect of the lens vesicle differentiate and elongate into primary lens fiber cells. The lens body, which is made up of primary lens fiber cells, is completely formed in the human by embryonic day 47. Secondary lens fiber cells then arise from the anterior epithelium beginning around the eighth week of development and continuing throughout the life of the lens (Larsen 1997).

The cells of the lens produce proteins called crystallins. Crystallins are water-soluble proteins that, together, make up approximately 80 – 90% of the proteins in the lens. In general, crystallins have polypeptide weights between 20 and 35 kiloDaltons. Crystallins are responsible for maintaining the transparency of the

lens by an ordered arrangement that minimizes absorbance and scatter of light. After lens fiber cell differentiation, the cells lose their organelles. In mammals, the lens fiber cells then extend in length from the equator to the centrally located lens suture (Bassnett 1992). Once the organelles are expelled, the lens fiber cells lose their ability to produce more proteins. Therefore, the crystallin proteins produced by the lens fiber cells are as old as the cells that have produced them and remain with these cells throughout the existence of the lens.

There are two main classes of crystallins, the alpha and the beta-gamma crystallins (Albert and Jacobiec 1994). Chromatography is commonly used to separate the crystallins in their native form and SDS-PAGE is commonly used to study the denatured crystallin proteins. The alpha crystallins form aggregates with a native molecular weight of 600,000 to 900,000 Daltons and a polypeptide weight of 20,000 Daltons. The beta crystallins are populations of aggregates divided into beta-high, beta-low 1 and beta-low 2. When separated using chromatofocusing, the beta-high, the beta-low 1 and the beta-low 2 populations are composed of beta subunits in different proportions (Bloemendal et al. 1990). The native molecular weights for beta crystallins range from 50,000 to 200,000 Daltons and the polypeptide weights from 23,000 to 35,000 Daltons (Albert and Jacobiec 1994). The gamma crystallins are synthesized predominately during embryogenesis and are therefore found in the oldest portion of the lens, the nucleus. They are small tightly packed protein monomers around 20,000 Daltons in their native and denatured state (Piatigorsky 1981). SDS-PAGE has been

used to study high molecular weight crystallin aggregates in lens extracts from many animals' lenses including rat, bovine and human (Turk et al. 1997), (Nagaraj and Sady 1996). In 20-week-old control rats, there was a slight increase (2.5%) in high molecular weight proteins with age when compared to 4-week-old rats. Additionally, a dramatic increase (30.5%) in high molecular weight proteins was found in diabetic rats, with a 20-week long duration of diabetes when compared to rats of shorter diabetic duration. (Turk et al. 1997).

In addition to the ubiquitous classes of crystallins, there are also taxon-specific crystallins. Taxon-specific crystallins are water-soluble lens proteins with peptide molecular weights that range from 35,000 to 70,000 Daltons. In general, most of these "species-specific" crystallins share structure and sometimes function with an enzyme. The most abundant taxon-specific crystallins have been reported in non-mammalian species such as reptiles, birds and fish (Wistow and Kim 1991). Taxon-specific crystallins have also been found in the lenses of some mammals including the guinea pig (Huang et al. 1987), the rabbit (Mulders et al. 1988) the elephant shrew and marsupials (Wistow and Kim 1991). All of these mammals are diurnal species. Taxon-specific crystallins are believed to play a structural and functional role. Structurally, they may replace the gamma crystallins in the lens making the lens softer for accommodation. Functionally, taxon-specific crystallins are thought to provide ultra-violet filtration or protection against oxidation and other stresses (Wistow 1995). This unusual expression of enzymes in the lens of some species has also been reported in the corneal epithelium and

is theorized to provide protection against ultra-violet irradiation (Cooper et al. 1993), (Piatigorsky 1998). Interestingly, the corneal epithelium, another transparent tissue of the eye, derives from the same embryonic ectoderm as the lens.

Since the cornea and the lens are avascular organs, they must receive nutrition from adjacent tissues. The ciliary body, a highly vascular tissue, produces a filtrate of blood called the aqueous humor. The aqueous humor surrounds the lens in the anterior segment of the eye. As the glucose levels of the blood rise, so does the glucose level of the aqueous humor. Glucose entry from the aqueous humor into the lens is not modulated by insulin or by glycolysis (Goodenough et al. 1980), (Mathias et al. 1997). Recently, Merriman-Smith, et al reported the presence of GLUT-1 transporters in the anterior epithelium of the lens and GLUT-3 in the lens fiber cells of rats (Merriman-Smith et al. 1999). GLUT-1 transporters are constitutive transporters found in brain, erythrocytes and endothelial cells and have a  $K_m = 20$  mmol/liter. GLUT-3 transporters are high affinity glucose transporters found in neurons and placenta, with a  $K_m = 10$  mmol/liter, and act independently of the GLUT-1 transporters. This recent report of GLUT-1 and GLUT-3 transporters in specific locations within the lens of rats may indicate independent movement of glucose into the lens fiber cells. This significantly contrasts other literature on the location of glucose transporters. One report found GLUT-1 transporters mainly localized in the cortical lens fiber cells of humans (Mantych et al. 1993) whereas, another study failed to detect GLUT-1

transporters anywhere in the lens (Kumagai et al. 1994). Transport studies also report conflicting results. Transport of glucose at both the anterior and posterior lens surfaces in the calf lens (Kern and Ho 1973) contrasts with the report of just the anterior epithelium as the main site for glucose uptake into the mouse lens (Goodenough et al. 1980).

Filling the space between the retina and the lens in the posterior segment of the eye is the gelatinous vitreous humor. The primary vitreous begins forming during the formation of the optic cup around embryonic day 32 (Larsen 1997). In the embryo there are vessels (tunica vasculosa lentis) that attach the retina to the lens but this vasculature degenerates and disappears. Retinal Muller cells and ciliary epithelial cells produce an acellular extracellular matrix called the definitive vitreous. The vitreous humor is made up of several types of collagen and vitreous proteins plus hyalocytes, resting macrophages that migrated from the hyaloid vessel (a part of the tunica vasculosa lentis). The hyalocytes are believed to produce hyaluronan, a major component of the glycosaminoglycan network seen in basement membranes (Albert and Jacobiec 1994). The hyaluronan molecules laterally associate with each other and form a three-dimensional lattice. The hyaluronan molecules of the lattice also associate with globular proteins or link proteins. This association stabilizes the vitreous structure in an orderly fashion that maintains media transparency (Brewton and Mayne 1992).

## Diabetic Cataract Formation

Cataracts are the number one cause of blindness worldwide (Leske et al. 1999). A cataract is any opacity of the lens of the eye that compromises sight. There are several clinical classification systems, however, in general, cataracts are classified by the location within the lens and the extent of opacity. Cataracts are a common complication of diabetes. During the course of Type 2 diabetes the blood glucose levels fluctuate between normal and high levels. Hyperglycemia leads to a parallel glucose elevation in the aqueous humor of the eye (Farr et al. 1999). In contrast, the glucose levels of the vitreous humor are generally lower than the glucose levels of the blood due to the anatomic isolation of the vitreous humor (Daae et al. 1978). The retinal vessels are believed to be the source for the vitreous glucose by facilitated and passive transport (Lundquist and Osterlin 1994). In the normal state, the rate of transport for the facilitated transport system is five times greater than the passive diffusion rate (Di Mattio et al. 1981). Yet, in experiments with diabetic animals, the facilitated transport of glucose is not affected while the passive diffusion rate is markedly increased (Di Mattio et al. 1984). This may explain why the glucose levels of the vitreous in the diabetic patient, are higher than the glucose levels of the vitreous in non-diabetic people (Lundquist and Osterlin 1994). Forensic evaluation of the vitreous for glucose is commonly used to determine if the patient was hyperglycemic prior to death since the blood glucose is rapidly converted to lactic acid (Daae et al. 1978), (Peclet et al. 1994). This elevation of the glucose levels in the aqueous and vitreous humors significantly impacts the glucose available for transport into the

lens and for glycation of crystallin proteins in the lens and the collagen of the vitreous.

#### **Hyperglycemia, Glucose Entry into the Lens and Cataract Formation**

Glucose enters the lens through insulin-independent GLUT transporters. As stated earlier, controversy exists over which GLUT transporters are located in specific locations in the lens and which location in the lens is predominately responsible for the major glucose uptake. The lens of the eye has a capsule covering the entire lens but no epithelium covering the posterior aspect of the lens. In humans, dogs and rats, diabetic cataracts are clinically apparent in the equatorial regions and posterior subcapsular region. The rat also has a much higher aldose reductase activity in the lens than the human or the dog (Albert and Jacobiec 1994). In the rat, the aldose reductase activity is 21 times higher in the anterior epithelium than all other areas of the lens (Hayman et al. 1966).

Aldose reductase activity and an increased flux of glucose through the sorbitol pathway in diabetes are reported as responsible for the osmotic changes such as anterior epithelial cell swelling, like that seen in the galactosemic rat (Robison et al. 1990). Robison reported the anterior epithelial cell changes occurred within 36 hours and intercellular vacuoles and cysts were seen in the equatorial regions of the lens within 48 hours of high galactose feeding to rats. The sand rat, which has aldose reductase in the lens (Cohen-Melamed et al. 1995), also produces vacuoles in the equatorial and posterior subcapsular regions, then subsequent opacities in the posterior cortical aspect of the lens within weeks of feeding a

standard rodent chow (personal observation via slit-lamp examination). The diabetic cataract then extends from the posterior subcapsular region through the posterior cortex and nucleus towards the anterior portions of the lens. The formation of the diabetic cataracts in the sand rat closely mimics the reported diabetic cataract pattern seen in the human, dog and galactosemic rat.

### **Hyperglycemia and Glycated Proteins in the Eye**

Glycosylation of proteins through a nonenzymatic mechanism is referred to as protein glycation. Protein glycation results from a series of reversible and irreversible steps called the Maillard reaction. Factors that determine the extent of protein glycation are the half-life of the protein and the degree and duration of the hyperglycemia (Cefalau 1988). A long duration of hyperglycemia results in the formation of irreversible advanced glycation end products (AGEs). There are reports suggesting that non-enzymatic glycosylation (glycation) may play a role in diabetic cataracts (Nagaraj et al. 1991), (Miksik and Deyl 1997). Since crystallins of the lens are known to be some of the oldest proteins in the body, it is not surprising that glycated crystallin proteins have been reported in diabetic (Perry et al. 1987), (Nakayama et al. 1993), (Ganea et al. 1994), (Ganea et al. 1994), (Sensi et al. 1995), (Ganea and Harding 1996), (Turk et al. 1997), (Crabbe 1998), (Swamy-Mruthinti and Carter 1999) and age-related cataracts (Lyons et al. 1991), (Araki et al. 1992), (van Boekel and Hoenders 1992), (van Boekel et al. 1996), (Das et al. 1998), (Shamsi et al. 1998), (Chellan and Nagaraj 1999), (Shamsi and Nagaraj 1999). Using spectrofluorescence, AGE formation of lens

proteins was found to be significantly higher in diabetic animals than in control animals (Sensi et al. 1995), (Turk et al. 1997). Levels of AGE products also increase in human lenses with an increase in age (Araki et al. 1992). AGE increases are also associated with an increased severity of lens pigmentation, which is seen in aged lenses (Miksik and Deyl 1997), (Nagaraj et al. 1991), (Saxena et al. 2000). Reports also indicate that non-enzymatic glycosylation (glycation) may play a role in diabetic vitreopathy (Shires et al. 1990), (Sebag et al. 1994), (Stitt et al. 1998), (Farr et al. 1999). The vitreous humor is an anatomically isolated collagen matrix that is commonly tested in forensic medical studies in humans. It has been shown that glycated protein (fructosamine) levels of the vitreous humor are a more consistent indicator of diabetes mellitus, at autopsy, than blood or other fluid glucose values (Osuna et al. 1999). Glucose is rapidly converted to lactate in cadavers whereas the glycated protein levels reflect the mean glucose values over a longer period of time. Significantly higher fructosamine levels are reported in the vitreous of diabetic cats and rabbits when compared to the vitreous of controls (Farr et al. 1999). A positive correlation of AGE production in the vitreous with increased age was shown when control patients were compared to age-matched diabetic patients (Stitt et al. 1998). Changes to the vitreous such as syneresis (liquefaction) are more common in diabetes (Lundquist and Osterlin 1994). Utilizing Raman spectroscopy on human vitreous, diabetic vitreous was distinguished from control vitreous based on a three-fold elevation in the spectroscopic peaks of the diabetic samples (Sebag et al. 1994). Even though controversy exists over whether high glucose levels or

oxidation products are the responsible glycation agents (Albert and Jacobiec 1994), based on reports in the literature, there must be a link in the elevation of the blood, aqueous and vitreous glucose levels to the glycation of crystallin proteins in the lens and collagen of the vitreous humor.

### The Fat Sand Rat and Other Common Rodent Models for Diabetes

The rat is, by far, the most commonly used induced model of diabetes. The rat was selected for use, over the mouse, for the study of diabetic cataracts since the mouse does not express aldose reductase in substantial quantities in the lens and thus cannot form diabetic osmotic cataracts. Chemical induction of diabetes in the rat includes alloxan or streptozocin ablation of the pancreatic beta cells creating a Type 1 diabetes model (Tarui et al. 1987). There are several genetically induced rat models such as the BB rat, also a Type 1 model, the Zucker fatty rat and the Japanese Goto-Kakizaki rat, both Type 2 models (Tarui et al. 1987), (Miyamoto et al. 1996). A Type 2 diabetes-like syndrome is nutritionally induced in the rat by feeding a diet of 50% galactose. This diabetes model is referred as the galactosemic rat (Robison 2001). Several genetically, chemically and nutritionally induced rodent models of diabetes exist but there are few naturally occurring rodent models of Type 2 diabetes. The spontaneous rodent models include two gerbil species, one of which is *Psammomys obesus*, "the fat sand rat," and a rare hamster species (Shafrir and Renold 1984), (Goodwin 1997), (Kalman et al. 1996). Few of these are available to researchers

and most have not been fully characterized with respect to the ocular changes of Type 2 diabetes.

Of these naturally occurring models, only the sand rat has been directly compared to a human population with one of the highest incidences of diabetes, the Pima Indians (Tarui et al. 1987). This comparison is based on the concept of the "thrifty gene" enabling a human to survive under feast or famine conditions in a desert climate. This concept of the "thrifty gene" in people living in desert regions should also apply to animals of a similar climate if the species is expected to survive. *Psammomys obesus* or the "Fat Sand Rat," is a *Cricetidae* rodent from the Northern African Desert region. In the wild, the Fat Sand rat consumes a plant diet low in energy and high in fiber, electrolytes and water. Type 2 diabetes is easily induced nutritionally by placing the animals on a high-energy, low fiber diet such as a standard rodent chow (Kalman et al. 1996). The diet change results in hyperinsulinemia, hyperglycemia, hyperlipidemia and obesity as early as 11 – 14 days after starting the high-energy diet (Adler et al. 1990). To achieve a consistently induced diabetic model and control, Adler, et al, began producing diabetes-prone (DP) and diabetes-resistant (DR) lines within the Hebrew University-Hassah Medical School breeding colony (Adler et al. 1990). Sand rats were fed a standard laboratory chow from weaning up to 5 months of age. They were bled for blood glucose on a biweekly basis. When the average of the three highest blood glucose values was > 120 mg/dl, these sand rats were selected as breeders for the DP line. When the average of the three

highest blood glucose values was < 120 mg/dl, these sand rats were selected as breeders for the DR line. Much of the diabetes literature on this model utilizes this technique (Kalman et al. 1996), (Kaiser et al. 1997), (Nesher et al. 1999). In general, the stages of Type 2 diabetes produced in this model are grouped as listed in Table 1.01 (page 29), (Kalderon et al. 1986), (Shafir and Gutman 1993). These blood glucose and insulin level shifts are similar to what is seen in humans at different stages of Type 2 diabetes. Aside from the biochemical changes that have been reported, cataracts are also a common ocular change seen in the diabetic sand rat (Hackel et al. 1965), (Gutman et al. 1976), (Adler et al. 1990), (Marquie et al. 1991). In fact, bilateral cataracts are produced in this spontaneous animal model within the first month of clinical diabetes (personal observation of the Uniformed Services University of the Health Sciences sand rat colony). This rapid and reasonably consistent manifestation of diabetes makes this model an excellent choice for the study of developmental mechanisms of diabetic cataracts, a common cause of blindness in man.

#### **U.S. Populations at Risk for Type 2 diabetes**

Type 2 diabetes is a serious problem in the Hispanic, African American and Native American populations in this country. Diabetes is 2 –3 times more common in Hispanic Americans than in non-Hispanic Caucasians (Flegal et al. 1991). The prevalence rate of diabetes in African Americans is 1.6 times the prevalence rate in Caucasians (Harris et al. 1998). Of the Native American populations, approximately 50% of the Pima Indians in the U.S. are diagnosed

with Type 2 diabetes by the age of 35 years (Schwab 1985). The Pima Indians originate from the Sonoran Desert region, which spans the Mexican State of Sonora and the U.S. State of Arizona. Peoples originating from desert climates are thought to have inherited a gene increasing their susceptibility to diabetes (Knowler et al. 1990). The genetic basis for the diabetes is attributed to the Neel Theory of the "thrifty gene" (Neel 1962). This gene enables carriers to adapt to extreme changes by enabling them to store fat needed in times of famine. With fewer "feast and famine" cycles occurring and an increased contact with Caucasian populations, dietary and exercise changes occurred in the Pima Indians and other populations. This change from 15% fat in the diet to a Caucasian diet of almost 40% fat, coupled with severely reduced physical activity, resulted in obesity, insulin resistance and Type 2 diabetes in Pima Indians in the U.S. The Mexican Pimas, who are genetically homogeneous with American Pimas, live in a remote area of the Sierra Madre Mountains. They are not overweight and have low incidence of diabetes in their population. The study of the Pima Indians of Arizona has lead to the identification of several candidate genes for Type 2 diabetes. The fatty acid binding protein locus, FABP2, may be one genetic factor responsible for the variability of insulin action seen in non-diabetic Pimas (Baier et al. 1995). The gene encodes for intestinal fatty acid binding protein (IFABP), an intracellular lipid binding protein. A polymorphism was found in the coding sequence that alters an alanine to a threonine. The threonine encoding allele, was found to be associated with an increased affinity

for long-chain fatty acids. This increased absorption of fatty acid into the blood is believed to contribute to the insulin resistance in Pimas.

In addition to the problems associated with obesity in these populations, blindness due to diabetic cataracts is also of great concern. Rates for cataract surgery are almost six times as high in the Pima Indians when compared to the estimated U.S. rates (Schwab 1985).

### Significance

Approximately 16 million people in this country are affected by Diabetes. The 1999 Report of the Expert Committee on the Diagnosis and Classification of Diabetes Mellitus states that "the chronic hyperglycemia of diabetes is associated with long term damage, dysfunction and failure of various organs, especially the eye, kidneys, nerves, heart and blood vessels." Diabetic patients are 25% more likely to become blind than non-diabetic people. The prevalence rate of cataracts in diabetes ranges from 18% - 25% (Klein et al. 1985), (Schwab 1985), (Klein et al. 1995), (Delcourt et al. 1995), (Kaimbo et al. 1995), (Hapnes and Bergrem 1996). The only common treatment for cataracts is surgical removal of the lens and replacement with a synthetic intraocular lens. Investigations are continuing in therapies aimed at the sorbitol pathway through aldose reductase inhibition (Robison et al. 1990), (Robison et al. 1995), (Jacot et al. 1997) and aimed at the Maillard Reaction by reducing advanced glycation end products (Friedman 1999), (Degenhardt et al. 1999), (Monnier et al. 1999). This drug therapy

research may identify medical interventions for alleviation of cataracts without requiring an already compromised patient to undergo surgery. With the devastating multisystemic complications of diabetes being so prevalent, it is imperative that new animal models be developed and characterized for future diabetes research.

Of the few spontaneously diabetic animal models, only the sand rat has been directly compared to a human population with a high incidence of diabetes. This easily handled rodent model consistently develops cataracts early in the course of clinical disease. To date, little research has been published exclusively on the diabetic cataract formation in this animal and there are no reports in the literature on the characterization of the lens crystallins of the normal and the diabetic sand rat. This absence of literature in the area of cataract formation, in this ideal diabetic animal model, led to the following research. In accordance with departmental rules, this thesis project was initiated in the format of a NIH grant application. The remainder of this chapter restates the hypothesis and specific aims of that proposal.

### Hypothesis

During the diabetic state, there are elevated glucose levels in the aqueous humor and, over time with a mean blood glucose elevation, subsequent elevated glucose levels in the vitreous humor. This elevation of glucose in ocular fluids results in increased glucose levels in the lens of the eye by way of insulin-

independent transporters. This glucose influx into the lens causes initial osmotic changes resulting in the well-characterized “diabetic cataract.” Later, this process may lead to glycation of the lens crystallins and subsequent aggregation. *The central hypothesis is that polymerized aggregates of lens crystallins enhance the formation of non-reversible cataracts, both diabetic and age-related, by a mechanism involving both elevated blood and ocular fluid glucose and glucose transport-dependent formation of crystallin glycoconjugates.*

#### Specific Aim #1

Determine the glucose levels of the aqueous humor, vitreous humor and blood in the diabetic and non-diabetic sand rat.

**Rationale:** Diabetic cataracts are common in sand rats. They often form within the first month the sand rat is placed on diabetogenic rodent chow. It has been reported that the aqueous levels of glucose parallel blood glucose levels in both the normal and diabetic states. Yet, in diabetic patients, some question remains concerning the glucose levels of the vitreous humor over time.

Comparing the glucose levels within the aqueous and vitreous to the blood glucose values will determine if a predictable relationship exists between the glucose levels in the eye and the blood of the sand rat.

**Specific Hypothesis to be tested:** The glucose concentration of the vitreous humor does not directly follow the blood glucose levels, as does the aqueous humor, but instead continues to increase over time in diabetic sand rats.

**Experimental Approach:** A hexokinase-based colorimetric glucose test (SIGMA Diagnostics) will be used for the glucose concentrations of the aqueous and vitreous humors. Blood glucose will be measured using a blood glucose meter. In the event the blood glucose values are too high to be read by the blood glucose meter, a serum glucose value will be determined using the hexokinase-based colorimetric glucose test.

**Significance:** This approach will establish the relationship of the glucose levels in the blood, aqueous and vitreous humors of the diabetic and non-diabetic sand rat.

#### **Specific Aim #2**

Determine glycated protein levels in the blood, the lens of the eye and the vitreous humor of the diabetic and non-diabetic sand rat.

**Rationale:** Forensic medical studies in humans have shown that glycated protein (fructosamine) levels of the vitreous humor are a more consistent indicator of diabetes mellitus, at autopsy, than blood or other fluid glucose values. Glucose is rapidly converted to lactate in cadavers whereas the glycated protein levels reflect the mean glucose values over a longer period of time.

**Specific Hypothesis to be tested:** As the mean blood glucose levels rise in diabetes, there is more protein glycation occurring in the blood, the lens of the eye and the vitreous humor.

**Experimental Approach:** A fructosamine-based colorimetric test (SIGMA Diagnostics) will be used for the glycated protein content of the vitreous humor

and lens. The HbA1c filter paper elution test will be used to determine the glycated hemoglobin level in the blood.

**Significance:** This approach will establish the relationship of the glycated protein levels in the blood, lens and vitreous humors to the mean blood glucose values of the diabetic and non-diabetic sand rat.

### **Specific Aim #3**

Determine if the sand rat has GLUT-1 and GLUT-3 transporters in the anterior lens epithelium and the lens fiber cells, respectively.

**Rationale:** Glucose transport into the lens of the eye is insulin-independent. Recently, GLUT-3 transporters were reported in the rat lens fiber cells and GLUT-1 transporters were reported in the anterior lens epithelial cells. GLUT-1 transporters are constitutive transporters and GLUT-3 transporters are high affinity glucose transporters and are mutually exclusive. Therefore, their rate of glucose transport into specific cell types of the lens may differ. This rate difference may impact the physical location of lens opacities in diabetes.

**Specific Hypothesis to be tested:** The sand rat has GLUT-1 transporters in the anterior epithelial cells and GLUT-3 transporters in the lens fiber cells.

**Experimental Approach:** Reverse Transcriptase Polymerase Chain Reaction (rtPCR) will be performed on the target tissues to determine if specific mRNAs are present.

**Significance:** This approach will establish whether the GLUT-1 and GLUT-3 transporter transcripts are present in the anterior epithelium and the lens fibers

cells, respectively. Determination of the location of the GLUT-1 and GLUT-3 transporters could lead to prevention of diabetic cataracts through the use of localized therapeutics aimed at reducing the flux of glucose through these transporters.

#### **Specific Aim #4**

Determine the normal crystallin pattern of the fat sand rat lens.

**Rationale:** Crystallins make up 80 – 90% of the water-soluble proteins in the lens. If glycation of crystallin proteins is occurring in diabetes and aging, it is essential to know the normal crystallin pattern of the sand rat prior to the study of the altered crystallin pattern of the cataractous state.

**Specific hypothesis to be tested:** The fat sand rat lens has a crystallin pattern that is similar to closely related rodent species.

**Experimental Approach:** Collect clear lenses from clinically normal non-diabetic sand rats for determination of native crystallin weights, denatured crystallin weights and crystallin identification. Native molecular weight determination will be accomplished with gel filtration chromatography for normal crystallin patterns. SDS-PAGE will be performed for determination of polypeptide molecular weights. Western blots will be performed for identification of the major crystallin classes.

**Significance:** This approach will establish the normal crystallin pattern of the fat sand rat.

### **Specific Aim #5**

**Determine the crystallin pattern of the diabetic fat sand rat with cataracts.**

**Rationale:** It is well documented that diabetic cataracts are a result of osmotic changes due to increased flux through the polyol pathway. Less studied is the impact of crystallin aggregates in the diabetic state. The cause of the crystallin aggregation is not well defined and the crystallin classes involved in aggregation have only recently been investigated.

**Specific hypothesis to be tested:** The normal crystallin pattern for the fat sand rat is altered with diabetic cataracts.

**Experimental Approach:** Cataractous lenses from diabetic sand rats will be collected for determination of native crystallin weights, polypeptide crystallin weights and crystallin identification. The same techniques used in Specific Aim #4 will be performed.

**Significance:** This approach will establish which crystallin classes are aggregating to form the cataracts and will demonstrate if changes in crystallin mobility occur due to diabetic complications such as crystallin glycation.

## **Expectations, Innovations and Impact**

The normal crystallin composition and the diabetic ocular changes of the Fat Sand Rat, a spontaneous model of Type 2 diabetes, have not been reported. Knowledge of the crystallin composition, the presence and location of lenticular glucose transporters, and the correlation of the glucose/glycated protein levels of the blood to those of the ocular fluids and tissues, will aid in research targeted at diabetic cataracts. Full characterization of the Fat Sand Rat lens, normal and cataractous, lends an opportunity for research into early medical intervention therapy. Medical therapies would be aimed at reversal/prevention of the disease process instead of surgical alleviation of the diabetic symptoms. This research will pave the way for developing a medical alternative to surgical lens removal, the only currently available therapy for diabetic cataracts.

**TABLE 1.01**

	<b>Group A</b>	<b>Group B</b>	<b>Group C</b>	<b>Group D</b>
<b>Clinical evaluation based on chemistry</b>	<b>Control Normoglycemic Normoinsulinemic</b>	<b>Diabetic Normoglycemic Hyperinsulinemic</b>	<b>Diabetic Hyperglycemic Hyperinsulinemic</b>	<b>Diabetic Hyperglycemic Normoinsulinemic</b>
<b>Blood glucose in mg/dl</b>	<b>&lt; 100</b>	<b>&lt; 100</b>	<b>&gt; 100</b>	<b>&gt; 100</b>
<b>Serum insulin in <math>\mu</math>U/ml</b>	<b>&lt; 100</b>	<b>&gt; 100</b>	<b>&gt; 100</b>	<b>&lt; 100</b>

Table 1 was derived from the reports of Kalderon, et al, and Shafrir, et al. Group A are considered normal or control animals. Group B sand rats are considered to be compensating diabetics. Group C animals are decompensated diabetics. Group D animals were termed as "failing  $\beta$ -cells." Based on more recent literature the diabetic Group D would more likely be listed as a group with insulin resistance, insulin receptor defects or defective insulin production.

## CHAPTER 2

**"Ocular Changes in a Spontaneously Diabetic Animal Model, the Fat Sand Rat (*Psammomys obesus*)."**

Submitted to *Comparative Medicine* in May 2001.

### Abstract

***Purpose:*** The purpose of this study was to characterize the formation of diabetic cataracts in this model by determining the relationship between elevated glucose and glycated protein levels within the blood and glucose influx into the ocular tissues, specifically the lens.

***Methods:*** Standard rodent chow converted sand rats to a diabetic state. Slit-lamp biomicroscopy was used for ocular examinations. Blood glucose and glycated hemoglobin (HbA1c) values were determined using standard techniques. Aqueous glucose, vitreous glucose, water-soluble lens extract glycated protein, vitreous glycated protein values and lens water-soluble protein levels were determined using colorimetric test kits. Location of glucose transporter (GLUT) transcripts was determined using reverse transcriptase polymerase chain reaction (rtPCR).

**Results:** Blood glucose, aqueous glucose, vitreous glucose and glycated hemoglobin (HbA1c) levels were all significantly elevated in the diabetic sand rats. Water-soluble lens protein levels were higher in the control sand rats. No significant difference was seen in glycated protein levels of the lens extracts. GLUT-1 and GLUT-4 transcripts were present in the anterior epithelial cells of the lens. GLUT-4 transcript was present but GLUT-1 transcript was absent in the lens fiber cells. The presence of GLUT-3 transcript was inconclusive due to the difficulty in determining a primer pair with consistent results.

**Conclusions:** The elevated glucose and HbA1c values in the blood of diabetic sand rats translate to high levels of glucose within the eye supporting the diabetic cataract formation which was seen with the slit-lamp biomicroscope. Assay constraints prevented reliable results for the glycated vitreal protein levels. Increased insolubility of the lens proteins accounts for the lower water-soluble protein levels found in the diabetic animals. More diabetes research is needed studying glucose entry into the lens by transporters. The easily handled diurnal sand rat is an excellent choice for such diabetes research due to the reliable formation of diabetic cataracts in a pattern consistent with the formation in humans with diabetes.

## Introduction

Approximately 16 million people in this country are affected by diabetes.

Cataracts are a common complication of diabetes. The prevalence rate of cataracts in diabetes ranges from 18% - 25% (Klein et al. 1985), (Schwab 1985), (Klein et al. 1995), (Delcourt et al. 1995), (Kaimbo et al. 1995), (Hapnes and Bergrem 1996). A cataract is any opacity of the lens of the eye that compromises sight and cataracts are classified by the degree of opacity and the location within the lens. During the course of Type 2 diabetes the blood glucose fluctuates between normal and high levels. Hyperglycemia leads to a parallel glucose elevation in the aqueous humor of the eye (Farr et al. 1999). In diabetic patients, the glucose levels of the vitreous humor are higher than in non-diabetic patients (Lundquist and Osterlin 1994). However, in general, the glucose levels of the vitreous humor are lower than the glucose levels of the blood (Daae et al. 1978). This elevation of the glucose levels in the aqueous and vitreous humors significantly impact the glucose available for transport into the lens and for glycation of crystallin proteins and vitreal collagen.

Glucose enters cells by either active transport sodium-linked glucose transporters, as in intestine and kidney cells, or through facilitated diffusion mediated by transmembrane proteins called GLUT proteins. GLUT proteins are encoded by specific genes and have distinct tissue distributions. GLUT-1 and GLUT 3 are glucose transporters found mainly in nervous tissue. GLUT-2 is found mainly in pancreatic beta cells. GLUT-4 is the insulin-dependent

transporter of striated muscle and adipose (Shepard and Kahn 1999). It is clear that glucose enters the lens but the isoform of glucose transporters present in the lens is still under investigation. Recently GLUT-1 and GLUT-3 transporters were identified in specific locations within the lens of the eye of the rat (Merriman-Smith et al. 1999). GLUT-1, a constitutive transporter was found located in the rat anterior lens epithelium. GLUT-3, a high affinity glucose transporter was found in the lens fiber cells. This indicates that the lens fiber cells may have the ability to take up glucose independently of the anterior epithelial cells.

Once glucose has entered the lens, aldose reductase and an increased flux through the sorbitol pathway are responsible for the osmotic changes seen in diabetic cataracts (Robison et al. 1990), (Shafrir 1996), (Belpoliti and Maraini 1993), (Lee et al. 1995), (Lackner et al. 1997), (Sato et al. 1998), (Jacob 1999). Along with the osmotic changes caused by an increased flux through the polyol pathway, non-enzymatic glycation may also play a role in diabetic cataracts and diabetic vitreopathy (Shires et al. 1990), (Nagaraj et al. 1991), (Sebag et al. 1994), (Miksik and Deyl 1997), (Stitt et al. 1998), (Farr et al. 1999). Glycated proteins are non-enzymatically formed compounds that have been reported to occur in the lens (Osuna et al. 1999), yet there is controversy over whether high glucose levels or oxidation products are the responsible glycating agents (Albert and Jacobiec 1994). Dramatic increases in one such glycation marker, pentosidine, are associated with age and the severity of lens pigmentation (Miksik and Deyl 1997), (Nagaraj et al. 1991). In humans, advanced glycation

end products (AGEs) form on the vitreous collagen network (Stitt et al. 1998) and this cross-linking by the AGEs may be responsible for vitreal liquefaction seen in diabetes and in aging. Fructosamine, another AGE product, was reported to be significantly higher in the vitreous of diabetic cats and rabbits when compared to the vitreous of controls (Farr et al. 1999). These cited reports indicate there may be a link in the elevation of the blood, aqueous and vitreous glucose levels to possible glycation of crystallin proteins in the lens and collagen of the vitreous humor.

There are several genetically, chemically and nutritionally induced rodent models of diabetes but few naturally occurring rodent models of Type 2 diabetes. Mouse models of diabetes are not appropriate for the study of diabetic cataracts since the mouse does not express aldose reductase in substantial quantities in the lens and thus cannot form diabetic osmotic cataracts. There are reports of transgenic mice with diabetic cataracts. These mouse models express either the human aldose reductase gene (Lee et al. 1995) or the bovine sodium/myoinositol cotransporter gene (Cammarata et al. 1999) both of which act in the sorbitol pathway and lead to diabetic cataract formation. Table 2.01 (page 53) summarizes some of the most common non-mouse rodent models of diabetes.

Of the spontaneous models listed in Table 2.01 (page 53), only a few are available to researchers from private breeding colonies. Most of these spontaneous models have not been fully characterized with respect to the ocular

changes of Type 2 diabetes. *Psammomys obesus* or the “Fat Sand Rat,” is a *Cricetidae* rodent from the subfamily *Gerbillinae*. This desert gerbil originates from the Northern African Desert region and is much larger than a jird (*Meriones sp*). An adult sand rat is approximately the size of a young adult laboratory rat, with an average weight range reported for males between 196 and 252 gm and for females between 186 and 207 gm (Kalman et al. 1996). Type 2 diabetes was first noted in this species when they were collected by the U.S. Naval Medical Research Unit in Egypt in the 1960's and placed on regular rodent chow in the laboratory (Strasser 1968), (Shafrir and Gutman 1993). In the wild, the sand rat consumes a diet of mainly salt bush (*Atriplex halimus*). Salt bush is low in digestible energy and high in fiber, electrolytes and water (Gutman et al. 1975). The sand rat, a diurnal rodent, is well adapted to desert life (Frenkel et al. 1972). It has the ability to highly concentrate its urine and therefore requires little water in the desert. This adaptive ability is believed to be due to a 60 – 70% higher relative weight of the kidney (as compared to a rat) and an extremely long renal papilla. Type 2 diabetes is easily induced nutritionally by placing the animals on a high-energy, low fiber diet such as a standard rodent chow (Kalman et al. 1996). This diet change results in hyperinsulinemia, hyperglycemia, hyperlipidemia and obesity as early as 11 – 14 days after starting the high-energy diet (Adler et al. 1990). Aside from the biochemical changes that have been reported, a common ocular change seen in the sand rat is cataracts (Hackel et al. 1965), (Shafrir and Renold 1984), (Marquie et al. 1991). Figure 2.01 (page 57) shows a sand rat from the Uniformed Services University of the Health Sciences (USUHS) colony

that has diabetes-induced cataracts. Once placed on a standard rodent chow, bilateral cataracts are produced in this spontaneous animal model within one month of the diet change. This rapid and consistent manifestation of diabetes makes this model an excellent choice for the study of mechanisms of development of diabetic cataracts. The purpose of this study was to characterize the formation of diabetic cataracts in this model by comparing the impact of elevated glucose and glycated protein levels within the blood to the glucose influx into the ocular tissues, specifically the lens.

## Materials and Methods

**Animals:** A total of 34 sand rats, 20 controls (8 males, 12 females) and 14 diabetic sand rats (9 males, 5 females), were studied. The animals were housed at the Uniformed Services University of the Health Sciences (USUHS) central animal facility, which is fully accredited by the Association for the Assessment and Accreditation of Laboratory Animal Care, International (AAALAC). All animals were handled in accordance with procedures approved by the USUHS Institutional Animal Care and Use Committee (IACUC). The sand rats were obtained from a USUHS breeding colony. This is a closed colony but on routine sentinel exam, the colony tested positive for the dwarf tapeworm (*Hymenolepis nana*). Approximately 50% of the sand rats on this study tested positive for *Hymenolepis nana* but were not treated. The animals on study were in various stages of diabetes at the determination of infection. Since they had no clinically apparent disease, we chose not to treat the animals. The sand rats on study

were divided initially into 2 groups, controls and diabetics. The control animals were fed a specially formulated Sand Rat Chow (Purina Sand Rat Diet 5L09, Ralston Purina, Richmond, IN) and the diabetic group was fed a standard rodent chow (certified Purina Rodent Diet 5002, Purina Mills, St. Louis, MO). Once on the chows, there were three control animals that became diabetic on the sand rat chow and six sand rats did not convert to a diabetic state (diabetes resistant) on the Purina Rodent Diet. Of the 34 sand rats, the diabetic group included 11 sand rats on standard rodent chow and 3 on Sand Rat chow for a total of 14. The control animals included 14 sand rats on sand rat chow and 6 sand rats on standard rodent chow (diabetes-resistant) for a total of 20. After the onset of diabetes, diabetic sand rats were approximately 30 – 40 gm heavier in average weight than the age and gender-matched control sand rats.

**Determination of the Diabetic State:** The animals were bled on a bi-monthly schedule for determination of diabetes. This determination was modified from the American Diabetes Association recommendations (ADA 1999a), (ADA 1999b) and based on obtaining two consecutive blood glucose values greater than 200 mg/dl or one value greater than 200 mg/dl and a glycated hemoglobin (HbA1c) level of greater than 8%. The blood sampling was then reduced to once a month thereafter. Determination of diabetes resistance was based on blood glucose values and HbA1c levels that were consistently in the normal range while the sand rat was on a diabetogenic diet. Based on our experience, if the animal did not convert within the first 2 – 3 months, the animal was considered

diabetes resistant and was then placed into the control group category. In addition to the clinical chemistry data, the lenses of all sand rats on study were photographed using the slit-lamp biomicroscope. This was performed to assure that control animals did not have any clinically apparent lenticular abnormalities prior to assignment in this study and to follow the course of the diabetic cataracts.

Sample Collection: Serial blood samples were collected from the sand rats using isoflurane anesthesia. The sand rats were masked down and blood was collected from the orbital sinus using a sterile Pasteur pipette. No greater than 70  $\mu$ l was collected from the animals during each serial bleed, which is within the acceptable limit for an animal weighing 200 gm. For the slit-lamp exams and photographs (Topcon Model #SL-7E, Topcon American Corporation, Paramus, NJ), the sand rats were sedated using 20 – 40 milligrams/kilogram (mg/kg) ketamine HCl and 2-5 mg/kg xylazine administered by intraperitoneal (IP) injection. One to two drops of tropicamide was administered, as needed, to each eye for pupil dilation during examination. All other tissue and fluid collection was performed at the time of euthanasia. The sand rats were anesthetized using 40 mg/kg ketamine HCl and 5 mg/kg xylazine administered by intraperitoneal (IP) injection. For maximal blood sampling, cardiac puncture was performed under anesthesia and the sand rats were then placed into a carbon dioxide chamber for euthanasia. A thoracotomy was performed and cardiac tissue removed ensuring death. The aqueous humor was collected using a micropipetter after puncture

into the cornea near the limbus with an 18 gauge needle. After globe enucleation, a limbal circumferential incision was made to remove the lens. The lens was convex in shape and had a firm zonular attachment. The vitreous humor was also removed using a micropipetter. The aqueous and vitreous were immediately frozen and stored at  $-20^{\circ}\text{C}$  until analyzed. The lenses were either placed in 1 ml of Tris-buffer (0.05 M Tris-Cl, 5mM 2-mercaptoethanol, pH =7) and frozen at  $-20^{\circ}\text{C}$  until analyzed or placed directly into a tube with a RNA preservation solution (RNAlater™, Ambion, Austin, TX) and stored at  $4^{\circ}\text{C}$ .

#### Sample processing for reverse transcriptase Polymerase Chain Reaction

(rtPCR): The lenses stored in RNAlater™ solution at  $4^{\circ}\text{C}$  from normal sand rats were carefully dissected to remove the capsule with anterior epithelial cells from the lens fiber cells. These samples were macerated using a FastPrep™ machine (Qbiogene, Carlsbad, CA). RNA was isolated and prepared in TRIzol solution (GIBCO BRL/Life technologies, Gaithersburg, MD) using the standard chloroform/ethanol extraction techniques recommended by the manufacturer. First strand synthesis from the RNA was performed using Ready-To-Go You-Prime-First-Strand Beads (Amershan Pharmacia Biotech, Piscataway, NJ). The reaction mixture contained prepared RNA added to a prepared product containing 50 mM Tris (pH 8.3), 75 mM KCl, 7.5 mM DTT, 10 mM  $\text{MgCl}_2$ , 0.08 mg/ml BSA and 2.4 mM of each dNTP (dATP, dTTP, dCTP, dGTP). The reaction mixture was incubated at  $37^{\circ}\text{C}$  for one hour. The cDNA product was then added to Ready-To-Go PCR Beads (Amershan Pharmacia Biotech,

Piscataway, NJ), which contained 1.5 units of *Taq* DNA polymerase, 10 mM Tris-HCl, 50 mM KCl, 1.5 mM MgCl<sub>2</sub>, 200 µM of each dNTP (dATP, dTTP, dCTP, dGTP) and primers specific for GLUT-1, GLUT-3 and GLUT-4. These oligomers listed in Table 2.02 (page 55) are based on rat sequences, obtained from Genbank, and were used for determining the presence of glucose transporter mRNA in the sand rat. Primer pairs for beta actin (Table 2.02, page 55) were used to test the quality of the cDNA. After 2 minutes at 94 °C, amplification was performed using a three-step thermal cycling program. There was a 30 second denaturation at 94 °C, a 30 second anneal at 55 °C for GLUT-3 and GLUT-4 and a 30 second anneal at 57 °C for GLUT-1. Extension was performed at 72 °C for 30 seconds. Thirty-five cycles were used followed by an extra 5 minutes at 72 °C for optimizing the elongation. Amplified PCR products were analyzed by electrophoresis on 5% TAE polyacrylamide gels, in accordance with techniques described by Sambrook et al (Sambrook et al. 1989).

Sample processing for clinical chemistry: Serial blood glucose was determined using a commercially available blood glucose meter (SureStep™ by Lifescan, Milpitas, CA). Serial HbA1c values were obtained using the filter paper elution test (Petnostics Glycohemoglobin Assay, Flexsite Diagnostics, Palm City, FL). Using a hexokinase test kit (SIGMA Diagnostics, St. Louis, MO), the glucose concentration of the aqueous and vitreous was determined. This enzymatic technique is similar to that described (Carroll et al. 1970) and determines glucose

concentration by using a colorimetric response for hexokinase presence at 520 nanometers (nm).

The lens was homogenized in 1 ml of Tris-buffer and centrifuged at 15,000 g for 15 minutes at 4°C. The water-soluble fraction was collected and is referred to as the lens extract. Protein values for the water-soluble lens extract were determined using a protein assay (BioRad, Hercules, CA) based on the Bradford dye-binding procedure (Bradford 1976). This is a quantitative test using a colorimetric response for protein level at a maximum absorption of 595 nm. Glycated protein levels of the lens extract and vitreous were determined using a fructosamine test kit (SIGMA Diagnostics, St. Louis, MO). Fructosamine is produced through non-enzymatic glycation of proteins and is proportional to the average prevailing glucose concentration. The SIGMA Fructosamine Test Kit, based on the technique of Johnson et al (Johnson et al. 1982), is a quantitative technique using glycated proteins to reduce nitrotetrazolium under alkaline conditions producing a colorimetric response with maximum absorption at 530 nm. The test kit uses a calculation based on change in absorbance. For blood samples this relationship is linear. Since a media other than blood was tested, a standard curve for the test kit was produced using multiple concentrations of the standard. This standard curve can be seen in Figure 2.02 (page 58).

## Results

Detection of cataract formation by slit lamp examinations: The course of the cataract formation was documented via slit-lamp biomicroscopic exam and examples of this routinely observed pattern are seen in Figures 2.03 through 2.07 (page 59). The sand rat produces vacuoles in the equatorial regions, then subsequent opacities in the posterior aspect of the lens within weeks of feeding a standard rodent chow (Figures 2.03 and 2.04, page 59). The diabetic cataract then extends from the posterior regions through the nucleus towards the anterior portions of the lens (Figures 2.05 and 2.06, page 59). This pattern of cataract formation was seen in most of the diabetic sand rats with several also exhibiting involvement of the lens suture. The cataract often appears segregated along the suture line as seen in Figure 2.07, page 59.

Detection of Glucose Transporter Transcripts by rtPCR: Using oligonucleotide primers specific for rat GLUT-1 mRNA, a 195 base pair amplicon is seen in the sand rat anterior epithelial cells, the sand rat brain and the rat brain (Figure 2.08, page 61). The gel is shown with two sets of 100 base pair markers so it is easy to see that the gel ran at an angle but bands are clearly present in lanes III, IV and V. Using beta actin primers (Weng et al. 1997) for the mouse resulted in a band present at 331 bp for lens fiber cells, anterior epithelial cells, sand rat brain and rat brain, indicating good quality cDNA from these tissues. The presence of GLUT-3 transcript could not be determined due to problems producing a primer pair from the rat GLUT-3 gene. A 201 bp amplicon is seen in sand rat lens fiber cells, anterior epithelial cells, sand rat brain and rat brain using primers specific

for the rat GLUT-4 mRNA (Figure 2.09, page 62). In the sand rat, GLUT-1 and GLUT-4 transporter transcripts were present in the lens anterior epithelial cells. GLUT1 transcript was absent in the lens fiber cells of the sand rat (Figure 2.08, page 61). GLUT-4 transcript was also present in the lens fiber cells of the sand rat (Figure 2.09, page 62).

Determination of concentrations of glucose, protein and glycated protein: The mean values for the glucose, glycated protein and protein values of blood and ocular tissues and fluids are listed in Table 2.03 (page 56). Blood, aqueous and vitreous glucose levels were elevated in the diabetic sand rats when compared to control animals. Analysis of Variance (ANOVA) yielded a highly significant difference (0.000, 0.004, 0.000, respectively) for the glucose values. The lens extract (water-soluble) protein concentration was higher in the control sand rats than in the diabetic sand rats. The ANOVA yielded a highly significant difference (0.001) between these groups. No significant difference between the diabetics and controls was seen in the glycated protein concentrations of the water-soluble lens extracts. Since the standard curve (Figure 2.02, page 58) for the fructosamine test kit did not allow for calculation of values with a change of absorbance less than 0.024, the glycated protein levels of the vitreous could not be determined by the described method. The HbA1c values were elevated in the diabetic sand rats when compared to controls with ANOVA testing yielding a highly significant difference (0.000).

## Discussion

The sand rat is a diurnal animal with strong lenticular attachments to the lens zonules. This is unlike many other rodents and may indicate the ability of this animal to accommodate its vision similar to higher species. Based on our slit lamp examinations, the pattern of formation of the irreversible diabetic cataracts in the sand rat mimics the reported diabetic cataract pattern seen in the humans, dogs (Albert and Jacobiec 1994) and galactosemic rats (Robison et al. 1990). This includes early vacuolization at the equators and posterior lens, due to the osmotic swelling of the lens fiber cells. Lens fiber cell rupture and disruption of the normal lens architecture results in opacities in the posterior aspects of the lens. Prominence of the lens sutures with segregation of the cataract along this line appears to be a common finding in diabetic cataracts and was seen in the diabetic sand rat. The rapid and consistent formation of diabetic cataracts in a pattern consistent with the formation in human diabetic patients supports the use of *Psammomys obesus* as an excellent spontaneous model for the clinical study of diabetic cataracts.

Identification of GLUT-1 and GLUT-4 transcripts in sand rat ocular tissues using primer pairs generated from rat mRNA indicates good homology for these glucose transporters between these rodent species. Different primer pairs were generated and utilized than those reported by Merriman-Smith, et al (Merriman-Smith et al. 1999) because of inadequate results using their primer pairs on

genomic DNA from sand rats. Using the primer pairs listed in Table 2.02 (page 55), GLUT-1 transcript was identified in sand rat anterior epithelial cells, sand rat brain and as expected in rat brain. The presence of three bands in the anterior epithelial cell lanes of Figures 2.08 and 2.09 (pages 61 and 62) could be attributed to annealing of transcripts to each other during the elongation phase or to gene duplication. Annealing of the transcripts to each other is the most probable explanation since the bands at 400 and 800 bp are exactly 2 and 4 times as large as the expected transcript size yet are quantitatively lower in concentration. Bands of equal density and thickness at the larger size of 400 and 800 bp have one half and one quarter, respectively, less transcript than the amount of transcript found in the 195 (Figure 2.08, page 61) and 201 bp (Figure 2.09, page 62) bands. These additional bands at 2 and 4 times the expected band size could also be explained by gene duplication. This is an unlikely cause for the additional bands since there is no additional data to support this and the duplicated genes would be expected to have bands 2 to 4 times as dense for an equivalent amount of transcript. Therefore, the probable cause of the additional bands is the annealing of transcript ends to each other.

With the presence of GLUT-1 and GLUT-4 transcript in the anterior epithelial cells of the sand rat lens, it is easy to speculate the glucose transporter protein is probably also located in these cells. With the presence of only GLUT-4 transcript in the lens fiber cells, it is more difficult to speculate the presence of any transporter protein but GLUT-4. That is unless consideration is given to the fact

that the anterior epithelial cells are the stem cells for the lens fiber cells and the lens fiber cells lose their organelles with maturation. The loss of the organelles prohibits the cell from transcribing and translating additional proteins. This, however, does not exclude the lens fiber cells from containing proteins translated earlier in the stem cells. If, in fact, only GLUT-4 protein were present in the lens fiber cells of sand rats, insulin would be required for glucose transport into this location. Cataracts form early in the clinical course of the disease, at a time when the sand rat is compensating for the diet change with an elevated blood insulin level (Kalderon et al. 1986), (Shafrir and Gutman 1993) so there is an abundance of insulin available to support glucose transport into the anterior epithelial and lens fiber cells. By the time the sand rat becomes insulin resistant, the cataracts are generally mature. At this point, the absence of the insulin for the GLUT-4 transporters in the lens is insignificant since the osmotic changes have irreversibly damaged the lens. If, in fact, other non-insulin dependent GLUT transporters, like GLUT-1, are present in the lens fiber cells, rapid movement of glucose into the lens fiber cells would occur with subsequent increased flux through the polyol pathway and rapid formation of diabetic cataracts. The identification of GLUT-1 transcript in the anterior epithelial cells of the sand rat could also explain the early diabetic cataract formation seen in the equators of the lens of the sand rat, if more transporters exist in the anterior epithelial cells that are at the equatorial regions of the lens. This is the transition area of the lens. The daughter cells of the anterior epithelium are becoming lens fiber cells. A higher number of transporters supporting a higher metabolic cell rate would

allow for increased glucose transport into the cells at a location where diabetic cataracts are seen to begin in the sand rat. All of these scenarios are feasible since the cataracts form quickly and early in this disease.

The presence of messenger RNA for GLUT-1 and GLUT-4 in the lens epithelial cells but the absence of GLUT-1 mRNA in the lens fiber cells of the sand rat differs from the results of Merriman-Smith et al, in the rat (Merriman-Smith et al. 1999). They reported GLUT-1 transporter as the dominant glucose transporter in lens anterior epithelial cells and GLUT-3 as the predominant transporter in lens fiber cells of the rat. This was significant because it showed differential uptake of glucose by lens fiber cells independent of the need for insulin. Since GLUT-3 has a faster rate of glucose uptake than GLUT-1, this independent uptake by the lens fiber cells would also explain the early characteristic differential opacity formation within the posterior of the lens. This pattern is seen in several species including galactosemic rats and sand rats. Still other reports found GLUT-1 transporters mainly localized in the cortical lens fiber cells of humans (Mantych et al. 1993) or failed to detect GLUT-1 transporters anywhere in the lens (Kumagai et al. 1994). Glucose transport studies are equally conflicting. Transport of glucose at both the anterior and posterior lens surfaces in the calf lens (Kern and Ho 1973) is in contrast to the report of the anterior epithelium as the main site for glucose uptake into the mouse lens (Goodenough et al. 1980). Clearly, more research is needed studying the glucose entry and transport mechanisms into the lens during diabetes. This is important for the study of early intervention therapy at the

site of the glucose transporter and for the study of how the presence of the elevated glucose levels affect the ocular proteins.

The clinical chemistry findings for the elevated glucose values of the blood and ocular fluids and the elevated HbA1c in the diabetic sand rats are consistent with the literature for other species. The hyperglycemia in the sand rats resulted in subsequent elevated glucose in the aqueous and vitreous and increased glycation of hemoglobin. Elevated ocular glucose levels are reported in the literature for human diabetic patients (Daae et al. 1978), (Peclet et al. 1994), (Lundquist and Osterlin 1994) and are related to an increased permeability of the blood-aqueous barrier (Waltman et al. 1978), (Coulter et al. 1983) and an increased passive diffusion rate of the retinal vessels in diabetes (Di Mattio et al. 1981). The factors that affect the extent of protein glycation are the half-life of the protein and the degree and duration of the hyperglycemia (Cefalau 1988). This is the reason glycated hemoglobin is so valuable in the determination of the diabetic state. HbA1c describes the glycemic conditions over a longer course of time. In the sand rat, HbA1c describes the blood glucose condition for the last 60 days (personal communication with Dr. Chenault). This indicates a much longer red blood cell half-life in the sand rat than the more common Mongolian gerbil (*Meriones unguiculatus*), which has a red blood cell half-life of only 9 - 10 days (Harkness and Wagner 1995).

The degree and duration of the elevated glucose levels of the aqueous and vitreous should affect the long-lived collagen proteins of the vitreous and crystallin proteins of the lens. An elevated level of glycated vitreal proteins is reported in diabetic humans (Stitt et al. 1998), (Osuna et al. 1999) and other species (Shires et al. 1990), (Farr et al. 1999). Unfortunately with small sample sizes in the sand rats, the test kit lacked the sensitivity required for accurate verification of glycated protein levels from the vitreous. Pooling of vitreal samples and concentrating these small samples for each group is indicated for future studies. The absence of a difference in glycated lens protein concentrations between control sand rats and diabetic sand rats conflicts with the literature for other species. Glycation of lens proteins in diabetes and aging has been reported for humans (van Boekel and Hoenders 1992), (Crabbe 1998) and animals (Perry et al. 1987), (Ramanakoppa et al. 1996), (Shamsi et al. 1998). This lack of a difference in the sand rats may be due to the lower water-soluble protein levels in the diabetic animals. The lower protein concentration in the water-soluble extracts of the diabetic sand rats may be attributed to protein aggregation and subsequent insolubility, resulting in loss of protein to the non-water-soluble fraction. Additionally, some water-soluble protein may be lost to the vitreous through capsular leakage during cataract maturation.

The fat sand rat is an excellent model for the study of diabetic cataracts because clinical cataract formation is rapidly induced with a simple diet change, the formation of cataracts and clinical chemistry is similar in progression to what is

seen in human diabetic cataract formation and the sand rat is easy to breed and handle. This spontaneous model is easily converted to a diabetic state without drug injections, like alloxan or streptozocin, and without costly food additives, like a diet of 50% galactose. The diabetic cataract formation in the sand rat is identical to diabetic cataract formation in the human, the dog (Albert and Jacobiec 1994) and the galactosemic rat (Robison et al. 1990). In addition, the sand rat, like humans and dogs and unlike the rat, has the lens of a diurnal animal. Rats and mice, being nocturnal species, have a hard round lens with minimal zonular attachments, since there is no reason for nocturnal animals to be able to accommodate. Not only are sand rats a more anatomically correct lens model than the other common rodent models seen in Table 2.01 (page 53) they are also much easier to handle. Sand rats can be readily handled without the behavioral acclimation that is required for rats and mice. The clinical chemistry data of the sand rat of the blood glucose and ocular glucose concentrations along with the glycated hemoglobin values also indicate similarity to human diabetic patients. Based on these anatomical, biological, behavioral and clinical chemistry parameters, the sand rat is an excellent model for the study of diabetic cataracts.

The only common treatment for cataracts is surgical removal of the lens and replacement with a synthetic intraocular lens. Therapies are currently aimed at the sorbitol pathway through aldose reductase inhibition (Robison et al. 1990), (Robison et al. 1995), (Jacot et al. 1997) and at the Maillard reaction by reducing advanced glycation end products (Friedman 1999), (Degenhardt et al. 1999), (Monnier and Cerami 1981). Identification of glucose transporters within the lens clearly needs to continue to be investigated as a potential mechanism for drug therapy. Advances in drug therapy research favor finding medical interventions that may alleviate or prevent cataracts without requiring an already compromised patient to undergo surgery. With the devastating multisystemic complications of diabetes being so prevalent, it is imperative that new animal models be developed and characterized for future diabetes research. The sand rat, a spontaneous model for Type 2 diabetes, is an excellent choice for diabetic cataract research.

### **Acknowledgments**

We would like to thank Dr. Steven Dalal, Ms. Carol Puligiese, Ms. Lee Lewis and Ms. Sue Pletcher of the Uniformed Services University of the Health Sciences (USUHS), Department of Laboratory Animal Medicine for their clinical expertise, animal care, clinical pathology and histopathology assistance, respectively. We also thank Drs. William P. Roach and Thomas Johnson, USUHS, Department of Preventive Medicine and Biometrics, for the generous use of their slit-lamp camera, digital camera and laboratory facilities and Mr. Mike Flora,

Bioinstrumentation Center, USUHS, for the GLUT primer production. This research was supported by the Uniformed Services University grant # T070IQ, National Institutes of Health, National Eye Institute (NEI) grant # EY11726 and the National Aeronautical Space Administration (NASA) grant # G276GT.

TABLE 2.01

Animal Model	Type	Characteristics and Use	Reference
Alloxan-induced rats	Drug Induced	Zinc chelating?/oxygen radical formation agent = Type 1 Model	(Tarui et al. 1987)
Streptozocin-induced rats	Drug Induced	Zinc chelating?/oxygen radical formation agent – Two methods 1. Single dose IV or IP in neonates – hyperglycemia, normoglycemia then hyperglycemia = Type 2 Model 2. Multidose in adults destroys pancreas by lymphocytic infiltration & reduces insulin production by Beta cell destruction = Type 1 Model	(Tarui et al. 1987)
BB rat	Genetically Induced	Overt diabetes after a period of autoimmune insulinitis caused by T-cell lymphocytic infiltration of pancreas = Type 1 Model	(Tarui et al. 1987)
Zucker rat ( <i>fa/fa</i> )	Genetically Induced	Obese and diabetic single recessive gene mutation in the leptin receptor = Type 2 Model	(Tarui et al. 1987), (Shepard and Kahn 1999)
Galactosemic rat	Diet Induced	Hyperglycemia induced with 50% galactose in diet; complications due to increased flux through the polyol pathway occur rapidly. Used to study multisystemic disease (especially ocular changes) in Type 2 diabetes	(Robison 2001)
Fat Sand Rat	Spontaneous	Obese and diabetic when on high energy diet due to “thrifty gene,” low insulin receptor density/insulin resistance = Type 2 Model	(Kalman et al. 1996), (Shafrir 1996)
Mongolian Gerbil	Spontaneous	Obese and diabetic when on high energy diet = Type 2 Model	(Tarui et al. 1987)

<b>Goto-Kakizaki rat (Japanese colony)</b>	<b>Spontaneous? or Genetically Induced?</b>	<b>Selective breeding (polygene) of Wistar rats with glucose intolerance creating a non-obese rat with glucose intolerance, impaired insulin secretion, hyperinsulinemia and decreased pancreatic insulin stores but no cataracts = Type 2 Model</b>	<b>(Miyamoto et al. 1996), (Tarui et al. 1987)</b>
<b>Egyptian Spiny Mouse</b>	<b>Spontaneous</b>	<b>Diabetes due to overeating and obesity, but no insulin resistance = Type 2 Model</b>	<b>(Shafrir and Renold 1984)</b>
<b>Djungarian hamster</b>	<b>Spontaneous</b>	<b>One colony had glycosuria +/- ketonuria, Beta cell de-granulation, glycogen deposition in Islets = Type 2 Model?</b>	<b>(Goodwin 1997)</b>

Table 2.01 shows the common rodent models of diabetes (excluding *Mus* genus mouse models).

TABLE 2.02

Protein	Oligonucleotide	Expected PCR Product Size
GLUT 1 (S68135*(Wadhvani et al. 1993))	Sense (20 bases, position 1) TCTTCCAACCTCAACCAACCA Antisense (20 bases, position 195) CAGGAGTGTCCGTGTCTTCA	195 bp
GLUT 3 (U17978*(Krishnan and Haddad 1995))	Sense (20 bases, position 618) CGAGAGTCCAAGGTTCTTGC Antisense (20 bases, position 1253) CGCAGCCGAGGGGAAGAACA	636 bp
GLUT 4 (J04524*(Charron et al. 1989))	Sense (20 bases, position 1285) ATATTTGGCTTTGTGGCCTT Antisense (20 bases, position 1485) GGCAAATAGAAGGAAGACGT	201 bp
Beta actin (X03672*)	Sense (23 bases, position 418) AGGCCAACCGTGAAAAGATGACC Antisense (22 bases, position 749) GAAGTCTAGAGCAACATAGCAC	331 bp

\*GenBank accession number

Table 2.02 shows the PCR primer sets and predicted product sizes.

TABLE 2.03

Parameters	Control Sand Rats Mean Values +/- S	Diabetic Sand Rats Mean Values +/- S	F value	Significance
Aqueous glucose concentration in mg/dl	78.5 +/- 32.19 n = 16	275.85 +/- 191.84 n = 13	16.498	.000
Vitreous glucose concentration in mg/dl	77.33 +/- 50.71 n = 15	190.92 +/- 128.65 n = 13	9.959	.004
Blood glucose concentration in mg/dl	103.95 +/- 65.99 n = 20	283.29 +/- 172.09 n = 14	18.120	.000
Lens water-soluble protein concentration in mg/ml	62.95 +/- 30.66 n = 10	17.25 +/- 21.69 n = 11	15.791	.001
Glycated water soluble lens protein concentration in mMol/L	3.46 +/- 2.37 n = 9	1.90 +/- 1.93 n = 3	1.046	.330
Glycated HbA1c concentration in %	5.37 +/- 0.59 n = 19	11.8 +/- 4.84 n = 14	33.193	.000

Table 2.03 is a comparison of mean glucose, protein and glycated protein concentrations in the control and diabetic sand rats. A One-Way Analysis of Variance (ANOVA) was used to determine significant differences between control and diabetic animals.

**FIGURE 2.01**



**Figure 2.01 shows a sand rat with diabetes induced bilateral cataracts. This sand rat was approximately 35 cm in length from the tip of the nose to the base of the tail.**

FIGURE 2.02

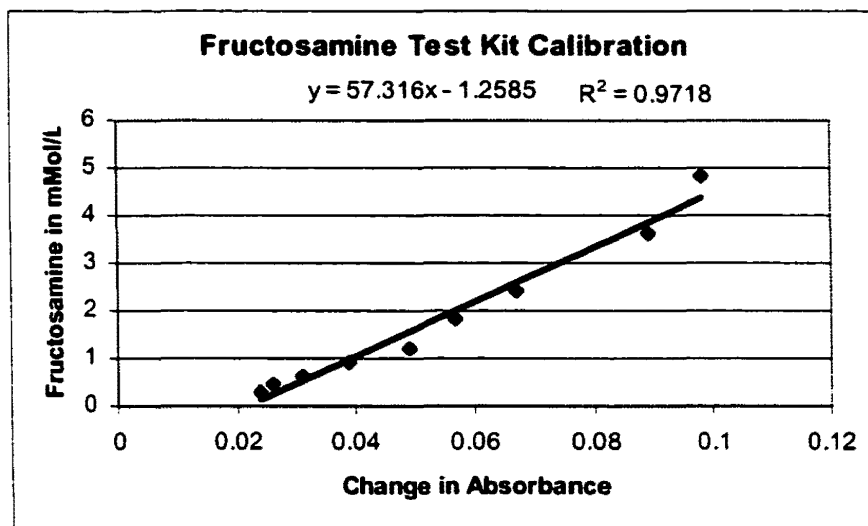


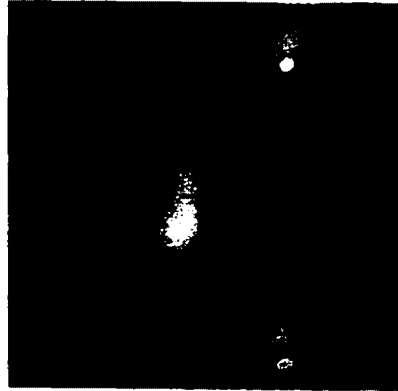
Figure 2.02 shows the standard curve for the fructosamine test kit.

FIGURE 2.03 THROUGH 2.07

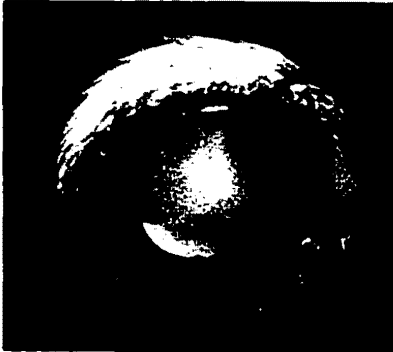
2.03



2.04



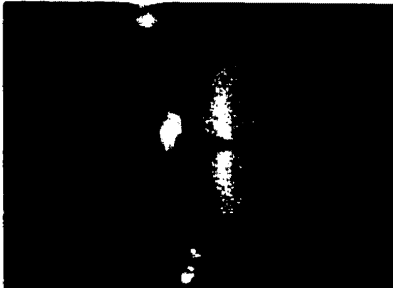
2.05



2.06



2.07



Figures 2.03 – 2.07 (page 59) show detection of diabetic cataracts by slit-lamp photography (16 X magnification)

Lens of sand rat that was diabetic for two months (2.03, 2.04). Camera is focused on the posterior aspect of the lens. Multiple small and large vacuoles are seen in the equatorial and posterior subcapsular region. There is also a low to medium grade cataract in the posterior cortical region (2.04). Lens of same sand rat three months later, at five months duration of diabetes has a more mature cataract (2.05, 2.06). Opacities are seen in the posterior aspects as well as the nuclear and anterior cortical regions (2.06). Lens from a 10-month-old sand rat that was diabetic for 5 months (2.07). Segregation along the suture line running through the cataract in an anterior to posterior fashion is seen (2.07).

2.03, 2.05 (frontal view); 2.04, 2.06, 2.07 (slit view)

**FIGURE 2.08**

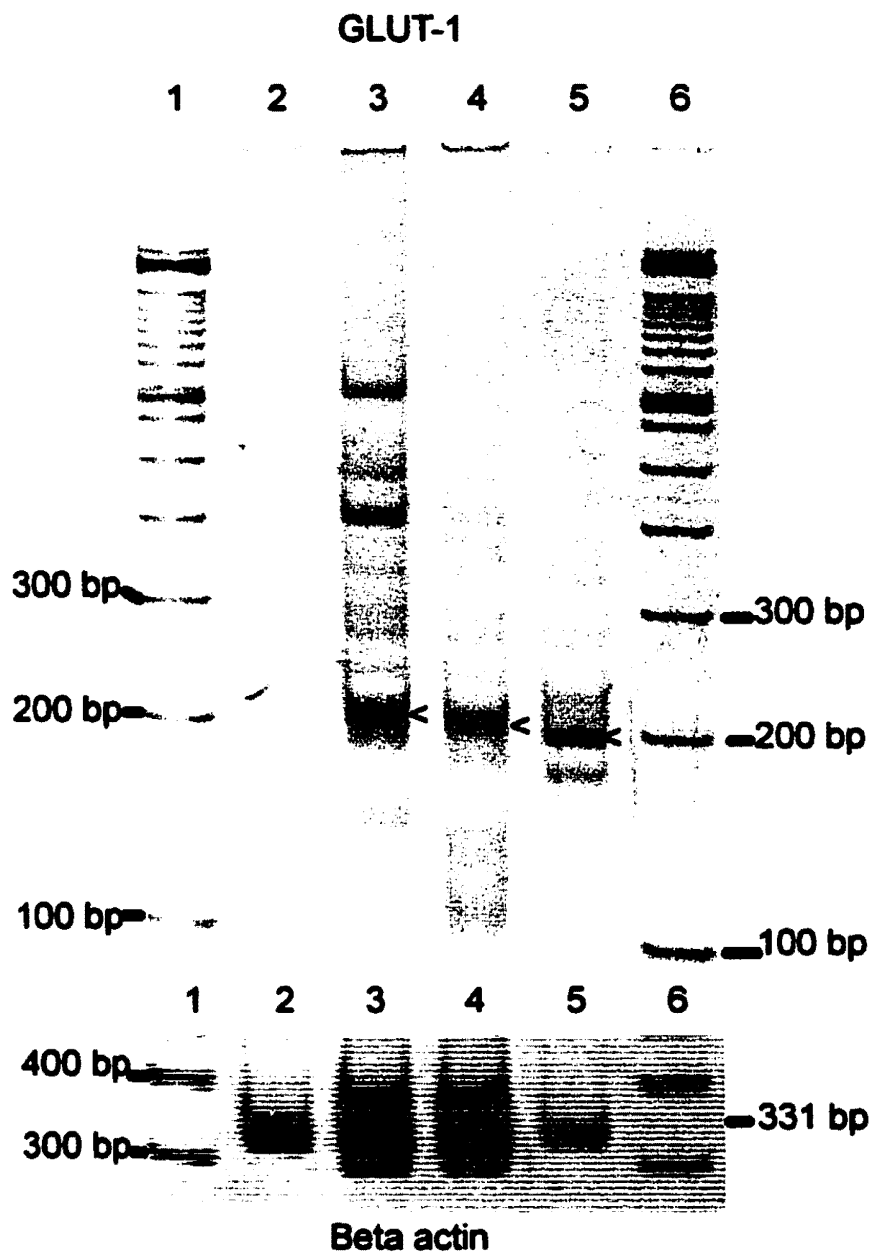


Figure 2.08 shows the detection of GLUT-1 isoform transcript. GLUT-1 transcript expression is indicated by a < at 195 bp for sand rat lens fiber cells (2), sand rat lens anterior epithelial cells (3), sand rat brain (4) and rat brain (5). A 100 base pair ladder is in lane 1 and lane 6.  $\beta$  actin transcript expression is at 331 bp for sand rat fiber cells (2), sand rat lens anterior epithelial cells (3), sand rat brain (4) and rat brain (5). A 100 base pair ladder is in lane 1 and lane 6.

**FIGURE 2.09**

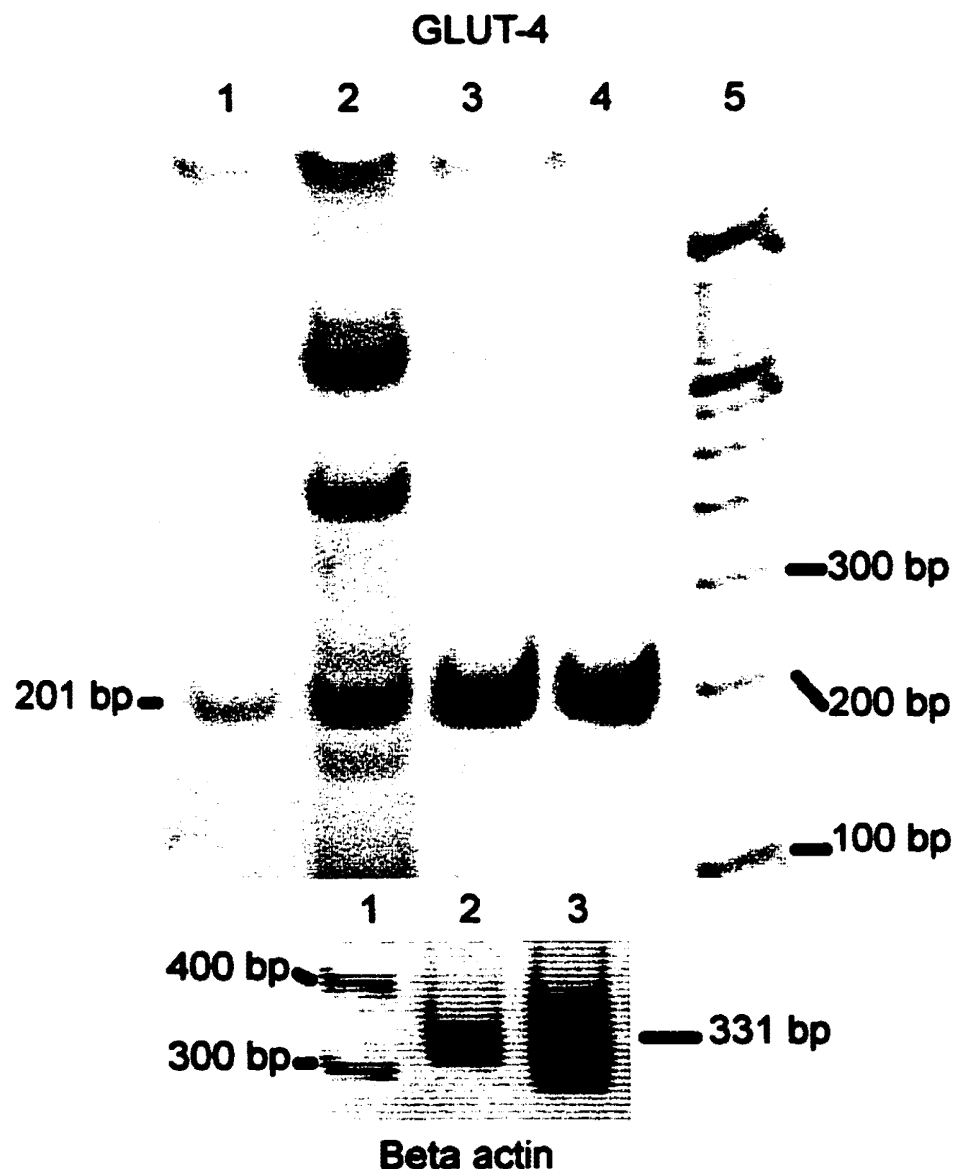


Figure 2.09 shows the detection of GLUT-4 isoform transcript. GLUT-4 transcript expression is at 201 bp for sand rat lens fiber cells (1), sand rat lens anterior epithelial cells (2), sand rat skeletal muscle (3) and rat skeletal muscle (4). A 100 base pair ladder is in lane 5.  $\beta$  actin transcript expression at 331 bp for sand rat fiber cells (2), sand rat lens anterior epithelial cells (3). A 100 base pair ladder is in lane 1.

## CHAPTER 3

### Additional Results from "Ocular Changes in a Spontaneously Diabetic Animal Model, the Fat Sand Rat (*Psammomys obesus*)."

In addition to the data presented in Chapter 2, a brief discussion on related data remains. This discussion will center around data collected on the body weights of controls and diabetics, slit-lamp photography and cataract formation in several other sand rats, and additionally, the glucose and glycated protein determinations using the previously described test kits.

#### Sand Rat Body Weights

The body weights of age and sex matched pairs of sand rats are seen in Figures 3.01 – 3.04 (pages 73 – 76). Figure 3.01 (page 73) shows an overlay of two male sand rats, one of which was diabetic for a total of three months. There was a characteristic weight gain in the diabetic animals. They rapidly gained weight on the high carbohydrate diet (standard rodent chow) to well over 200 gm. This pattern is also seen in Figures 3.02, 3.03 and 3.04 (pages 74 – 76). Although an age matched control can be seen to increase in weight greater than 200 gm (Figure 3.04, page 76), the rise is much more gradual with age of the animal. The animals in Figure 3.04 (page 76) were both 13 month-old males and the diabetic experienced a rapid drop in weight, 26 gm in just 5 days, in March 2000. This suggests that the diabetic animal at this point was no longer able to move glucose into its muscle and adipose. This was probably due to insulin resistance

or the production of a defective insulin product, as suggested by Kaiser et al (Kaiser et al. 1997). This type of drastic weight loss was seen in many of the diabetics and was a primary consideration for euthanasia since allowing an animal to “starve to death” was not ethically or scientifically justifiable. The inability to follow the course of the blood insulin levels simultaneously with the blood glucose was a serious drawback. Although a dramatic loss of body weight is usually an excellent indicator of the endstage of diabetes, additional insulin testing using microliter quantities of blood or serum, if a test were available, would aid in following the entire course of the disease in this model. The reason this is so important is that a loss in body weight may also indicate an animal has compensated for its hyperglycemia and is no longer diabetic. This was seen in a few animals and is discussed further in the Diabetic Blood Glucose section of this chapter.

#### **Slit-lamp Examinations and Photography**

Slit-lamp photographs were obtained using the Topcon Model #SL-7E seen in Figure 3.05 (page 77). Using the slit-lamp, the anterior segment of the eye can be clearly visualized, magnified and photographed. Animals were initially screened for any ocular abnormalities prior to study. The slit-lamp was additionally used for following the course of the diabetic cataract formation in the sand rats. Annotations at the time of the exam along with hand drawn diagrams were essential for correlating the photographic findings. Figures 3.06 – 3.09 (page 79) shows the lenses of control sand rat #803 and indicates the animal has

clear lenses. The presence of “retroillumination” or a reflection back from the retina indicates an unobstructed passage of light (Figure 3.07, page 79). Figures 3.08 and 3.09 (page 79) are included to illustrate the focusing capabilities of the slit-lamp. Figure 3.08 (page 79) is a slit focused on the anterior aspect of the lens and Figure 3.09 (page 79) on the posterior aspect of the lens. Specular reflections (Figure 3.06 and 3.07, page 79) are a common artifact from flash photography and do not indicate an opacity in the lens.

Sand rat # 803 was age and sex matched to sand rat # 805 (Figures 3.10 – 3.12, page 80). The photograph of sand rat # 805, using an open aperture of light (Figure 3.10, page 80) shows vacuolization predominately around the equatorial areas of the lens with some vacuoles in the cortical regions of the lens, within the first month of clinical diabetes. A slit image (Figure 3.11, page 80) of the same eye on the same day additionally shows the segregation of the cataract along the lens suture. Within only 2.5 months of clinical diabetes, this 9 month-old sand rat has a high grade opacity uniformly distributed throughout the lens as indicated by the high amount of scattered light seen in this slit-lamp image (Figure 3.12, page 80).

Sand rat # 820 (Figure 3.13 – 3.16, page 81) has a vacuolated lens in the posterior cortical and equatorial areas within only two months of clinical diabetes (Figures 3.13 and 3.14, page 81). Within three more months, the nuclear and cortical regions have progressed to moderate grade opacities (Figures 3.15 and

3.16, page 81) with vacuoles completely filling the equatorial areas of the lens. A small amount of retroillumination can be seen in the equatorial areas indicating some light is being transmitted back to the retina.

A 7 month-old female sand rat # 158 developed a “mushroom shaped” cataract (Figure 3.17, page 82) at 2 months of clinical diabetes. The cap of the mushroom is the opacity that partially obscures the posterior subcapsular and posterior cortical regions. The stem of the mushroom is an opacity that fills the nuclear and central anterior cortical regions (Figure 3.17, page 82, with focus on anterior cortex). By 4.5 months of diabetes, the entire posterior cortical region has a diffusely mild “mushroom cap” cataract (Figure 3.18 and 3.19, page 82) and a much denser “stem region” in the nucleus of the lens (Figure 3.19, page 82). Figure 3.19 (page 82) is focused on the posterior of the lens and shows the dense opacity in the posterior cortical and nuclear region of the lens. Several longer duration diabetic animals developed this pattern of cataracts. Based on the location of these opacities, minimal light was being received by the retina. These diabetic animals were clinically blind.

The only drawback to the use of the slit-lamp is the sensitivity of the instrument. It is only as good as the operator in detecting opacities in the lens. Newer technologies such as optical coherence technology (OCT) for the imaging of the lens (DiCarlo et al. 1999) and dynamic light scattering for cataracts (Chenault et al. 1999) enables the operator to detect opacities in the lens that are not visible

to the operator's eye. Both techniques detect light scattered back from the lens using a diode laser light source. A high resolution lens image is obtained from OCT. A histogram style graph called a "cataractogram" is obtained using the DLS. Full pupil dilation through the use of mydriatics is required for optimal viewing of the lens using any of these techniques. The use of the newer technologies in conjunction with the slit-lamp would provide a more comprehensive evaluation of cataract formation in the sand rat.

#### Diabetic Blood Glucose Levels

The formation of the cataracts was related to the glucose levels of the blood, aqueous and vitreous humors (Figure 3.20, page 83). Blood was collected by cardiac puncture under anesthesia prior to euthanasia of the sand rat. The blood glucose concentration was determined using a commercially available blood glucose meter (SureStep™ by Lifescan, Milpitas, CA). The aqueous humor was collected using a micropipetter after puncture into the cornea near the limbus with an 18 gauge needle. After globe enucleation, the lens was removed and the vitreous humor was removed also using a micropipetter. The glucose concentration of the aqueous and vitreous was determined using a hexokinase test kit (SIGMA Diagnostics, St. Louis, MO.). The values listed in Figure 3.20 are from blood and ocular fluid samples collected at the time of euthanasia of the sand rats. As explained in Chapter 2, there was a significant difference in glucose values between the diabetic and control sand rats. Scatter plots of blood glucose concentrations over time for 4 of the diabetic animals with normal range

terminal values are seen in Figures 3.21 – 3.24 (pages 84 – 85). The graphs clearly show that blood glucose levels during diabetes fluctuate dramatically. This indicates that a single blood glucose value is not adequate for determining clinical diabetes in the sand rat. What remains much more clinically consistent for blood glucose determination is the glycated hemoglobin (HbA1c) values, which are more representative of the glucose concentration over time. Figures 3.25 – 3.28 (page 87 – 88) shows scatter plots of the HbA1c levels for the same animals. Interestingly, two of the four animals (sand rats # 823 and # 825) were originally control animals that converted on sand rat chow. These two were never placed on the diabetogenic rodent chow, but were considered as part of the diabetic group. The HbA1c values for all 4 animals indicate they were probably compensating for the diabetes at the time of euthanasia. Their body weights had also dropped but much more gradually than an endstage diabetic. These animals are examples of the difficulty that exists in consistently creating diabetic animals in this colony since diabetic-resistant (DR) and diabetes-prone (DP) lines have not been developed.

#### **Glycated Protein Determination using the Fructosamine Test Kit**

Figure 3.29 (page 90) shows how lenses were homogenized and separated into water-soluble and pellet fractions. Upon centrifugation, the lens pellet was noticeably larger in the diabetic samples. This observation was consistent with cataractous lenses. Based on the observed difference in pellet size, additional tests were performed using the insoluble pellets. Evaluation of glycated protein

levels using the SIGMA Fructosamine Test kit and SDS-PAGE of the pellets were attempted. The lens pellets were tested for glycated protein levels based on the theory that crystallins were becoming glycated, aggregating and becoming insoluble. The results of the tests were unreliable. This was not based on an absorbance difference of less than 0.024, as explained in Chapter 2, but was related to extreme differences in values each time the test was performed. Both groups of tests revealed a significant difference between the controls and diabetics. The first set of tests yielded a mean value of 32.95 mMol/L for the diabetics and 17.57 mMol/L for the controls. Unfortunately, the second group of tests produced a mean glycated pellet value of 0.94 mMol/L for the diabetics and 4.96 mMol/L for the controls. So, the significant difference seen between the groups is nullified. The second set of tests included some of the same samples that were tested in the first group. Plausible explanations for this difference in test results are insolubility and the freezing and re-thawing of test samples. The insoluble nature of the pellet material even after repeated homogenization was evident during the testing procedure. The kit is designed for a water-soluble medium. The first problem was related to pipeting an insoluble solution. There was no clear way to guarantee the pipeted sample contained uniformly homogenized media even when volume could be readily assumed to be consistent. During the test procedure, several techniques were tried. The samples were mixed and rapidly read and allowed to settle and re-read. Additionally samples were also centrifuged and re-read. These techniques interfered with the 10-minute incubation instructed by the test kit and also yielded

dramatic differences in sample values. Additionally, the process of freezing and re-thawing samples is also a potential problem that may have impacted the glycated protein values of the samples. Further research on the nature of the composition of the pellets, with respect to crystallin glycation, would be of value in diabetic cataract research but this particular test kit for fructosamine was not valuable in this case. Additional research on the pellets, running them on SDS-PAGE gels, was performed and the results are discussed in Chapter 5.

#### rtPCR for GLUT-3 Transporter Transcript

There was some difficulty in generating primer pairs for the rat GLUT-3 gene that would yield definitive results in the sand rat. A 636 bp amplicon is seen in Figure 3.30 using one set of many primer pairs that were tried in this species. Various conditions were tried including the addition of  $MgCl_2$  and changing the annealing temperature. This set of primer pairs yielded a definitive band at 636 for rat brain cDNA. Bands were also present at 636 bp in the anterior epithelial cells and brain of the sand rat but the results are not as definitive because there are additional bands in the lanes. This lack of specificity could be due to poor homology of the GLUT-3 gene between the sand rat and the rat but this is unlikely since GLUT-1 and GLUT-4 have good homology between the species. The additional bands could also be attributed to cDNA contaminated with genomic DNA. The cDNA was tested using primer pairs for mouse beta actin (Figure 3.30). The expected size of the transcript is 331 bp for mRNA, which is the band size detected using the cDNA from sand rat lens fiber cells, anterior epithelial cells, brain and rat

brain. No other bands were present in any of the lanes; this indicates the cDNA was free from contamination (data not shown). The appearance of the additional spurious bands is probably due to misprimed products. The most likely choices for primer pairs have already been tried so it is more likely to be the conditions for the rtPCR causing the misprimed products. As explained, numerous conditions were already tried with this primer pair. Changing the  $MgCl_2$  and increasing the annealing temperature is usually adequate to remove these spurious bands since these interactions are usually less stable than the correct one. There are other techniques in which the annealing temperature is changed several times during the rtPCR reaction. Using these techniques the optimum annealing temperature is increased or decreased by one or two degrees centigrade every cycle (or every other cycle) for the entire reaction. These are not trivial techniques to utilize since it may be difficult to determine which annealing temperature to begin with and then how much to vary the temperature. Once this is determined, additional factors like  $MgCl_2$  may also need to be varied to obtain the optimum reaction conditions.

## Summary

Body weight, blood glucose concentration and glycated hemoglobin values used together are reasonably good indicators of the diabetic state of the sand rat.

Additional factors that would vastly improve the use of the sand rat as a diabetes model are the generation of diabetes resistant and diabetes prone lines within the colony and the use of insulin testing to determine diabetic state of the animal.

The use of the slit lamp for staging cataracts is an excellent tool but additional new technologies such as optical coherence tomography (OCT) and dynamic light scattering (DLS) may be more useful in detecting opacity formation prior to visualization by slit-lamp. Detection of glycated protein values of the lens and vitreous would be vastly improved using a test kit with better sensitivity and using larger pooled samples. This would most likely yield glycated protein results similar to the literature for the lens and the vitreous of diabetic humans. For a more complete evaluation of glucose transport into the lens, additional rtPCR for GLUT-3 transcript would assist in determining the differences in the sand rat from other diabetic models. Additional research into the localization of all glucose transporters within the lens using in-situ fluorescent antibody techniques, if antibody for the sand rat glucose transporters was available, would be best for determining the presence of a specific glucose transporter within a specific location in the lens. In conclusion, the sand rat is an excellent diabetes model that develops cataracts early in the course of the disease. This animal provides a unique opportunity to study biochemical changes associated with Type 2 diabetes along with specific ocular changes that may lead to the prevention of blindness due to diabetic cataracts.

FIGURE 3.01

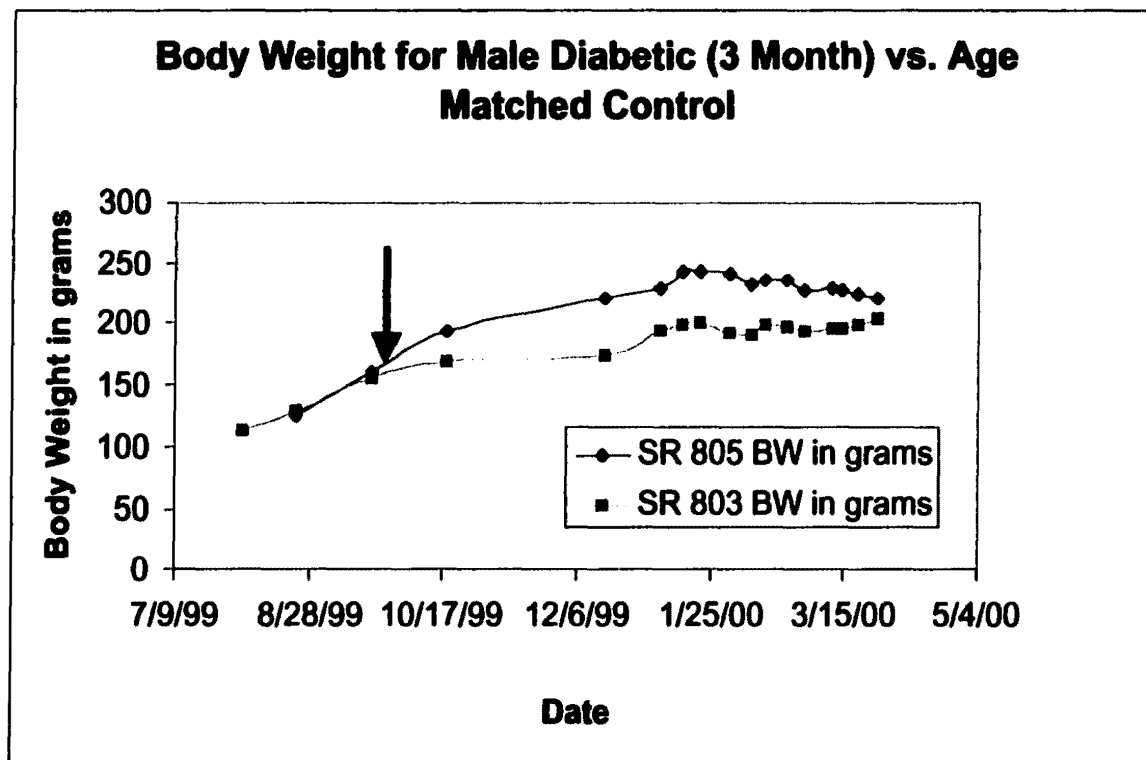


Figure 3.01 shows the body weights of sand rats # 805 (diabetic male) and # 803 (control male) over several months. Sand rat # 805 was clinically characterized as diabetic for 3 months duration. Both animals were 9 months of age at euthanasia. Arrow indicates diet change on 9/7/99.

FIGURE 3.02

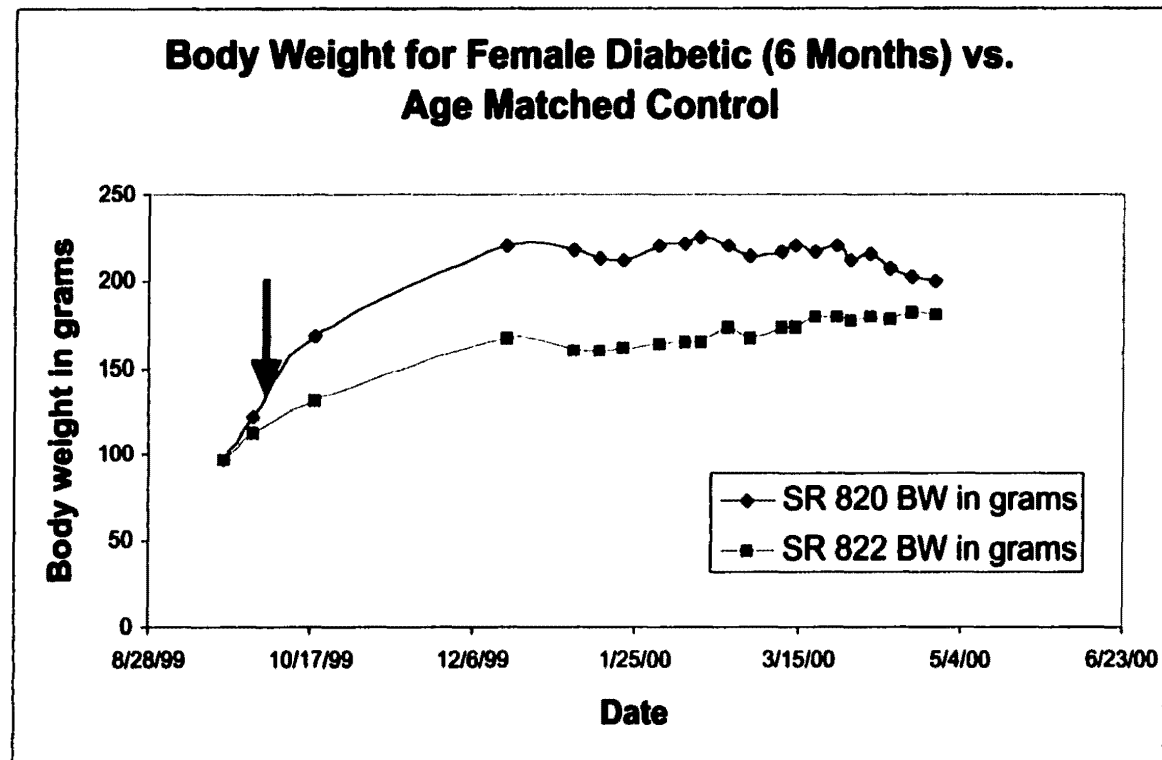


Figure 3.02 shows the body weights of sand rats # 820 (diabetic female) and # 822 (control female) over several months. Sand rat # 820 was clinically characterized as diabetic for 6 months duration. Both animals were 7.5 months of age at euthanasia. Arrow indicates diet change on 10/4/99.

**FIGURE 3.03**

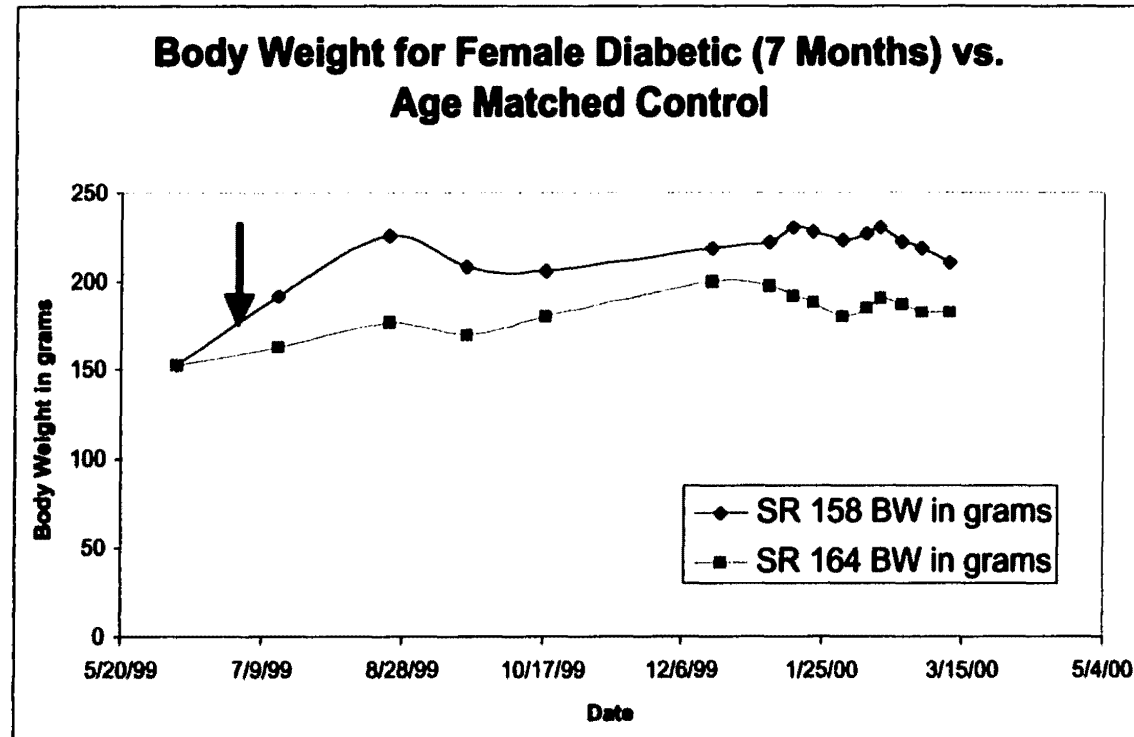


Figure 3.03 shows the body weights of sand rats # 158 (diabetic female) and # 164 (control female) over several months. Sand rat # 158 was clinically characterized as diabetic for 7 months duration. Both animals were 12 months of age at euthanasia. Arrow indicates diet change on 7/6/99.

FIGURE 3.04

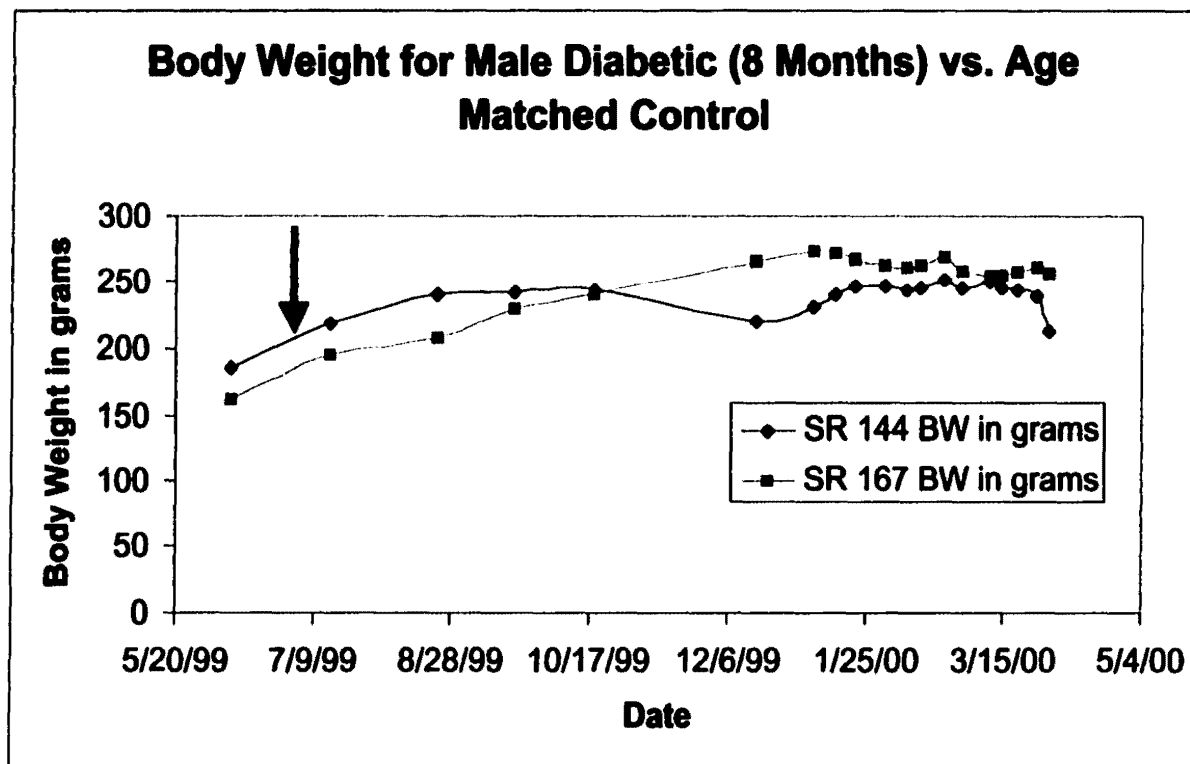
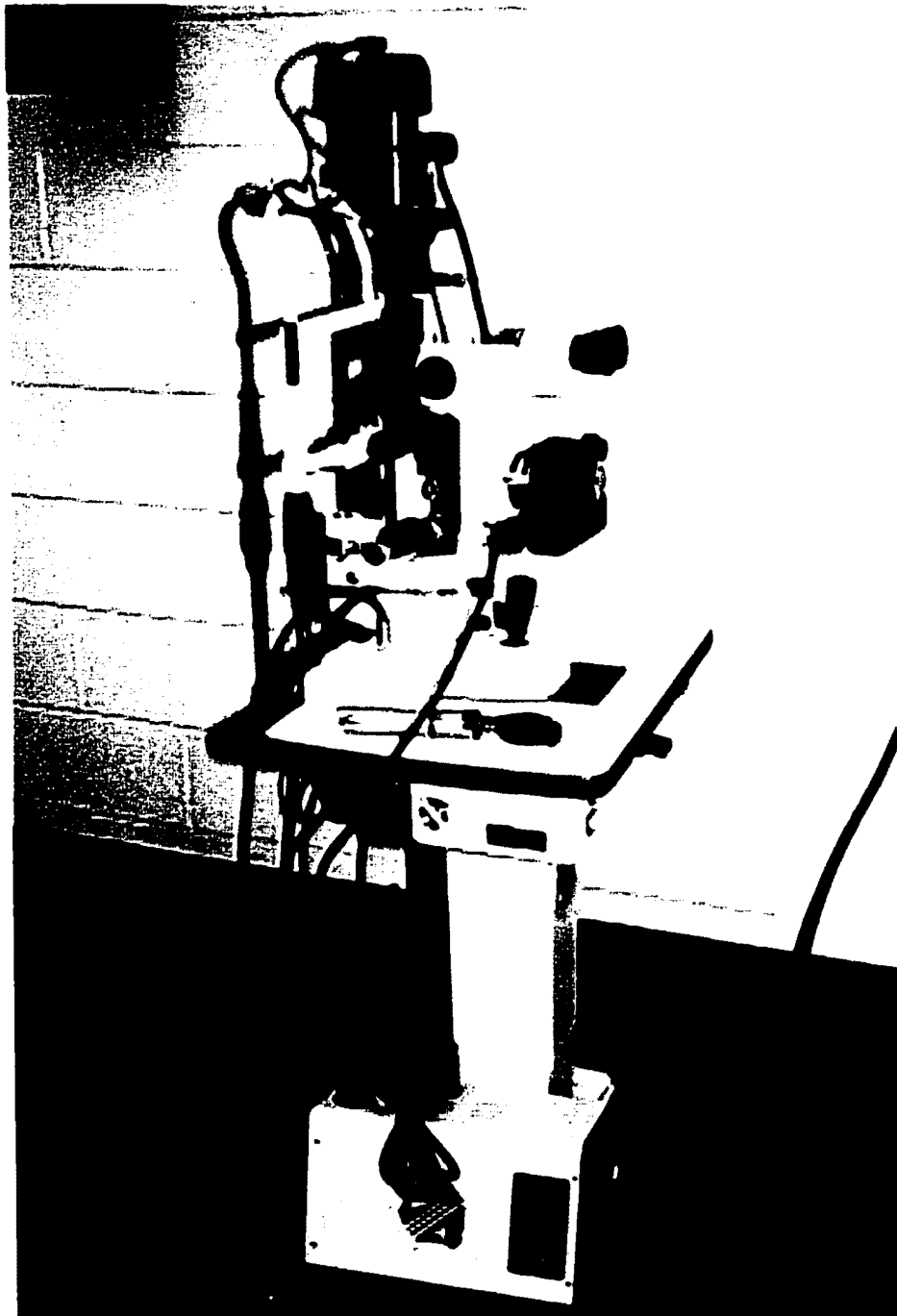


Figure 3.04 shows the body weights of sand rats # 144 (diabetic male) and # 167 (control male) over several months. Sand rat # 144 was clinically characterized as diabetic for 8 months duration. Both animals were 13 months of age at euthanasia. Arrow indicates diet change on 7/6/99.

**FIGURE 3.05**



**Figure 3.05 shows the Topcon slit-lamp (Model # SL-7E) used to photograph the sand rat eyes.**

Figures 3.06 – 3.19 show the open aperture views (3.06, 3.10, 3.13, 3.15, 3.17, 3.18) and the slit views (3.07, 3.08, 3.09, 3.11, 3.12, 3.14, 3.16, 3.19) of several sand rats. Control sand rat # 803 (3.06 – 3.09) views show a clear lens in the right eye (3.07, 3.08, 3.09) and also in the left (3.06). Views of age and sex matched diabetic # 805 (3.10- 3.12) shows cataract formation in the left eye within the first month of diabetes (3.10, 3.11) and the progression later at 2.5 months duration (3.12). At only 2 months duration of diabetes, 4.5 month-old female sand rat # 820 has a cataract in the left eye (3.13, 3.14), which shows only a mild progression three months later (3.15, 3.16). Views of a 7.5 month-old female sand rat # 158 with the first two months of diabetes (3.17) shows a “mushroom shaped cataract in the right eye and the progression of the cataract at 4.5 months of diabetic duration (3.18, 3.19).

FIGURES 3.06 THROUGH 3.09

3.06



3.07



3.08



3.09



FIGURES 3.10 THROUGH 3.12

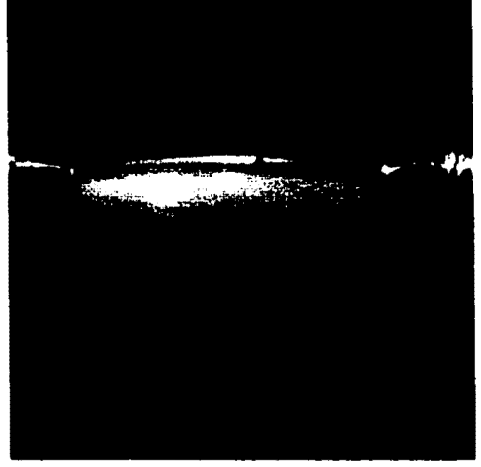
3.10



3.11



3.12



FIGURES 3.13 THROUGH 3.16

3.13



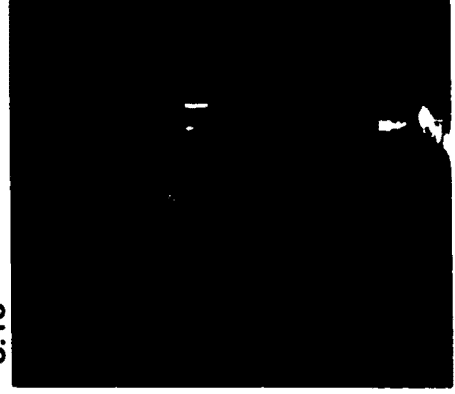
3.14



3.15

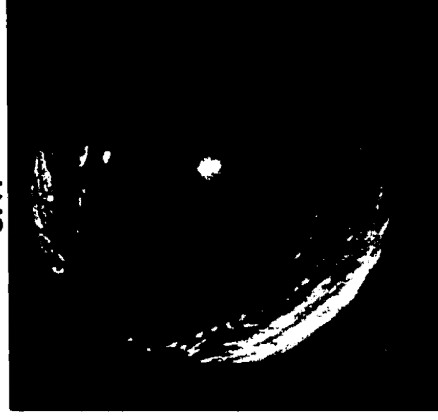


3.16



FIGURES 3.17 THROUGH 3.19

3.17



3.18



3.19

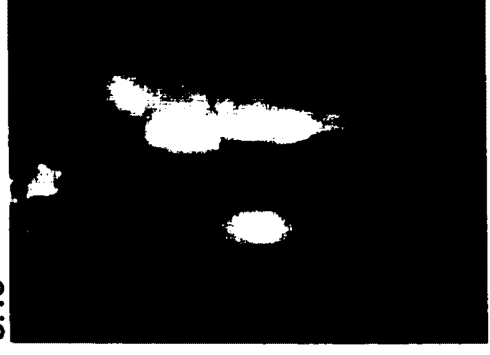


FIGURE 3.20

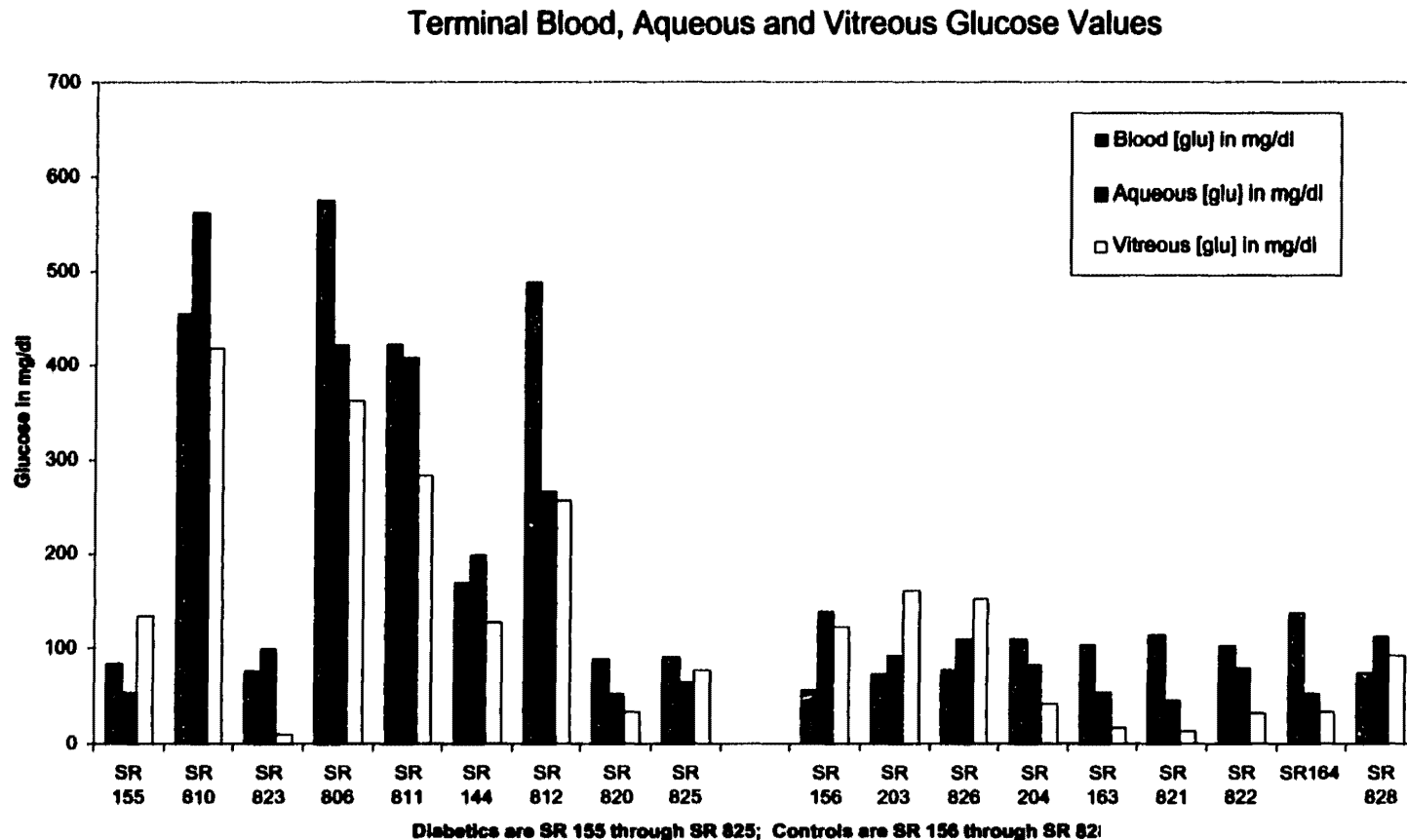
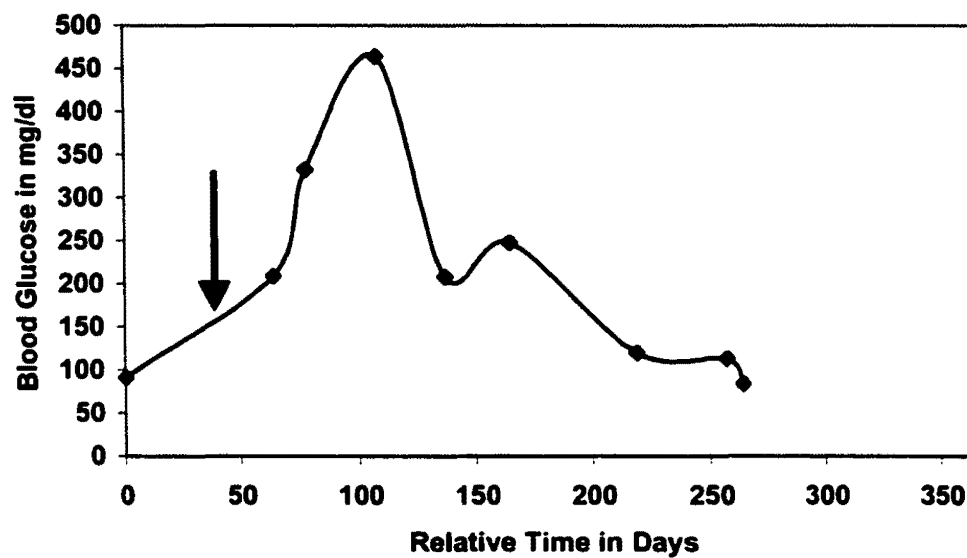


Figure 3.20 shows the blood glucose, aqueous glucose and vitreous glucose values for diabetic sand rats (# 155, 810, 823, 806, 811, 144, 820, 825) on the left of the graph and the blood glucose, aqueous glucose and vitreous glucose values for control sand rats (# 156, 203, 826, 204, 163, 821, 822, 164, 828) on the right side of the graph. All samples were collected at time of euthanasia.

FIGURES 3.21 AND 3.22

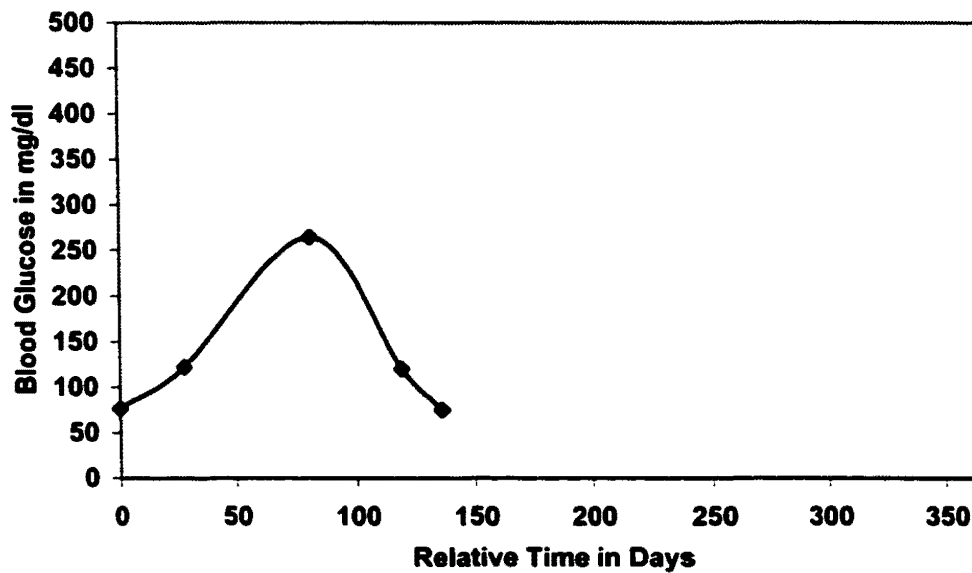
3.21

**Blood Glucose Concentration for SR # 155**



3.22

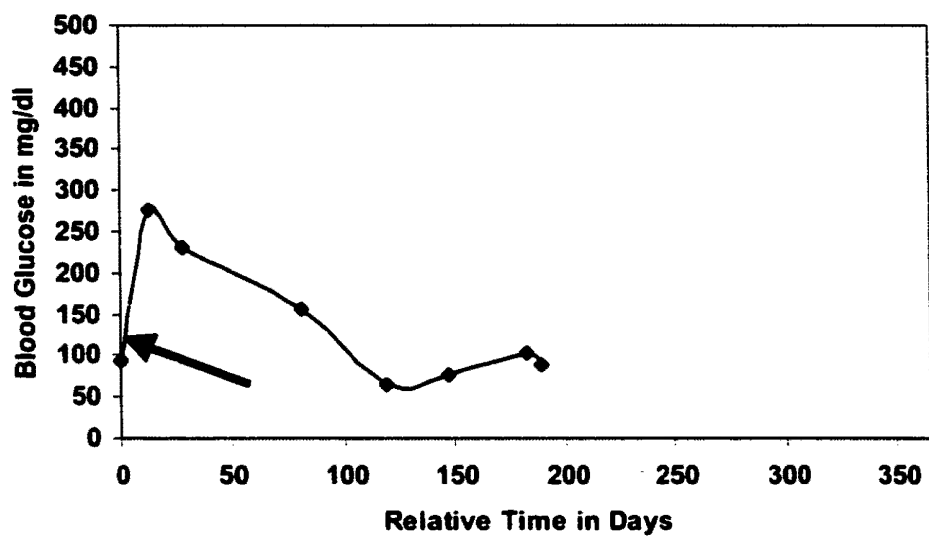
**Blood Glucose Concentration for SR # 823**



FIGURES 3.23 AND 3.24

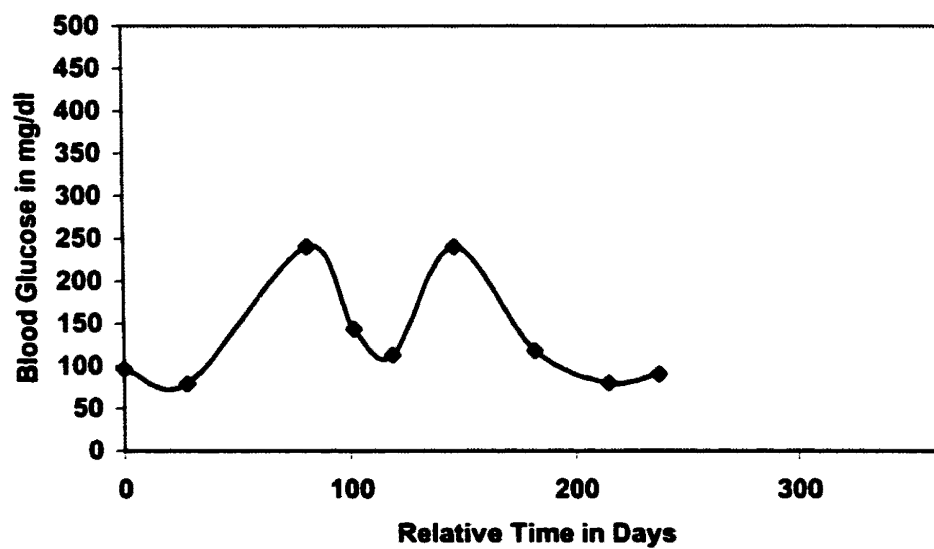
3.23

Blood Glucose Concentration for SR # 820



3.24

Blood Glucose Concentration for SR # 825

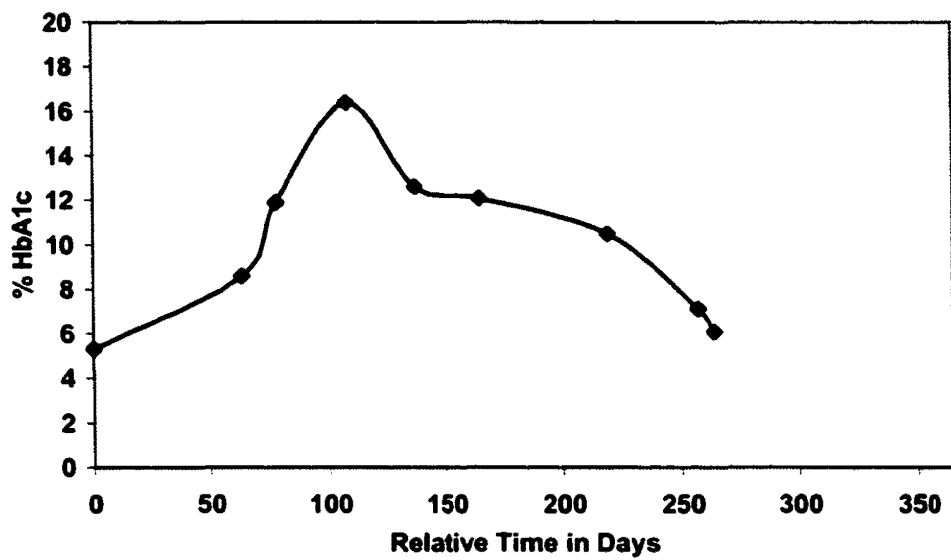


Figures 3.21 – 3.24 shows the blood glucose concentration of SR # 155, an 11 month-old male sand rat that was diabetic for 6 months (3.21); the blood glucose concentration of SR # 823, a 6 month-old sand rat that was diabetic for 2 months (3.22); the blood glucose concentration of SR # 820, a 7.5 month-old female sand rat that was diabetic for 6 months (3.23) and the blood glucose concentration of SR # 825, a 9.5 month-old female sand rat that was diabetic for 5 months (3.24). The arrow indicates the diet change. There is no arrow for sand rats # 823 and # 825 since these were sand rats that converted on normal sand rat chow.

FIGURES 3.25 AND 3.26

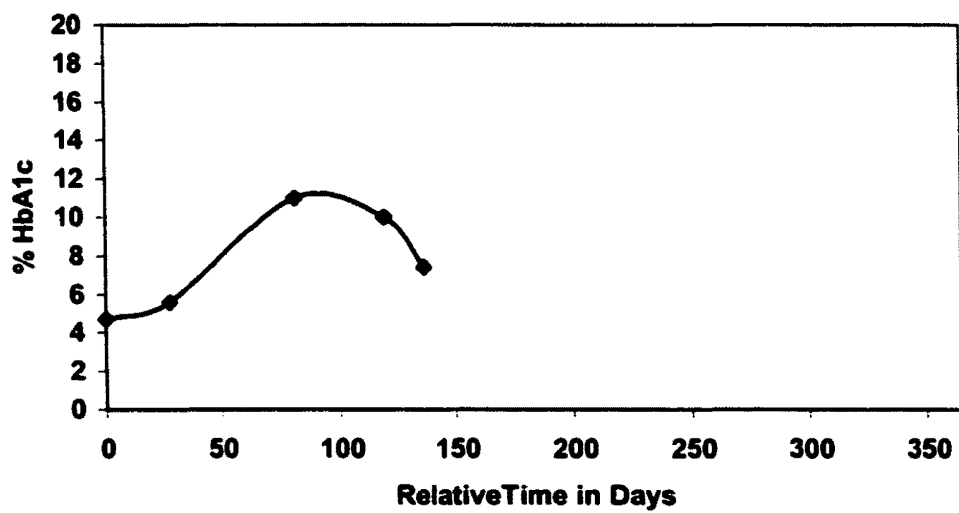
3.25

HbA1c for SR #155



3.26

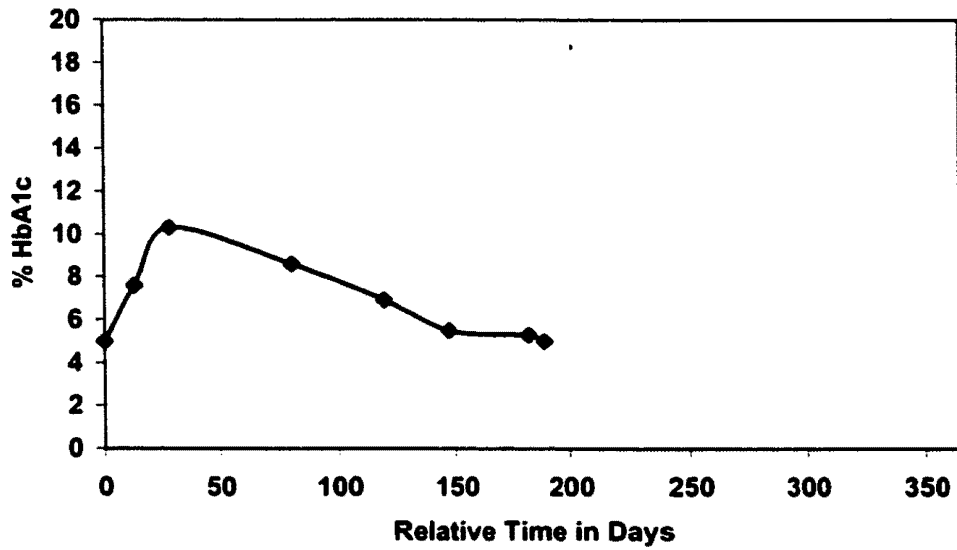
HbA1c for SR #823



FIGURES 3.27 AND 3.28

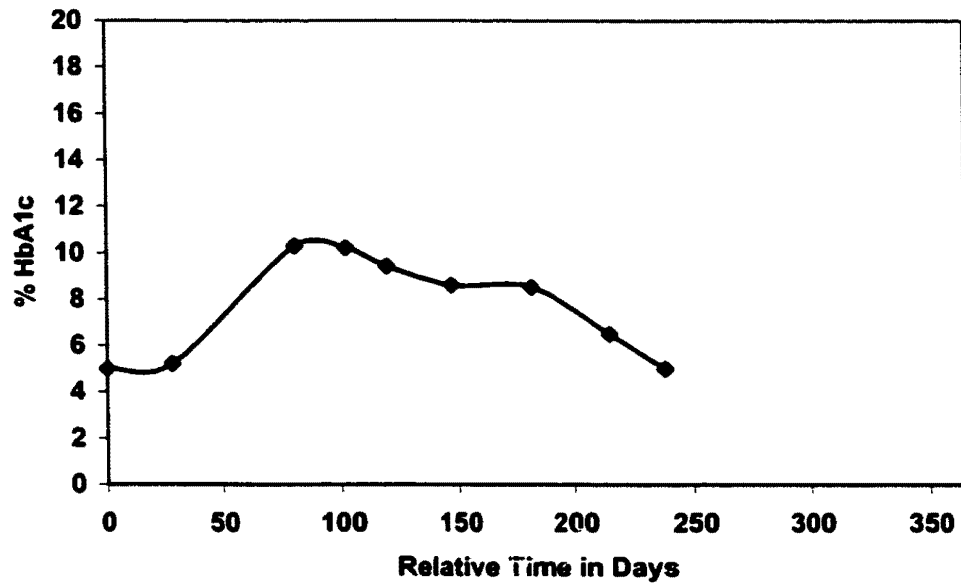
3.27

HbA1c for SR #820



3.28

HbA1c for SR #825



Figures 3.25 – 3.28 show the glycated hemoglobin concentration of an 11 month-old male sand rat that was diabetic for 6 months (3.25); the glycated hemoglobin concentration of a 6 month-old female sand rat that was diabetic for 2 months (3.26); the glycated hemoglobin concentration of a 7.5 month-old female sand rat that was diabetic for 6 months (3.27) and the glycated hemoglobin concentration of a 9.5 month-old female sand rat that was diabetic for 5 months (3.28).

FIGURE 3.29

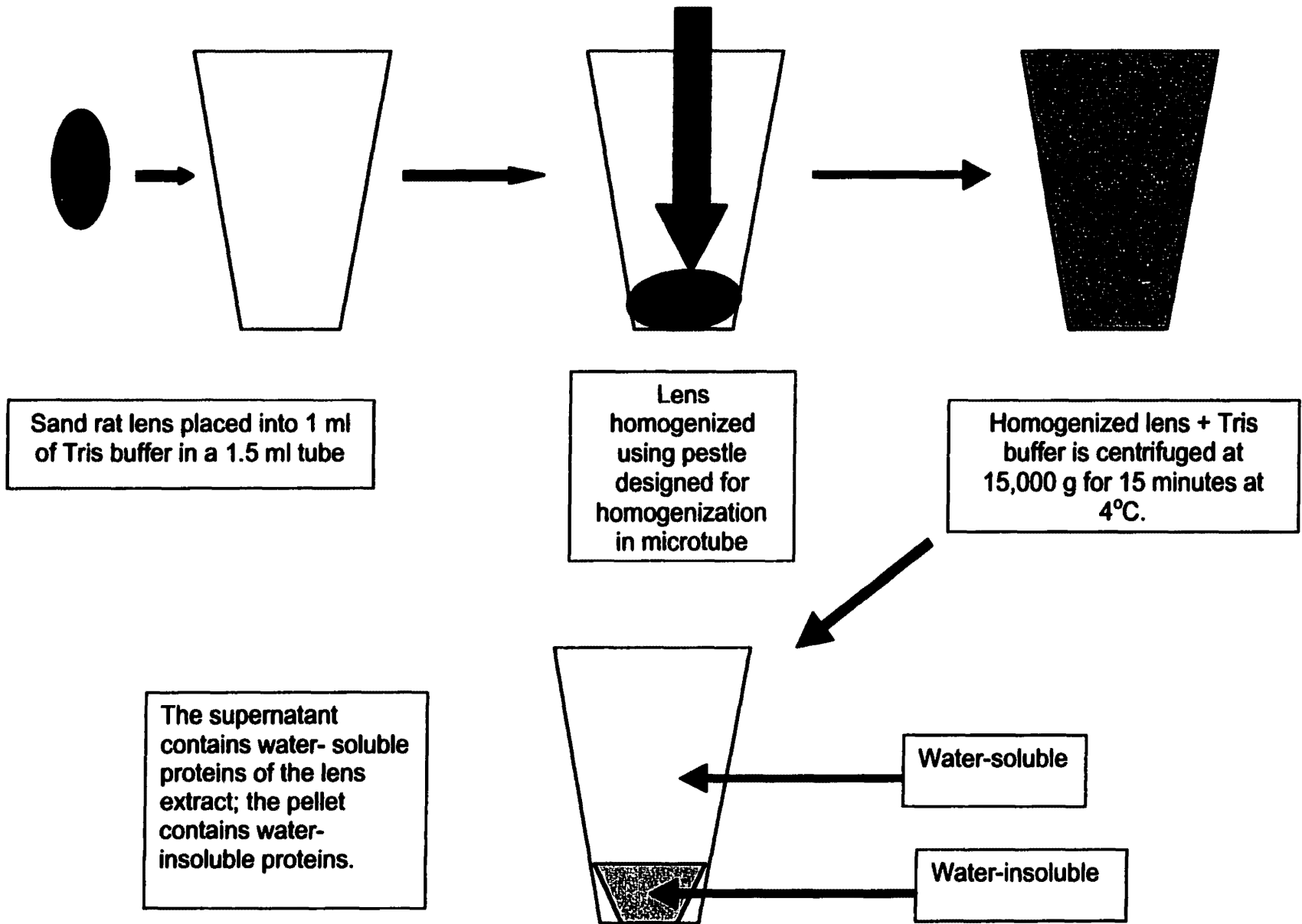


Figure 3.29 shows how the lens of the eye is homogenized and separated into a water-soluble fraction and a pellet (water-insoluble fraction).

FIGURE 3.30

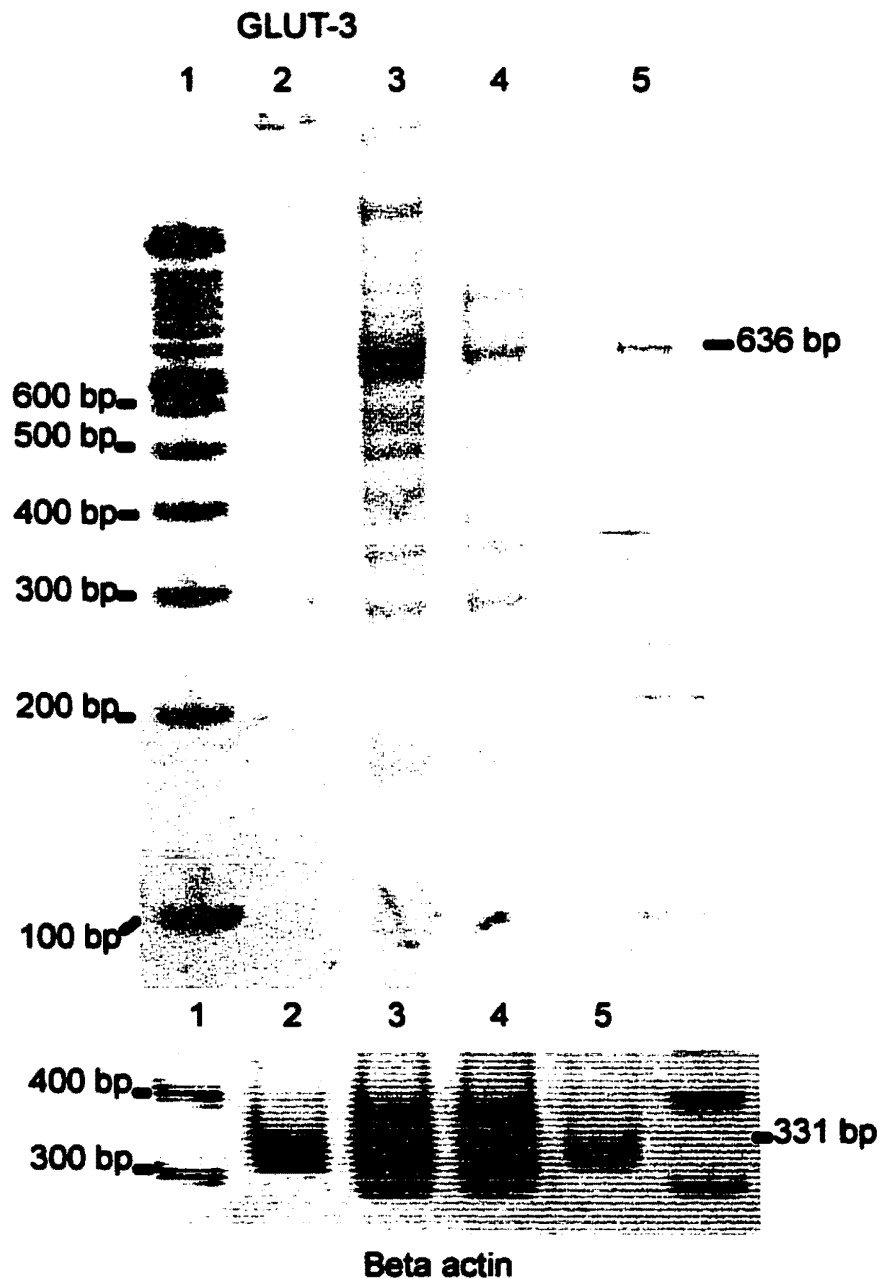


Figure 3.30 shows the detection of GLUT-3 isoform transcript. GLUT-3 transcript expression is at 636 bp for sand rat lens fiber cells (2), sand rat lens anterior epithelial cells (3), sand rat brain (4) and rat brain (5). A 100 base pair ladder is in lane 1.  $\beta$  actin transcript expression is at 331 bp for sand rat fiber cells (2), sand rat lens anterior epithelial cells (3), sand rat brain (4) and rat brain (5). A 100 base pair ladder is in lanes 1 and 5.

## CHAPTER 4

The Unique Lens Crystallin Pattern of the Fat Sand Rat (*Psammomys obesus*)

Submitted to *Experimental Eye Research* in May 2001.

### Abstract

**Purpose:** The purpose of this study was to identify the crystallin classes of the fat sand rat, a spontaneous model of Type 2 diabetes. The fat sand rat, *Psammomys obesus*, is a desert rodent in the subfamily, Gerbillinae. Obesity and subsequent diabetes occur in this animal upon feeding with a standard laboratory rodent chow. Diabetic cataracts occur within days of clinical diabetes.

**Materials and Methods:** Lens extracts from several control and diabetic sand rats and other species were prepared and centrifuged to remove particulate matter. The supernatants (water-soluble fraction) were collected and gel filtration chromatography was performed to separate the crystallin classes. Protein concentration was determined for each chromatography fraction. An equivalent amount of denatured protein from each fraction was then electrophoresed on TRIS-Glycine gels. The gels were stained with Invitrogen SimplyBlue™ SafeStain and de-stained for analysis of lens crystallins. Western blotting was used to determine crystallin classes. Verification of crystallin classes was obtained by mass spectrometry using the MALDI technique.

**Results:** The molecular weights of the chromatography fraction peaks from the control and diabetic sand rats were essentially the same, although the protein concentration was considerably lower in the diabetic fractions. On SDS-PAGE, in addition to the bands for the major crystallin classes, sand rats have three distinct bands at 51 kDa, 47 kDa and at 42 kDa. Western blots of gels containing these bands were negative for alpha, beta or gamma crystallins using antibodies to bovine alpha, beta and gamma crystallins. Mass spectrometry determined the bands to be a retinaldehyde dehydrogenase,  $\alpha$ -enolase and phosphoglycerate kinase, respectively. Western blots did confirm the presence of  $\alpha A^{\text{ins}}$  crystallin in the sand rat. Additionally SDS-PAGE of the diabetic animals revealed an increased banding pattern at 35 – 42 kDa and a banding shift from 22.5 to 23.5 kDa. Western blotting and mass spectrometry confirmed alpha A crystallin aggregates at 35 – 42 kDa and beta B 2/beta B3 crystallin banding shifts from 22.5 to 23.5 kDa.

**Discussion:** In conclusion, the normal sand rat has a crystallin pattern similar to a closely related gerbil with some unique differences. The presence of aldehyde dehydrogenase and glycolytic enzymes may be related to providing ultraviolet and heat shock protection for this diurnal desert animal. Additionally in the diabetic sand rats, there are  $\alpha A$  crystallin aggregates and  $\beta B2/\beta B3$  crystallin ratio shifts with cataracts. The cataractous changes seen in the sand rat lens are possibly indicative of post-translational modifications to the crystallins. This is the first report of characterization of the lens crystallins in the sand rat.

## Introduction

Crystallins are water-soluble proteins that make up approximately 80 – 90% of the proteins in the lens. In general, crystallins have polypeptide weights within the range of 20 to 35 kiloDaltons. There are two main classes of crystallins, the alpha and the beta-gamma crystallins (Albert and Jacobiec 1994). Alpha crystallins are large polymers made up of two subunits: alpha A and alpha B. The alpha crystallins are generally highly conserved among species (Hendricks et al. 1987) and they have been shown in numerous studies to be related to heat shock proteins and to function as molecular chaperones (Piatigorsky 1990), (Roquemore et al. 1992), (Rao et al. 1994), (Albert and Jacobiec 1994), (Raman et al. 1995), (Hook and Harding 1996), (Andley et al. 1998). Beta crystallins, the second major group, share a 30% peptide sequence identity with the gamma crystallins (Wistow et al. 1981). The beta crystallins are populations of aggregates divided into beta-high, beta-low 1 and beta-low 2. When separated using chromatofocusing, the beta-high, the beta-low 1 and the beta-low 2 populations are composed of beta subunits in different proportions (Bloemendal et al. 1990). Based on their protein sequence and x-ray crystallographic analysis, the beta crystallins are thought to be related to stress proteins (Wistow et al. 1988b). This is based on a similarity of the Beta crystallins to a protein superfamily containing Protein S, a component of the spore coat of *Myxococcus xanthus* and Spherulin 3a, a component of the cyst stage of the slime mold, *Physarum polycephalum* (Wistow 1990). The gamma crystallins, also of the beta-

gamma crystallin class, are synthesized mainly in embryogenesis and are found predominately in the nucleus of the lens. The gamma crystallins are small tightly packed protein monomers around 20 kiloDaltons in weight. The gammas are believed to be responsible for the lower refractive index of the nucleus of the lens (Slingsby and Miller 1983).

In addition to the alpha and beta-gamma crystallins, taxon-specific crystallins have been reported in numerous species. Taxon-specific crystallins have peptide molecular weights that range from 35 to 70 kiloDaltons. In general, most of these "species-specific" crystallins share structure and sometimes function with an enzyme. The first of these taxon-specific crystallins to be recognized is the delta crystallin of birds and reptiles. The delta crystallin shares structure and function with a urea cycle enzyme, argininosuccinate lyase (Nickerson et al. 1985), (Piatigorsky et al. 1988), (Barbosa et al. 1991), (Cvekl et al. 1995), (Li et al. 1997, Li et al. 1995). The discovery of species-specific crystallins within the lens lead to the theory of "Gene Sharing." This is the double use within the body of a distinct protein (Piatigorsky et al. 1988), (Piatigorsky 1998). This is accomplished by either one gene producing a product in more than one organ or by one gene being duplicated and then producing more than one product that is closely related. An example of gene sharing is seen with the zeta crystallin. Zeta is found in the lens of hystrichomorphs and camelids and has a peptide sequence similar to an alcohol dehydrogenase protein found in the liver (Borras et al. 1990), (Gonzalez et al. 1994a, Gonzalez et al. 1995, Gonzalez et al. 1994b),

(Richardson et al. 1995), (Rao et al. 1997), (Sharon-Friling et al. 1998). Another of the numerous examples is the epsilon crystallin of crocodiles and waterfowl, which shares structure and function with the enzyme lactate dehydrogenase (Wistow and Piatigorsky 1987). The Tau crystallin of lampreys, birds and aquatic turtles shares its structure and function with alpha-enolase, a glycolytic enzyme (Wistow et al. 1988a), (Kim et al. 1991), (Kim and Wistow 1993). The Eta crystallin makes up approximately 25% of the total lens proteins of elephant shrews. Eta crystallin shares a partial protein sequence and immunochemical reactivity with cytoplasmic aldehyde dehydrogenase (Wistow and Kim 1991). The lenses of Australian marsupials contain Mu crystallins. Mu is a mammalian homologue of *Agrobacterium* ornithine cyclodeaminase (Kim et al. 1992). Another enzyme crystallin is lambda, which is seen in rabbits and hares. Lambda is related by sequence to hydroxyacyl- and hydroxybutyryl-CoA dehydrogenases. The enzyme activity of lambda has not yet been determined (Mulders et al. 1988). This unusual expression of enzymes in the lens of some species has also been reported to occur in the corneal epithelium and is theorized to provide protection against ultra-violet light (Cooper et al. 1993), (Piatigorsky 1998).

*Psammomys obesus*, the Fat Sand Rat, or simply the “sand rat” is a *Cricetidae* rodent from the subfamily *Gerbillinae*. This desert gerbil originates from the Northern African Desert region. Type 2 diabetes is easily induced nutritionally by placing the animals on a high-energy, low fiber diet such as a standard rodent

chow (Kalman et al. 1996). This diet change results in hyperinsulinemia, hyperglycemia, hyperlipidemia and obesity as early as 11 – 14 days after starting the high-energy diet (Adler et al. 1990). Aside from the biochemical changes that have been reported, a common ocular change seen in the sand rat is cataracts (Hackel et al. 1965), (Shafrir and Renold 1984), (Marquie et al. 1991). Once placed on a diabetogenic rodent chow, bilateral cataracts are produced in this spontaneous animal model within one month of the diet change. This rapid and reasonably consistent manifestation of diabetes makes this model an excellent choice for the study of mechanisms of the development of diabetic cataracts. To date, there are no published reports in the literature characterizing the normal crystallin pattern of the lens of this species. The purpose of this study was to identify the major crystallin classes of the sand rat and determine if the lens of this diurnal desert rodent contains any species-specific crystallins.

## **Materials and Methods**

**Animals:** Control and diabetic sand rats were studied. These sand rats were obtained from the Uniformed Services University of the Health Sciences (USUHS) sand rat breeding colony. The animals were housed at the USUHS central animal facility, which is fully accredited by the Association for the Assessment and Accreditation of Laboratory Animal Care, International (AAALAC). All animals were handled in accordance with procedures approved by the USUHS Institutional Animal Care and Use Committee (IACUC). The animals on study were divided initially into 2 groups, controls and diabetics. The

control sand rats were fed a specially formulated Sand Rat Chow (Purina Sand Rat Diet 5L09, Ralston Purina, Richmond, IN) and the diabetic group was fed a standard rodent chow (certified Purina Rodent Diet 5002, Purina Mills, St. Louis, MO).

**Determination of the Diabetic State:** Diabetes was determined as described by DiCarlo, et al (manuscript in preparation) (DiCarlo et al. 2001). All sand rats on study were photographed using the slit-lamp biomicroscope. This was performed to assure that control animals did not have any clinically apparent ocular abnormalities prior to assignment in this study and to follow the course of the diabetic cataracts.

**Sample Collection:** Serial blood samples were collected from the sand rats using isoflurane anesthesia. The sand rats were masked down and blood was collected from the orbital sinus using a sterile Pasteur pipette. No greater than 70  $\mu$ l was collected from the animals during each of the serial bleeds. For the slit-lamp exams and photographs (Topcon Model #SL-7E, Topcon American Corporation, Paramus, NJ), the sand rats were sedated using 20 – 40 milligrams/kilogram (mg/kg) ketamine HCl and 2-5 mg/kg xylazine administered by intraperitoneal (IP) injection. One to two drops of tropicamide was administered, as needed, to each eye for dilation during examination. All other tissue and fluid collection was performed at the time of euthanasia. The sand rats were anesthetized using 40 mg/kg ketamine HCl and 5 mg/kg xylazine

administered by intraperitoneal (IP) injection. For maximal blood sampling, cardiac puncture was performed under anesthesia and the sand rats were then placed into a carbon dioxide chamber for euthanasia. A thoracotomy was performed and cardiac tissue removed ensuring death. After globe enucleation, a circumferential limbal incision was made to remove the lens. The lenses of the sand rats were convex in shape and had a firm zonular attachment. The lenses were placed in 1 ml of Tris-buffer (0.05 M Tris-Cl, 5mM 2-mercaptoethanol, pH =7) and frozen at – 20°C until analyzed (Borst and McDevitt 1987). Lenses from other animal species were obtained through IACUC approved tissue-sharing protocols. All of these lenses were handled and stored using the same methods and solutions for the sand rats.

**Preparation of Lens extracts:** The lenses were homogenized in 1 ml of Tris-buffer and centrifuged at 15,000 g for 15 minutes at 4°C. The water-soluble fraction was collected and is referred to as the lens extract. Protein values for the water-soluble lens extract were determined using a protein assay (BioRad, Hercules, CA) based on the Bradford dye-binding procedure (Bradford 1976). This is a quantitative test using a colorimetric response for protein level at a maximum absorption of 595 nm. The water-soluble lens extracts were then stored at – 20°C.

**Gel Filtration Chromatography:** Filtration chromatography was performed using a Sephacryl S-300 high resolution gel filtration column (Amersham Pharmacia

Biotech, Piscataway, NJ) on a Biologic Chromatography System (BioRad, Hercules, CA). Elution profiles were performed using high and low molecular weight standards (Amersham Pharmacia Biotech, Piscataway, NJ) and a calibration curve was developed for the column. Combined lens extract samples from control or diabetic sand rats were run through the column using an elution buffer (0.05M Tris-Cl, 0.1M KCl, 5 mM 2-Mercaptoethanol, 1 mM EDTA). Salts from the elution buffer were removed from fraction peaks by dialysis cassettes (Pierce, Rockford, IL). Protein values for the water-soluble lens extract fractions were determined using a protein assay (BioRad, Hercules, CA) based on the Bradford dye-binding procedure (Bradford 1976). Samples of low protein concentration were concentrated using Slide-A-Lyzer cassettes and concentrating solution (Pierce, Rockford, IL).

**SDS-PAGE and Western Blots:** The whole water-soluble lens extract and lens chromatography fractions were analyzed by electrophoresis on 14 - 16% Tris-Glycine gels (Invitrogen Corporation, Carlsbad, CA), in accordance with techniques described by Sambrook et al (Sambrook et al. 1989). For SDS-PAGE, the gels were stained with Coomassie Simply Blue SafeStain (Invitrogen Corporation, Carlsbad, CA) and destained for analysis of lens crystallins. Protein transfer to a nitrocellulose membrane was performed using the technique of Towbin (Towbin et al. 1979) and accomplished using the XCell Surelock Mini-Cell Blot Module (Invitrogen Corporation, Carlsbad, CA). The nitrocellulose membranes were incubated with rabbit anti-bovine crystallin antibodies to alpha,

beta and gamma crystallins (supplied by Dr. Zigler's laboratory at NEI).

Secondary antibody incubation was performed using goat anti-rabbit antibody labeled with peroxidase (Kirkegaard & Perry Laboratories, Inc., Gaithersburg, MD). The nitrocellulose membranes were then stained using the 4 CN Membrane Peroxidase Substrate System (Kirkegaard & Perry Laboratories, Inc., Gaithersburg, MD).

**Mass Spectrometry:** Crystallins were separated on one-dimensional Tris-Glycine gels (Invitrogen Corporation, Carlsbad, CA). Mass spectrometry was performed essentially as described by Colvis, et al (Colvis et al. 2000). A brief description of the technique is as follows. The individual bands from the Tris-Glycine gels were cut out using a #11 scalpel blade and destained until clear. The gel bands were dehydrated and rehydrated with trypsin to break lysine and arginine bonds. The extracted peptides were spotted onto a stainless steel plate and analyzed using the Matrix-Assisted Laser Desorption/Ionization (MALDI) technique (Johnstone and Rose 1996, Siuzdak 1996). MALDI was performed using a PE Biosystems Voyager DE STR (Framingham, MA) using the GRAMS/386 software package. A 337 nm wavelength laser is pulsed at the MALDI matrix spotted with the crystallin peptide sample. The matrix absorbs the laser light and vaporizes, carrying gaseous sample with it. The vaporized matrix ionizes sample molecules and the charge enables electrostatic lenses to direct the charged molecules into the mass analyzer. Time-of-flight analysis separates the ions based on their mass to charge ratio. The data is then entered into a University of California at San

Francisco website ([pospector.ucsf.edu](http://pospector.ucsf.edu)). This software program returns protein matches based on the input of mass-to-charge ratio and taxonomical information.

## Results

**Results of Gel Filtration Chromatography:** Seven major peaks were found on using gel filtration chromatography. Figures 4.01 and 4.02 (pages 115 and 116) show the results of gel filtration chromatography for control (4.01) and diabetic sand rats (4.02), both with a mean age of 11 months. The molecular weights of the fraction peaks are listed. Seven peaks are clearly seen for the control sand rats (4.01). Diabetic samples yielded only 5 clearly discernible peaks (4.02). The diabetic chromatogram (4.02) was on a much lower scale due to the lower protein concentration of the diabetic sample. The water-soluble protein concentration of the control sample was 50 mg/ml and of the diabetic sample was 7 mg/ml. There was not enough water-soluble sample to load an equivalent protein concentration of the diabetic samples.

**Results of SDS-PAGE and Western Blots:** Chromatography fractions 1 – 5 from a control sand rat run on a SDS-PAGE gel are seen in Figure 4.03 (page 117). The corresponding western blot for alpha crystallins is shown in Figure 4.04 (page 117). Alpha crystallins eluted off the column within the first two chromatography peaks (4.04). There are three main bands seen for the alpha crystallins between the weights of 20 kDa to 25 kDa and an additional band is seen at around 45 kDa. Figure 4.05 (page 118) shows control sand rat

chromatography fractions from peaks 1- 6 run on a SDS-PAGE gel. The corresponding western blot for beta crystallins is seen in Figure 4.06 (page 118). Beta crystallins eluted off the column in fraction peaks 1 - 6 (4.06). Approximately 10 bands are seen for the beta crystallins between the weights of 20 kDa and 35 kDa and an additional small group of 4 bands are seen at 45 – 50 kDa. Chromatography fractions 2 -7 from a control sand rat run on a SDS-PAGE gel is seen in Figure 4.07 (page119). The western blot for gamma crystallins in Figure 4.08 (page 119) shows that gamma crystallins eluted off in all fractions but fraction number 4 with the majority of gamma crystallins found in the 7<sup>th</sup> peak. The gammas appeared as one large band from 20 kDa to 22 kDa. Whole water-soluble lens extracts run on a SDS-PAGE gel for several species are seen in Figure 4.09 (page 120). A western blot of this gel for alpha crystallins is seen in Figure 4.10 (page 120). Three to four main bands are seen for most of the animals between 20 kDa to 25 kDa. A prominent band at 25 kDa is only in the mouse, gerbil and sand rat. The guinea pig has a band at a slightly higher weight, about 26 kDa. Most of the species had 1 – 2 bands at around 44 – 45 kDa.

Results of Mass Spectrometry by MALDI technique: Figures 4.11 and 4.12 (pages 123 and 124) show the results of the protein identification by MALDI. Chromatography fraction peaks 1 – 7 were run on a SDS-PAGE gel (4.11). Band identification is listed in Table 4.01 (page 113). An aldehyde dehydrogenase (retinal dehydrogenase) and glycolytic enzymes were identified along with the

major alpha and beta-gamma crystallin classes. Control and diabetic whole water-soluble lens extracts were run on a SDS-PAGE gel (4.12). The corresponding protein identification is seen in Table 4.02 (page 114). Bands 1 and 2 (4.12) were identified as the same beta crystallins in the control and diabetic sand rats (lanes 1 and 5) even though staining patterns are different. Bands 3 – 5 (lane 8) were all identified as alpha A crystallins (4.12).

## Discussion

Gel filtration chromatography for the diabetic and control runs yielded peaks for the water-soluble lens extracts with similar molecular weights. The native protein chromatography separated the water-soluble fraction of the lens extract into different crystallin fractions. There is a sharp difference in the ratio of the amplitude of the first two peaks between the control and diabetic animals. Since the animals are age-matched, this cannot be accounted for as an age-related  $\alpha B$  to  $\alpha A$  ratio shift as is seen in humans (Ma et al. 1998). A similar shift in the ratio of the amplitude of the first two peaks was also seen in chromatography of aged control animals when subjectively compared to the younger controls (data not shown). In that case, aging changes such as an  $\alpha B$  to  $\alpha A$  ratio shift may be responsible. Due to the lower protein concentration of the diabetic sample, the chromatogram was on a much lower scale and did not present all seven peaks clearly seen in the control chromatogram. The chromatography fractions obtained were further characterized by SDS-PAGE and subsequent western blots for major crystallin class identification.

crystallin dimers since they are two times the weight and they reacted to antibody specific for beta crystallins.

Gamma crystallins generally have a native molecular weight in the 20,000 Dalton range. In the sand rat they appeared in all but one of the fractions. Gamma crystallins may be eluting off the column non-specifically because gamma crystallins were found in several fractions. This was seen for all runs including the first run through the column. This suggests that the gamma crystallins, specifically gamma S crystallins due to the slightly higher molecular weight of 21 - 22 kDa, were complexing with larger crystallins as they moved through the column. As expected, the majority of the gammas eluted off the column in the sixth and seventh peaks from around 23 kDa down to 11kDa.

Along with the chromatography fractions, whole water-soluble lens extracts were also run on SDS-PAGE and used for comparison to related animal species. This was performed to specifically identify alpha insert crystallin in the sand rat. Alpha insert is an elongated alpha A-like crystallin subunit, which has a higher molecular weight than the alpha A and alpha B subunit (Cohen et al. 1978). It has been reported in some rodents, like the rat (Cohen et al. 1978), and the mouse (King and Piatigorsky 1983). The main bands seen from 20 to 25 kDa in the sand rat are alpha A, alpha B and alpha A insert, respectively based on their molecular weights and their reactivity to the antibody for alpha crystallins. This 25 kDa weight band was seen in the mouse, the gerbil and the sand rat. Alpha A

insert was not seen in this rat lens sample, which is unusual, and this may be due to a low protein concentration of the sample. The guinea pig had a slightly higher molecular weight band than the alpha insert, which was not expected in this rodent (De Jong et al. 1980). The chinchilla, which is from the same suborder of rodents as the guinea pig, did not have a band at this molecular weight. The rabbit, which is from a different order than the rodents, also did not have the alpha A insert as has been previously described (De Jong et al. 1980). The additional bands seen at 44 – 45 kDa represent dimerization of the alpha crystallins. This pattern was seen in all of the lanes except for the rat species.

Whole water-soluble lens extracts run on SDS-PAGE gels revealed a unique pattern for the sand rat. The pattern was similar to a closely related gerbil species, *Meriones unguiculatus*, but had a significant banding pattern at 42,000, 47,000 and 51,000 Dalton. Western blots for alpha, beta and gamma crystallins were unable to identify the three bands as belonging to a major crystallin class. Western blots for alpha crystallins did confirm the presence of the alpha A<sup>ins</sup> crystallin in the sand rat. Alpha A insert, which is identical to alpha A crystallin except for an insertion of 23 amino acids, is commonly seen in rodents of the Myomorpha suborder (King and Piatigorsky 1983) but this is the first report confirming its presence in the sand rat. These additional non-crystallin proteins and specific crystallin isoforms were then specifically identified using mass spectrometry.

Mass spectrometry by the MALDI technique not only confirmed the major crystallin classes identified by western blot technique but also specifically identified the crystallin isoforms. This was of particular interest in the diabetic animals where a consistent shift in the beta B2 to beta B3 ratios occurs regardless of duration of diabetes. Since the diabetic and control animals were age-matched, the change cannot be accounted for by a simple loss of beta B3 due to age, as seen in humans (Ma et al. 1998). It is difficult to tell which beta crystallin is lost to aggregation since the mass spectrometry technique is not quantitative but it is noteworthy that it occurs early in diabetic cataract formation and continues throughout the duration. Extensive Alpha A crystallin dimerization was seen in some diabetic sand rats (5 total) that were diabetic from 4 – 6 months duration. Mass spectrometry identified these bands as alpha A crystallins, which would generally be 20 kDa in weight. If these crystallin subunits dimerized they would appear where they are seen at around 40 kDa. Alpha crystallins associate with the lens fiber cell membranes and the association increases with the aging of the lens (Takemoto and Boyle 1998). Alpha A crystallin subunits are present in high molecular weight aggregates of senile human and bovine lenses (Takemoto et al. 1988), (Takemoto 1999). In the diabetic sand rats, once the alpha crystallins continue aggregating during cataracts, the proteins are probably becoming insoluble due to association with the membranes and segregating off into the pellet fraction. This may explain why extensive alpha A crystallin dimerization was not seen in our diabetic animals of greater than 6 months of duration (2 total).

In addition, the MALDI technique identified 3 enzymes of significant enough concentration that bands on SDS-PAGE gels were consistently seen in all animals, control and diabetic. Wistow reported that moderately abundant non-crystallin proteins might be seen in some mammalian species in quantities up to 1% of the total protein concentration without being considered a taxon-specific crystallin (Wistow and Kim 1991). A band at 51 kDa was identified as retinal dehydrogenase. Retinal dehydrogenase, a cytosolic aldehyde dehydrogenase, is an enzyme that is specifically involved with the biosynthesis of 9-cis and all-trans retinal to retinoic acids (Labrecque et al. 1995). In some species, like the elephant shrew, aldehyde dehydrogenase functions to replace gamma crystallins and provide a softer lens for accommodation (Lee et al. 1993). It has previously been theorized that aldehyde dehydrogenase in the lens may play a role to bind dinucleotide cofactors thus serving as an energy reserve or have reducing potential or even serve as ultraviolet filters for the eye (Wistow and Piatigorsky 1987). The theories of retinal dehydrogenase providing a softer lens and aldehyde dehydrogenase providing ultraviolet protection justify the presence of this enzyme at a higher concentration in the lens of the diurnal desert rodent.

The other two bands of high molecular weight, 47 kDa and 42 kDa, are glycolytic enzymes,  $\alpha$ -enolase and phosphoglycerate kinase, respectively. Glycolytic enzymes are present in lenses of many animals but usually do not appear in concentrations similar to crystallin protein concentrations.  $\alpha$ -enolase was

reported as a novel crystallin in several reptiles, birds and the lamprey (Stapel and De Jong 1983). Based on sequence information, this 48,000 Dalton protein is theorized to play a role as a heat shock protein (Iida and Yahara 1984). In mammals,  $\alpha$ -enolase is an abundant enzyme but generally does not exceed 0.1% of the total lens protein (Wistow and Kim 1991). Wistow suggests that recruitment of taxon-specific enzyme crystallins may occur in response to an animal migrating to a brighter light environment (Wistow 1995). These enzyme bands were consistently seen on SDS-PAGE in all of the sand rat lenses studied, but were not present in a closely related gerbil from the same subfamily, *Meriones unguiculatus*. Based on this, it is entirely possible that the sand rat lens has evolved to recruit enzymes such as retinal dehydrogenase and  $\alpha$ -enolase to protect the eye against the glare and heat of its native desert environment. In conclusion, the unique crystallin composition of the normal sand rat lens has now been identified, so that in the future, the changes to the crystallins from diabetic cataractous lenses may be elucidated.

#### Acknowledgments

We would like to thank Dr. Robert Horowitz, NIAMS, NIH for the generous use of his chromatography unit and Ms. Amy Herrera for her technical expertise on the use of the equipment. We thank Dr. Paul Russell, NEI, NIH for consultation on the western blotting techniques. We also thank Dr. William P. Roach, Uniformed Services University of the Health Sciences (USUHS), Department of Preventive Medicine and Biometrics, for the use of his slit-lamp camera and Dr. Steven Dalal and Ms. Carol Puligiese of the USUHS, Department of Laboratory Animal

Medicine for their clinical expertise and animal care, respectively. We also appreciate the sharing of animal tissues from Drs. Helke, Shea-Donohue, Cross, Roach and Maurelli at USUHS along with Dr. Shannon Stutler at the Air Force Research Laboratory, Wright-Patterson AFB, OH. This research was supported by the Uniformed Services University grant # T070IQ, National Institutes of Health, National Eye Institute (NEI) grant # EY11726 and the National Aeronautical Space Administration (NASA) grant # G276GT.

TABLE 4.01

Band #	Column #	Primary protein	GenBank Accession #	MW in kDa
1	1	Aldehyde dehydrogenase Eta crystallin	1706392 P51647	51.0
2	5	$\alpha$ enolase-Tau crystallin	P04764	47.0
3	5	Phosphoglycerate kinase	P09411	42.0
	5	Actin	P02570	42.0
4	1	$\beta$ B2	P43320	25.0
	1	60S ribosomal protein	P18124	25.0
5	1	$\beta$ A3	117403 P11843	22.5
	1	$\alpha$ A	P24623	22.5
	1	$\beta$ A2	117409	22.5
6	1	$\alpha$ B	P23928	21.0
7	1	$\alpha$ A	P24623	18.0
8	1	$\alpha$ A	P24623	17.0
9	5	$\beta$ B2	P43320	24.5
	5	$\beta$ A1	P14881	24.5
10	5	$\beta$ A3	P05813	22.0
	5	$\beta$ B2	P26775	22.0
11	6	$\gamma_s$		21.0
12	7	$\gamma$ C	117465	20.0
	7	$\gamma$	71511	20.0
13	6	$\gamma_s$		16.0
14	6			13.5
15	6			11.0
16	3	$\beta$ B1	1628435	27.5
17	3	$\beta$ B1	5326792	26.5
	3	$\beta$ B3	9789594	26.5
18	3	$\beta$ B3	9789594	25.5
	3	$\beta$ B1	9739217	25.5

Table 4.01 shows the MALDI Protein Band Identification for Figure 4.11 (page 123).

**TABLE 4.02**

<b>Band #</b>	<b>Column #</b>	<b>Protein</b>	<b>GenBank Accession #</b>	<b>Molecular Weights in kilo Daltons</b>
1	1	$\beta$ B2	P43320	23.5
1	5	$\beta$ B2	P43320	23.5
2	1	$\beta$ B2	P43320	22.5
2	1	$\beta$ B3	P02524	22.5
2	5	$\beta$ B2	P43320	22.5
2	5	$\beta$ B3	P02524	22.5
3	8	$\alpha$ A	P24623	42.0
4	8	$\alpha$ A	P24623	38.0
5	8	$\alpha$ A	P24623	35.0

Table 4.02 shows the MALDI Protein Band Identification for Figure 4.12 (page 124).

**FIGURE 4.01**

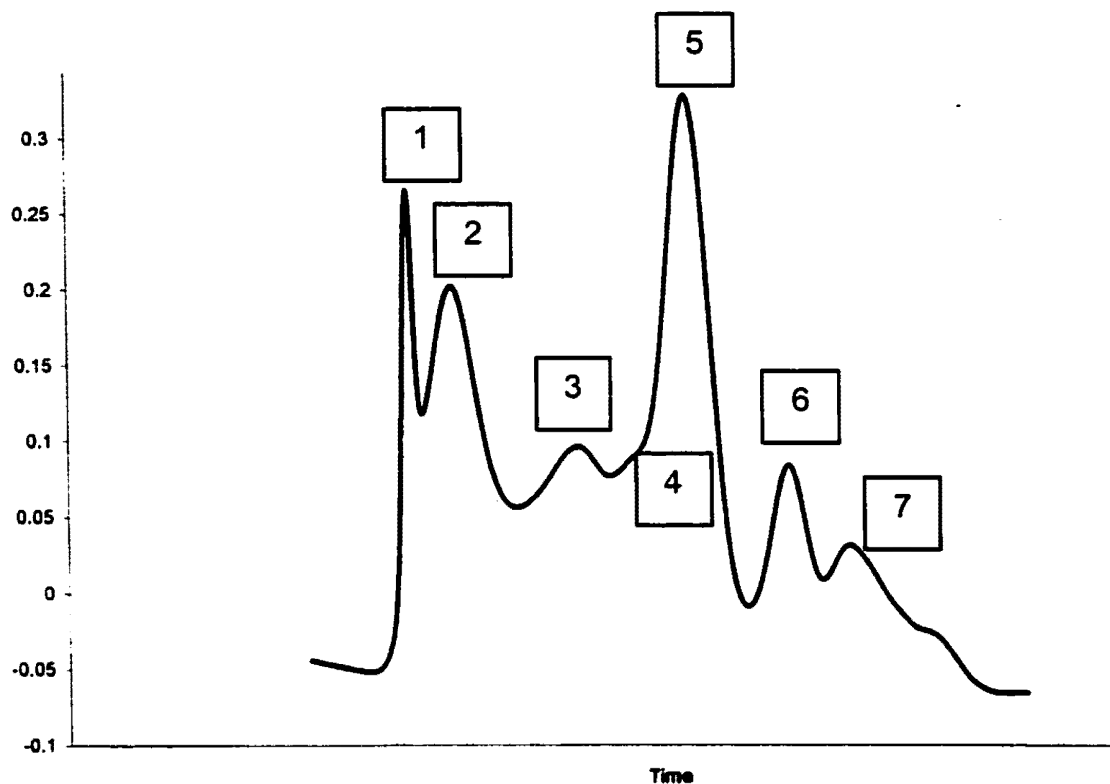


Figure 4.01 shows the separation of major water-soluble lens proteins by gel filtration chromatography for control sand rats. Seven major peaks are seen with the following calculated molecular weights in Daltons; >300,000 (1); 250,000 (2); 96,000 (3); 64,000 (4); 42,000 (5); 21,000 (6) and 13,000 (7).

**FIGURE 4.02**

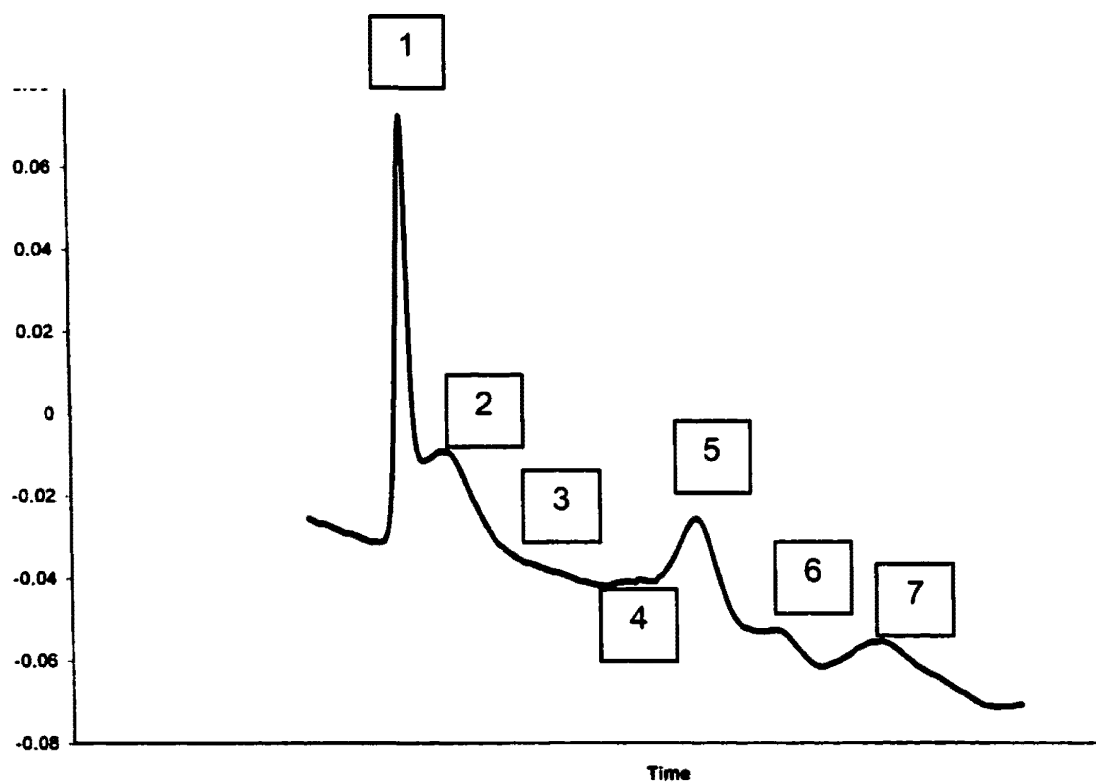
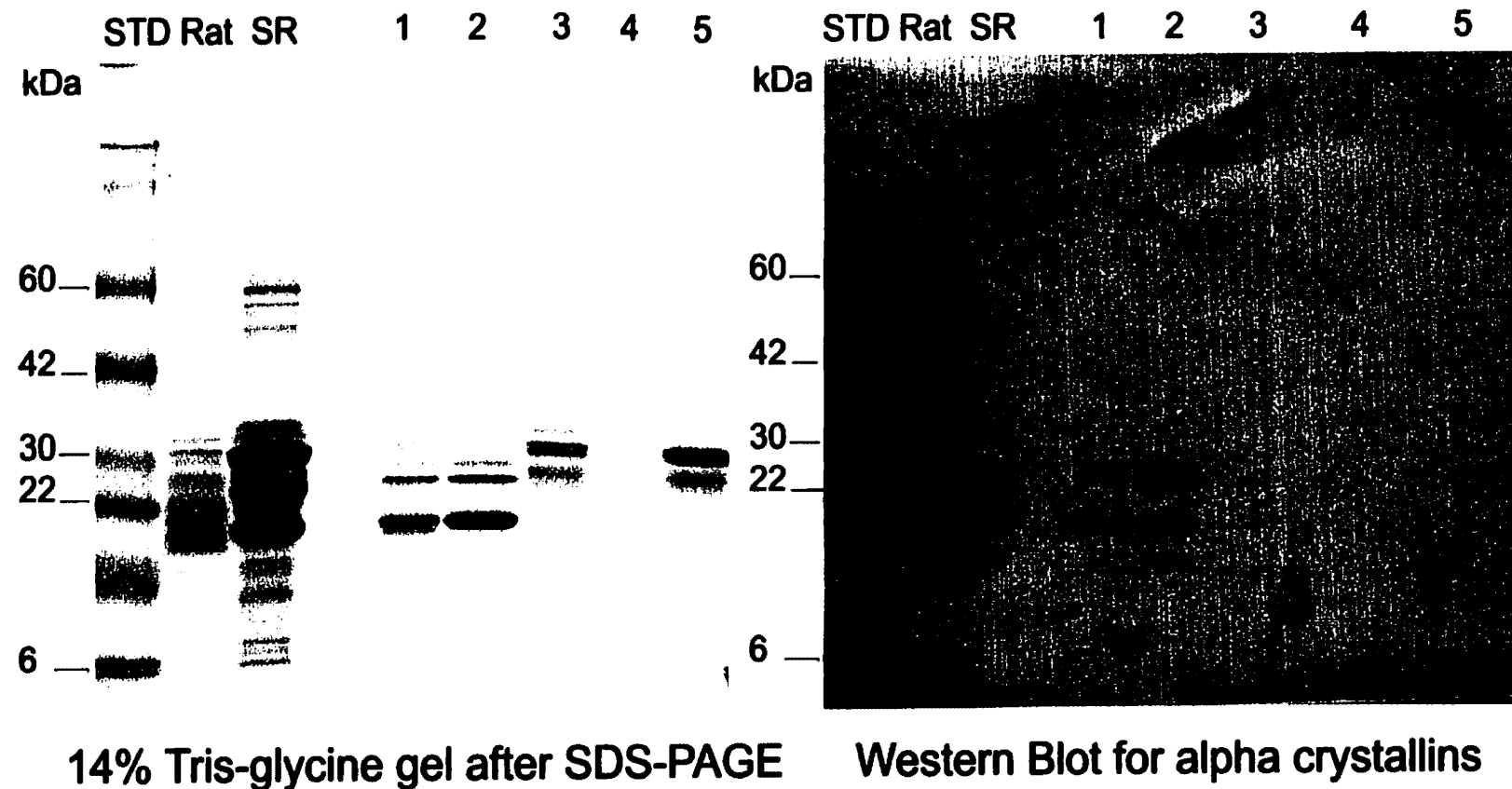
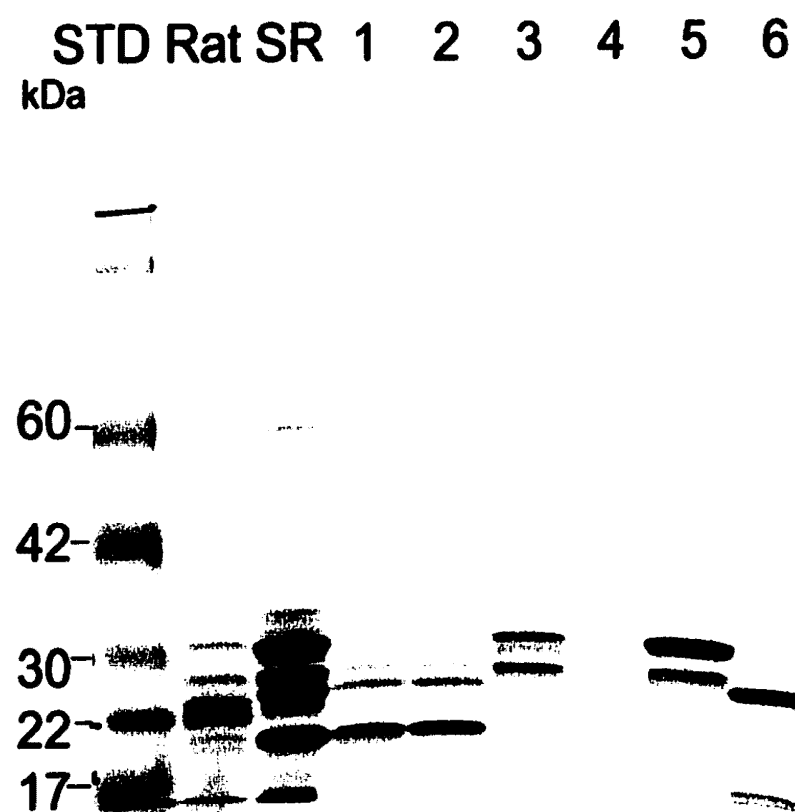


Figure 4.02 shows the separation of major water-soluble lens proteins by gel filtration chromatography for diabetic sand rats. Seven major peaks are seen with the following calculated molecular weights in Daltons; >300,000 (1); 260,000 (2); 96,000 (3); 64,000 (4); 43,000 (5); 24,000 (6); 11,000 (7).

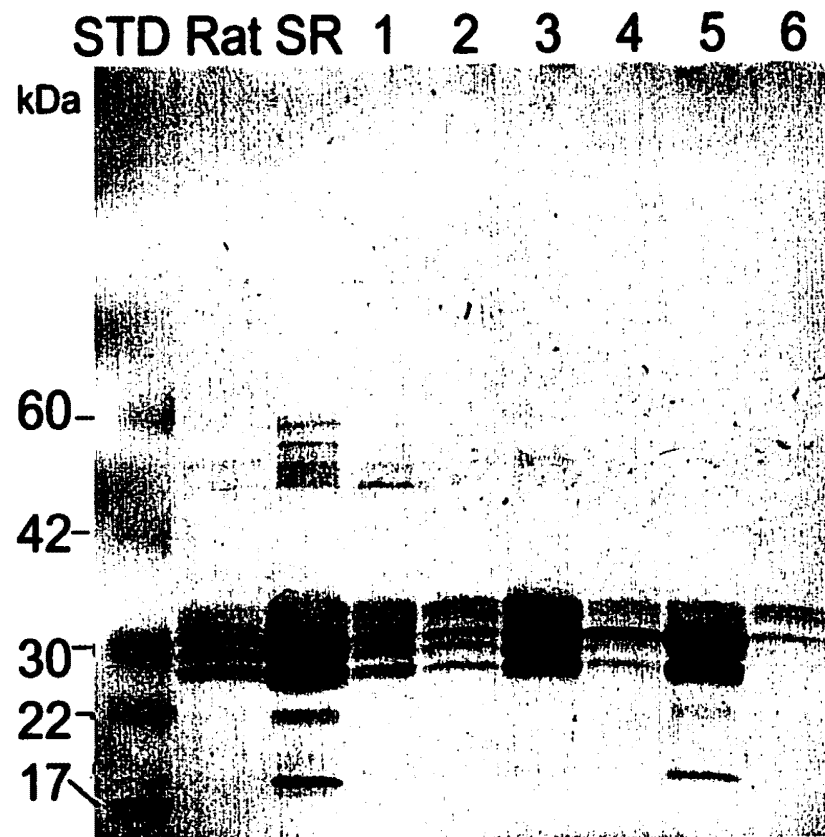
FIGURES 4.03 AND 4.04



FIGURES 4.05 AND 4.06

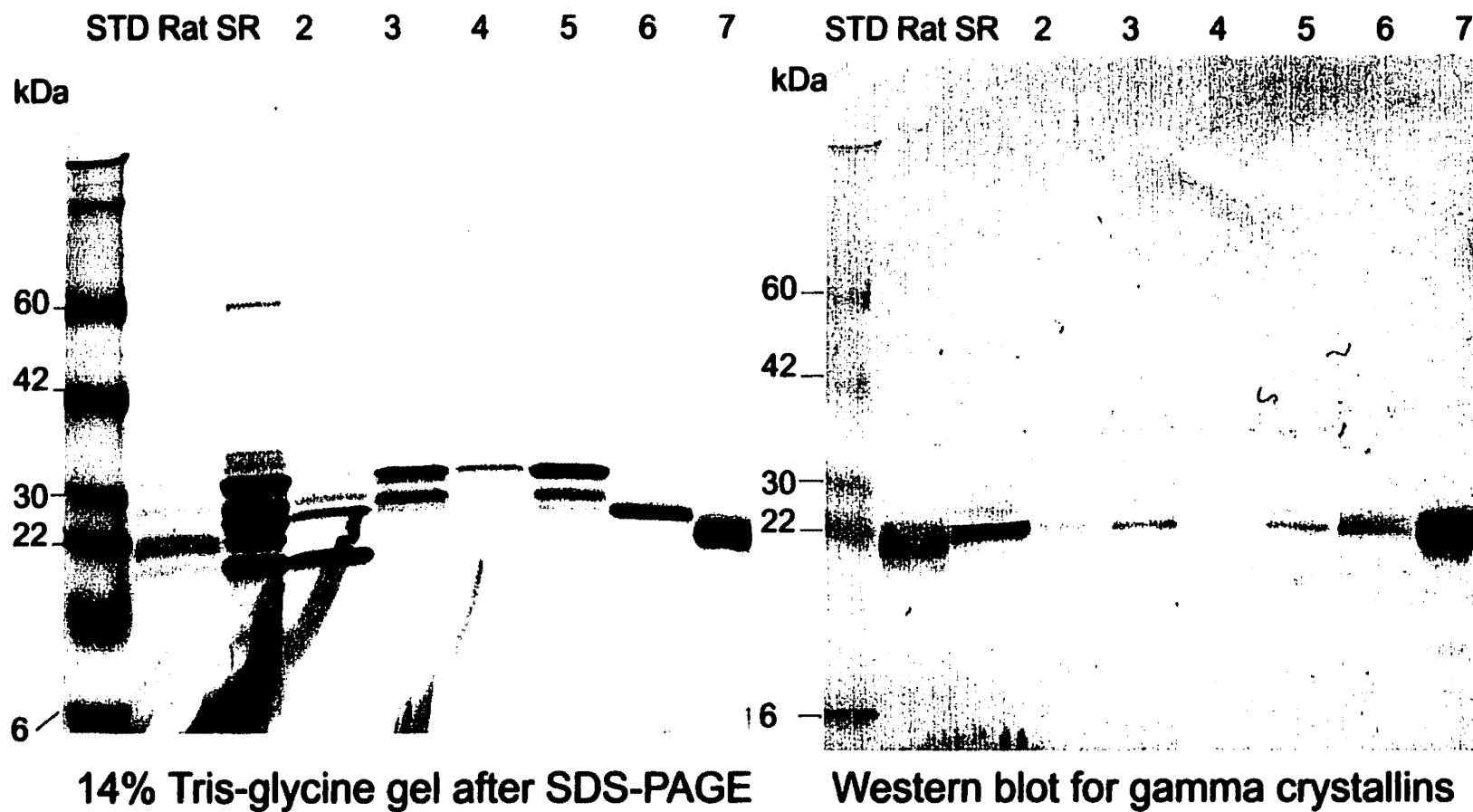


12% Tris-glycine gel after SDS-PAGE



Western Blot for beta crystallins

FIGURES 4.07 AND 4.08



FIGURES 4.09 AND 4.10

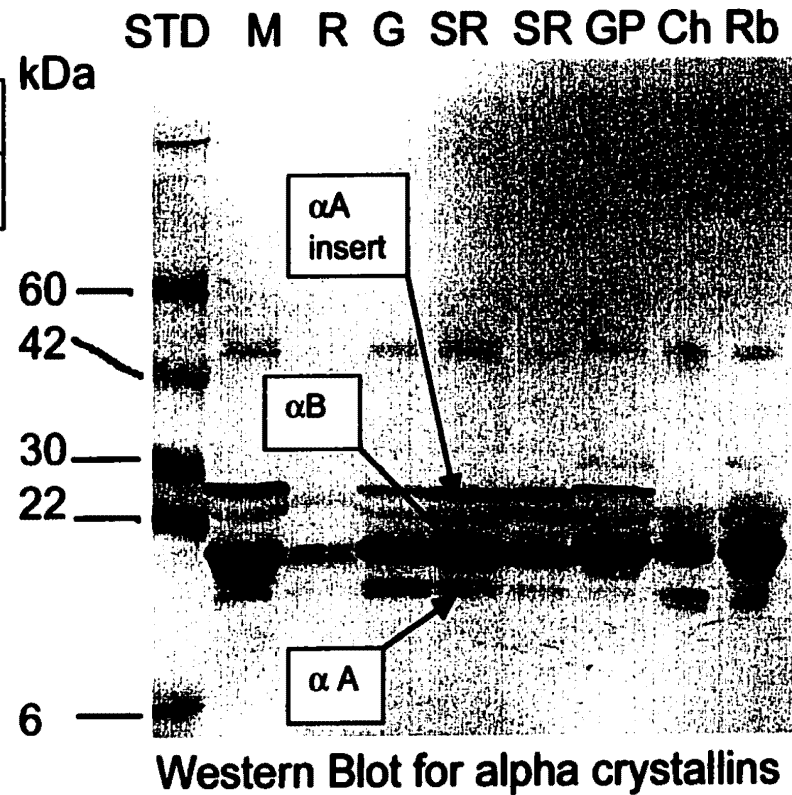
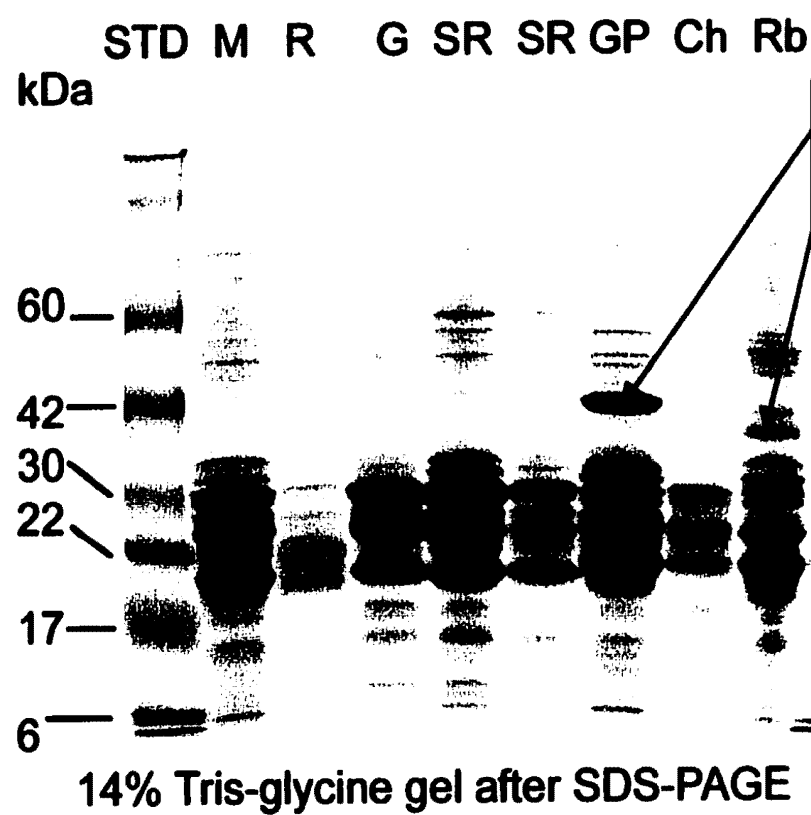


**Figure 4.03 – 4.10: Detection of Major Crystallin Classes by SDS-PAGE and Western Blot**

**SDS-PAGE of chromatography fractions (4.03) and western blots for alpha crystallins (4.04). Protein standard (STD); whole water-soluble lens extract from the rat (Rat); whole water-soluble lens extract from the sand rat (SR); lens extract fraction from chromatography peak #1 (1); lens extract fraction from chromatography peak # 2 (2); lens extract fraction from chromatography peak # 3 (3); lens extract fraction from chromatography peak # 4 (4); lens extract fraction from chromatography peak # 5 (5)**

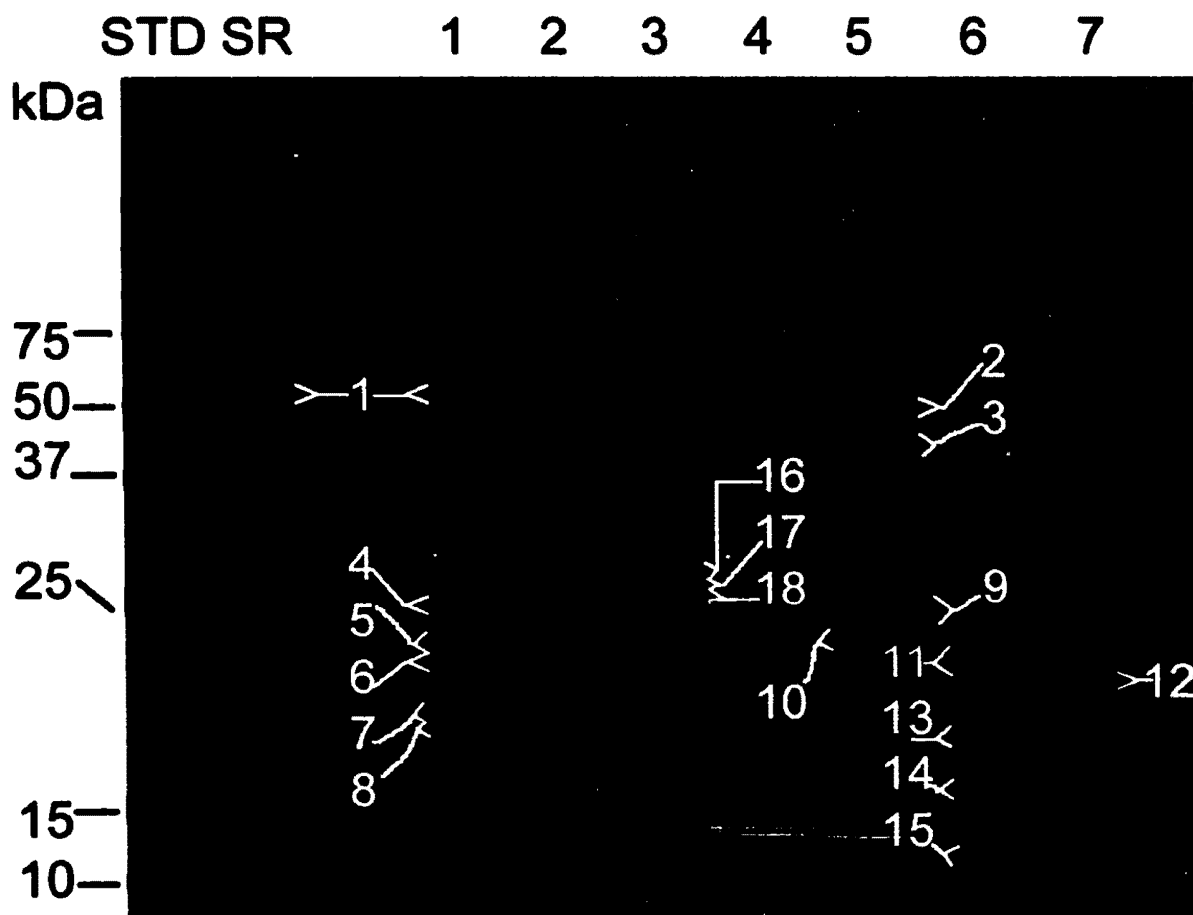
**SDS-PAGE of chromatography fractions (4.05) and western blots for beta crystallins (4.06). Protein standard (STD); whole water-soluble lens extract from the rat (Rat); whole water-soluble lens extract from the sand rat (SR); lens extract fraction from chromatography peak #1 (1); lens extract fraction from chromatography peak # 2 (2); lens extract fraction from chromatography peak # 3 (3); lens extract fraction from chromatography peak # 4 (4); lens extract fraction from chromatography peak # 5 (5); lens extract fraction from chromatography peak # 6 (6)**

**SDS-PAGE of chromatography fractions (4.07) and western blots for gamma crystallins (4.08). Protein standard (STD); whole water-soluble lens extract from the rat (Rat); whole water-soluble lens extract from the sand rat (SR); lens extract fraction from chromatography peak # 2 (2); lens extract fraction from**

chromatography peak # 3 (3); lens extract fraction from chromatography peak # 4 (4); lens extract fraction from chromatography peak # 5 (5); lens extract fraction from chromatography peak # 6 (6); lens extract fraction from chromatography peak # 7 (7)

SDS-PAGE of whole water-soluble lens extract (4.09) and western blots for alpha crystallins (4.10) of several species. Protein standard (STD); mouse (*Mus musculus*) (M); rat (*Rattus norvegicus*)(R); gerbil (*Meriones unguiculatus*) (G); sand rat (*Psammomys obesus*) (SR); guinea pig (*Cavia porcellus*) (GP); chinchilla (*Chinchilla laniger*) (Ch); rabbit (*Oryctolagus cuniculus*) (Rb); taxon-specific zeta crystallin ( $\zeta$ ); taxon-specific lambda crystallin ( $\lambda$ ) alpha A crystallin ( $\alpha$ A); alpha B crystallin ( $\alpha$ B); alpha A insert crystallin ( $\alpha$ A insert)

FIGURE 4.11



### 14% Tris-glycine gel after SDS-PAGE

Figure 4.11 shows the identification of specific crystallin isoforms and non-crystallin proteins by mass spectrometry on a SDS-PAGE gel (14% Tris-glycine gel). This is a SDS-PAGE of control sand rat chromatography fractions; Protein standard (STD); whole water-soluble lens extract from the sand rat (SR); chromatography peak 1 (1); chromatography 2 (2); chromatography peak 3 (3); chromatography peak 4 (4); chromatography peak 5 (5); chromatography peak 6 (6); chromatography peak 7 (7). Table 4.01 (page 113) lists the protein identifications of the numbered bands and the calculated molecular weights.

FIGURE 4.12

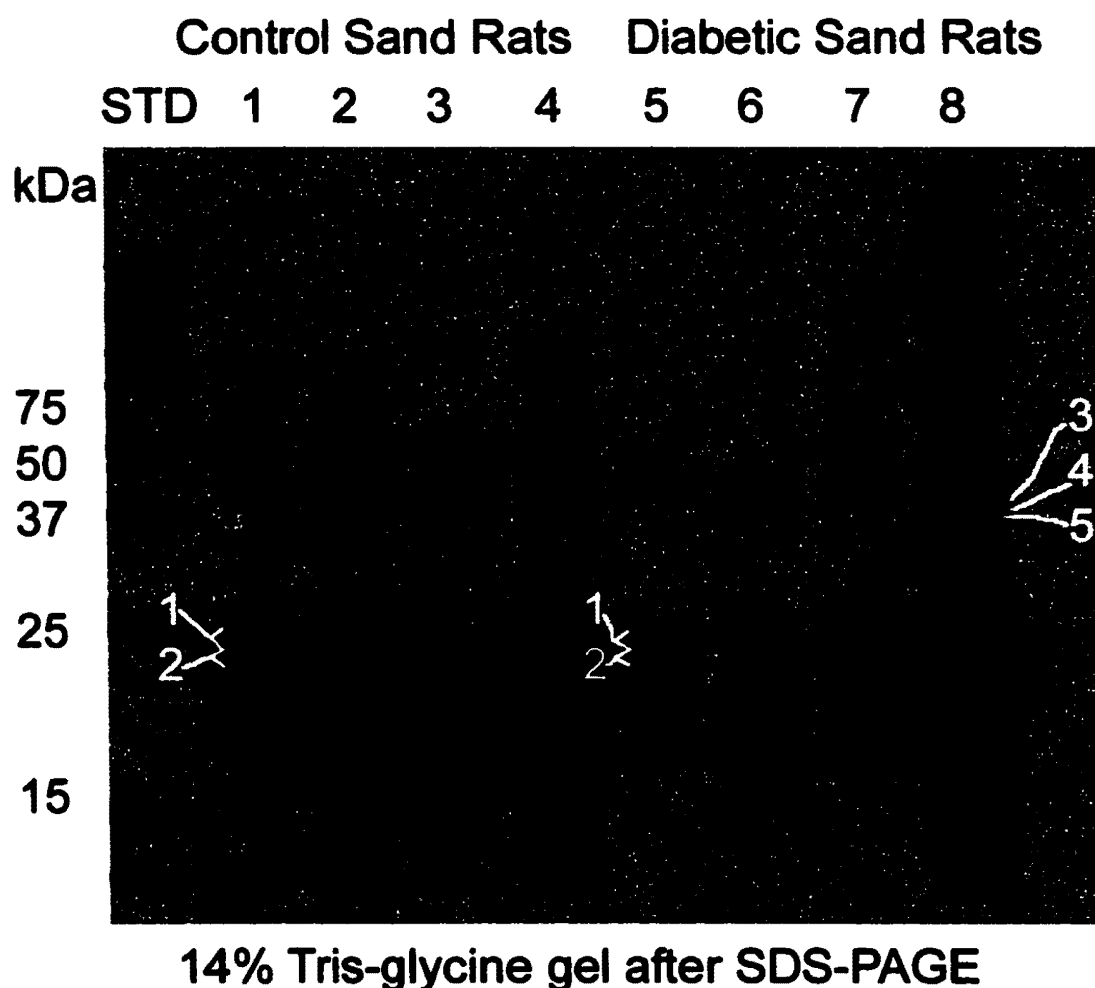


Figure 4.12 shows the identification of specific crystallin isoforms by mass spectrometry on a SDS-PAGE gel (14% Tris-glycine gel). This is a SDS-PAGE of whole water-soluble lens extracts from control and diabetic sand rats; Protein Standards (STD); control sand rats (1,2,3,4); diabetic (5, 6, 7, 8); 8 months of age (6); 9 months of age (8); 11 months of age (1, 2, 5); 12 months of age (3, 4, 7); diabetes duration of 4 months (6); diabetes duration of 5 months (8); diabetes duration of 6 months (5); diabetes duration of 7 months (7). Table 4.02 (page 114) lists the protein identifications of the numbered bands and the calculated molecular weights.

## CHAPTER 5

Additional results from "The Unique Lens Crystallin Pattern of the Fat Sand Rat (*Psammomys obesus*)."

In addition to the data presented in Chapter 4, several other related topics will be discussed in this chapter. The chromatography calibration and all of the sand rat chromatography curves will be discussed. Isoelectric focusing, 2-dimensional analysis and SDS-PAGE gels of the lens crystallins of the sand rat will be reviewed along with a brief discussion on the enzyme crystallins identified in the sand rat. Experiments on the pellet (non-water-soluble) fractions are also discussed in this chapter.

### Chromatography Set-up and Column Calibration

Column calibration was performed using high and low molecular weight standards calibration kits (Amersham Pharmacia Biotech, Piscataway, NJ). The standards were run through the Sephacryl column (Amersham Pharmacia Biotech, Piscataway, NJ) attached to a Biologic Chromatography System (BioRad, Hercules, CA) described in Chapter 4 and seen in Figure 5.01 (page 136). A calibration curve was determined using the elution of standards with known molecular weights. The standards used included ribonuclease A (13,700 Daltons), chymotrypsinogen A (25, 000 Daltons), ovalbumin (43,000 Daltons), albumin (67,000 Daltons), catalase (232,000 Daltons) and blue dextran

(2,000,000 Daltons). They were plotted on a logarithmic scale. The curve is linear from chymotrypsinogen (25,000 Daltons) to catalase (232,000 Daltons) and is seen in Figure 5.02 (page 137). It was assumed that the same relationship exists between the molecular size and molecular weight for determining molecular weights of the unknowns.

### Chromatography Curves

As explained previously, the lens extracts of 2 to 3 sand rats (1 lens each) were combined to obtain a 1 ml sample, which contained various lens protein concentrations. The samples were run through the column attached to the chromatography unit seen in Figure 5.01 (page 136). Molecular weights were determined using the calibration curve in Figure 5.02 (page 137). The chromatography curves and the molecular weights for each peak are listed in Figures 5.03 – 5.06 (pages 140 – 143). The calculated molecular weights for the major crystallin classes correlate well to the published values for the beta and gamma crystallins. The exact value for the first peak, alpha crystallins, on all of the chromatography curves in Figures 5.03 – 5.06 (pages 140 – 143) could not be accurately calculated and is therefore listed as a “greater than” value. This is due to the column not being able to separate compounds of molecular weight greater than 300,000 and also due to the calibration curve not being linear above 232,000 Daltons (catalase). There is some question concerning the calculated value for the second peak, which contains mainly alpha and some beta crystallins. In other species, alpha crystallins would not be found in this second

peak at a molecular weight of 250,000 Daltons. However, alphas were present in the second peak for the sand rat as described in Chapter 4. This is unusual for alpha crystallins since their native molecular weight is 600,00 to 900,00 Daltons (Albert and Jacobiec 1994). An overlay of all of the sand rat and gerbil runs is seen in Figure 5.07 (page 144). The gerbil chromatography peaks are well aligned over the sand rat peaks suggesting similar molecular weights for their crystallin classes. The protein level of the diabetic sample seen in the chromatography curve of Figure 5.05 is so low that only 3 peaks are apparent. The additional peaks marked on the graph are based on the fractions where peaks occurred for the control animals. Unfortunately, it was not possible to determine whether the peaks are lost due to cataract formation in the lens or simply due to low protein levels. Ideally, diabetic sample volumes large enough to provide an equivalent amount of protein for chromatography are needed. This requires larger numbers of animal lenses.

### **Isoelectric Focusing and 2-Dimensional Gels**

Along with the determination of molecular weight, the determination of the isoelectric point (pI) helps to identify a protein. Two control sand rat lenses were used specifically for the pI and molecular weight determination of the water-soluble lens proteins. These lens extracts were run on an isoelectric focusing gel (Invitrogen, Carlsbad, CA) and the results are seen in Figure 5.08 (page 145). The major bands seen are at a pH of 8.1, 7.5, 6.2 and 4.7 and 4.6. Alpha crystallins generally have a pI range of 4.8 – 5.0 and a polypeptide weight of 20

kDa (Albert and Jacobiec 1994). Beta crystallins have a pI range of 5.7 – 7.0 and a polypeptide weight of 23 – 35 kDa (Albert and Jacobiec 1994). Gamma crystallins have a pI range of 7.1 – 8.1 and a polypeptide weight of weight of 20 kDa (Albert and Jacobiec 1994). Based on the reference information, the bands at 4.6 and 4.7 are most likely alpha crystallins. The band at 6.2 is most likely beta crystallins. The bands at 7.5 and 8.1 are probably gamma crystallins. A lane from both edges of the gel in Figure 5.08 (page 145) was cut and inserted into a 2-D Tris-Glycine gel for SDS-PAGE. The results for each control animal, # 156 (Figure 5.09, page 146)) and # 165 (Figure 5.10, page 147), were almost identical. The results for both gels included higher molecular weight proteins with the following isoelectric point and molecular weight; pI 5.5, 175 kDa (a); pI 4.5 - 5.5, 100 kDa (b); pI 5.5, 60 kDa (c) and pI 6.5 - 7.0, 50 – 54 kDa (d). These bands and spots are not easily identified as being from the major crystallin classes mainly due to their high polypeptide weights. Some of these proteins are most likely the enzymes identified in Chapter 4, glycolytic enzymes and the aldehyde dehydrogenase. This would include the points estimated to be around 50 – 60 kDa in weight on the 2-D gels. The points at 100 and 175 kDa are unknown proteins. Alpha crystallin dimmers were seen on SDS-PAGE and Western Blots (Figures 4.03, 4.04, 4.09 and 4.10 on pages 117 and 120) but it is unlikely that these higher molecular weight spots are aggregates of this major crystallin class. The pI for the largest point (a) is slightly higher than the range for the alpha crystallins. The pI range for the next point (b) is within the range for alpha crystallins but the molecular weight is 5 times the polypeptide weight of the

alpha crystallin and the technique used for the 2-D gels denatures the proteins, so aggregates this large should not appear on this gel. The last three bands seen on the 2-D gels (Figures 5.09 and 5.10) are from the major crystallin classes. Beta crystallins are seen at the pI of 5.0 – 7.5 with a polypeptide weight of 28 – 32 kDa (e). Beta and probably some alpha, although the molecular weights are slightly high for alphas, crystallins are seen at a pI of 5.0 – 7.5 with a polypeptide weight of 24 – 26 kDa (f). Gamma crystallins with possibly some alphas, although the pH is high for alphas, are seen at a pI of 6.0 – 8.0 with a polypeptide weight of 20 kDa (g). The main problem with the use of this 2-D system was the streaking of specific protein points into bands. This horizontal streaking is due to inadequate immobilization of the proteins in the first dimension gel, during isoelectric focusing. In order to try to remedy this problem, a 2 dimensional gel was run using immobilized pH gradient gel (IPG) strips (BioRad, Hercules, CA). The IPG strips are designed to fix the protein to a spot on the strip and thus reduce the horizontal streaking on the 2-D gel. The positive attribute of this system is the ability to run numerous IPG strips at one time. But there are also drawbacks. The first problem encountered with the use of this system was the inability to get a pI reading off the first dimension. The IPG strips are not stained after running the first dimension and all information on the proteins is obtained only after the second dimension is run. Additionally, the programming time for the isoelectric focusing unit must be determined based on the proteins of interest and therefore requires multiple samples in order to optimize the unit. These problems, especially the need for multiple samples to optimize, along with the cost of the

unit made this technique prohibitive. Some chromatography fractions were run on this unit during a demonstration (data not shown) but unfortunately horizontal streaking was still seen, only to a slightly lesser extent. Additional research obtaining specific molecular weights and isoelectric points for the sand rat crystallins using the IPG unit and 2-D gels would add to the crystallin knowledge base. With the ability of the mass spectrometry to identify proteins in a band from a 1-D SDS-PAGE gel, it may be more appropriate to run IEF gels and cut the bands for mass spectrometry identification, if this technique is available.

#### Enzymes or Taxon-Specific Crystallins?

To investigate the relative concentrations of the enzymes identified by mass spectrometry, the NIH Image densitometry program was used. The results of a densitometry measurement on a lane of an SDS-PAGE gel from a control sand rat are seen in Figure 5.11 (page 148). As was determined by MALDI mass spectrometry, the enzymes are (a) retinaldehyde dehydrogenase, (b)  $\alpha$ -enolase and (c) phosphoglycerate kinase. In addition to phosphoglycerate kinase, actin is also present in this band. The bands containing major crystallin classes of comparable density are (d)  $\beta$ B1, (e)  $\beta$ B1/ $\beta$ B3 and (f)  $\beta$ B3/ $\beta$ B1. The peaks for (a) retinal dehydrogenase, (d)  $\beta$ B1 and for (f)  $\beta$ B3/ $\beta$ B1 are essentially the same height and appear to have a similar concentration. The peaks for (b)  $\alpha$ -enolase and (c) phosphoglycerate kinase/actin are approximately 2/3 of the height of peaks a, d and f. Wistow defines taxon-specific crystallins as "minor protein species constituting 0.1% - 1% of total proteins, about one or two orders of

magnitude lower than typical crystallins" (Wistow and Kim 1991). The enzymes (a – c) are either 2/3 or equal the approximate concentration of the identified beta crystallins (d – f). Based on the sizes of the peaks, there are certainly grounds to consider these enzymes as being taxon-specific crystallins. The case for retinal dehydrogenase, a cytosolic aldehyde dehydrogenase also seen in the lenses of elephant shrews, is of particular interest. This enzyme, called eta ( $\eta$ ) crystallin, is thought to play a role in softening the lenses of elephant shrews, a diurnal species, or possibly, since it was found to be enzymatically active, acting as a detoxifying agent for toxic aldehydes (Wistow 1995). Aldehyde dehydrogenase has also been thought to play a role in ultraviolet (UV) light absorbance (Wistow and Piatigorsky 1987). The sand rat, a diurnal desert species with a convex-shaped lens and firm zonular attachments would have some need for a softer lens in order to accommodate its vision and certainly a requirement for reducing glare in a desert environment. Retinaldehyde dehydrogenase may serve as a taxon-specific crystallin in this species aiding in lens accommodation and UV absorbance. Alpha enolase, a glycolytic enzyme referred to as tau ( $\tau$ ) crystallin in the lenses of reptiles birds and fish (Stapel and De Jong 1983), (Williams et al. 1985), is thought to possibly have some heat-shock function (Wistow and Piatigorsky 1987). Based on the diurnal behavior of the sand rat in its desert environment, the  $\alpha$ -enolase present in the sand rat lens may also be considered a taxon-specific crystallin in this species. Making a case for phosphoglycerate kinase as being a taxon-specific crystallin is much more difficult. First, the band this glycolytic enzyme was identified as being located in, is shared with the

protein actin. Since actin is abundant in many cell types and no quantification was made of either protein, it is difficult to compare with densitometry alone this band to one of the major crystallin bands. As explained in Chapter 4, glycolytic enzymes have been found in the lens of many animals. This particular glycolytic enzyme, phosphoglycerate kinase, has not been reported to date as a taxon-specific crystallin in any species. Additional research in the area of enzyme activity of all three enzymes would be of interest to help determine if these proteins are playing a structural or functional role in the lens of the sand rat.

#### **Special Staining of the Water-soluble and Pellet Fractions of Lens Extracts**

Lenses were prepared for crystallin evaluation as explained in Chapters 2, 3 and 4 (see Figure 3.29 on page 90 for diagram of preparation). Several experiments were performed to help determine differences between the crystallins of the water-soluble extract and the pellet. Figure 5.12 (page 149) shows a SDS-PAGE gel stained with a Coomassie safe stain (Invitrogen Corporation, Carlsbad, CA). The wells were loaded with water-soluble lens extracts and pellets from two diabetic (DE, DP) sand rats and with water-soluble lens extracts and pellets from two control sand rats (CE, CP). The lens pellet is in the lane to the right of the lens extract from the same animal. Aside from the differences discussed in Chapter 4 of beta crystallin ratio shifts no discernable differences were noted with these sand rat samples between diabetics and control. There were also no apparent differences between the pellets and the water-soluble extracts run on the gel. Additional special staining techniques were attempted using a

glycoprotein gel stain kit (Molecular Probe, Eugene, OR). This stain was designed to detect as low as 1  $\mu\text{g}$  of glycated protein. In order to test this kit, the red blood cell fraction of blood from a diabetic animal with an HbA1c value of 19.4% was run on an SDS-PAGE gel. The results yielded positive band identification with a concentration of 1.2  $\mu\text{g}$  of glycated protein. Very slight staining was observed at the dilution just below this level at 0.8  $\mu\text{g}$ . The only difficulty in interpretation was the observation of the bands well below the expected molecular weight of hemoglobin (64,500 Daltons). The bands were seen far below 18,000 Daltons (results not shown due to poor reproduction of the scanned gel). Since the staining technique was accurate for the glycated protein quantity, an additional gel was run using the lens extracts and pellets from a diabetic and a control sand rat. Again bands were identified at the bottom of the gel as seen in the SDS-PAGE of HbA1c. What is interesting is the presence of the bands for both lanes of pellets had approximately the same calculated percentage of glycated proteins. The control pellet had 2.9% and the diabetic pellet had 2.5% glycated protein. The lane for the water-soluble extract of the diabetic did not stain at all. The lane for the water-soluble extract of the control did however stain, but very faintly. This was the only lane to have protein staining in the region where the major crystallin classes would be located from 32,000 to 18,000 Daltons. In conclusion, the glycoprotein staining kit was accurate for detecting as low as 1  $\mu\text{g}$  of glycated protein but did not reveal a difference between potential crystallin glycation in control and diabetic sand rats.

## Summary

The fat sand rat is a diurnal desert rodent with a unique crystallin pattern. The normal crystallin composition of the sand rat lens includes the major crystallin classes and some species-specific enzyme crystallins. Generally, the major crystallin composition is similar to other rodent species with some minor exceptions. The native molecular weights of the alpha crystallins of the sand rat are lower than the other rodent species (250 kDa versus 600 – 900 kDa). In addition, the gamma crystallin concentration is slightly lower than in nocturnal rodents; this may allow the sand rat to accommodate its lens. The presence of the aldehyde dehydrogenase and glycolytic enzymes in the sand rat lens may be protecting the eye against the glare and heat of its native desert environment. Additionally, the lens of the diabetic sand rat varies from the lens of the control animal. Alpha A crystallin aggregates are seen in some diabetic sand rats with cataracts (at 4 – 6 months diabetic duration). These alpha crystallin aggregates may be associating with the lens fiber cell membranes during advanced cataract formation. Subsequent insolubility of the alpha crystallin aggregates would then explain the disappearance of these aggregates from the water-soluble fraction of the diabetic sand rats of longer duration. The lenses of all sand rats with diabetic cataracts showed a shift on SDS-PAGE in the beta B2/beta B3 ratio. This may be related to changes in the N-terminus or the C-terminus of the protein. This would change the charge of the beta crystallins and cause beta crystallin aggregation and subsequent cataract formation. In summary, the fat sand rat has a unique crystallin composition perhaps because it is a diurnal desert species but the sand

rat remains an excellent model for the study of diabetic cataracts because of its close similarity to cataract formation in humans and other diabetic animal models.

FIGURE 5.01

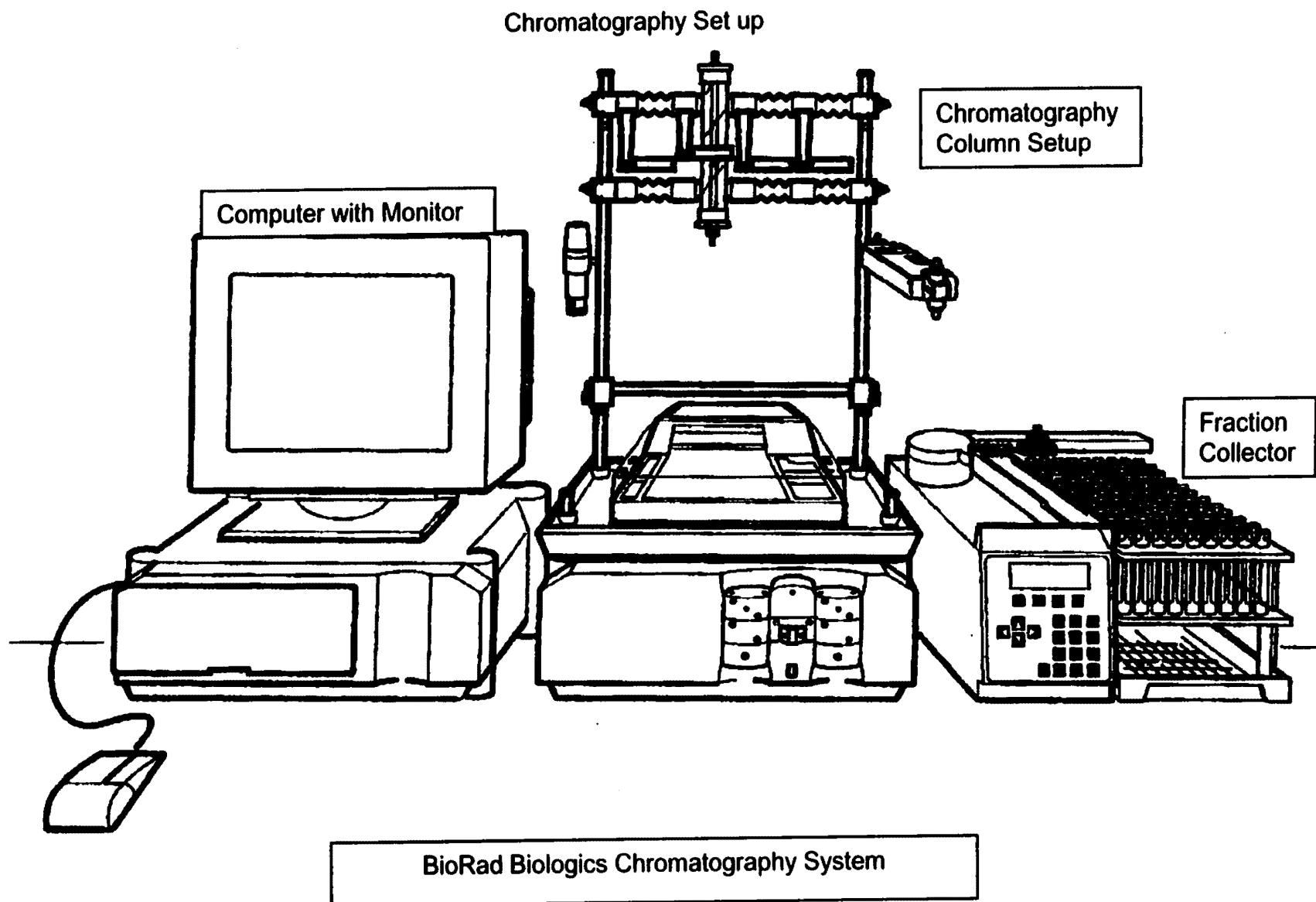


FIGURE 5.02

Calibration Curve for Gel Filtration Chromatography Molecular Weight Standards

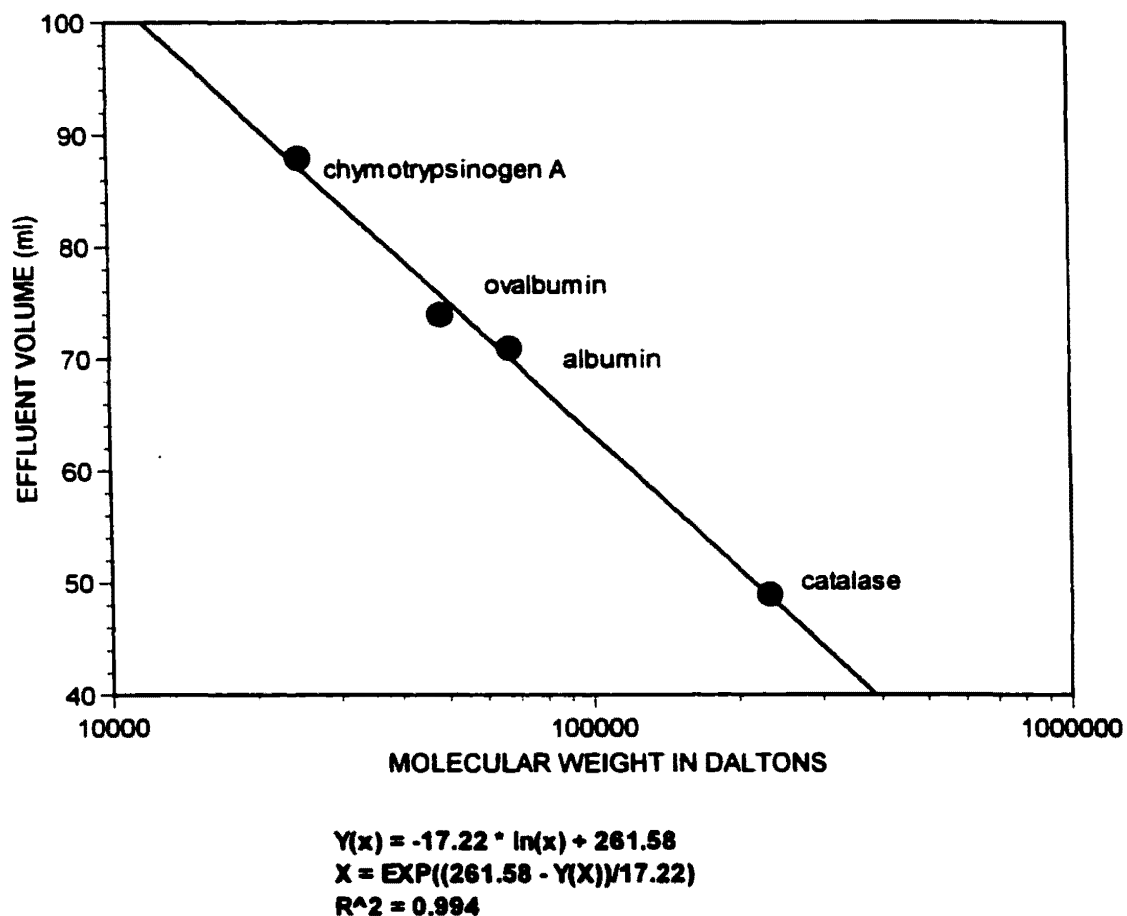


Figure 5.02 the calibration curve is linear from chymotrypsinogen (25,000 Daltons) to catalase (232,000 Daltons). The formula for the line was used to calculate molecular weight values for curves in Figures 5.03 – 5.07 (pages 140 – 144).

Figures 5.03 – 5.07 shows chromatography curves of lens extracts for control sand rats (5.03, 5.04), diabetic sand rats (5.05), normal gerbil (5.06), and an overlay of several chromatography runs (5.07).

Figure 5.03 shows peaks for alpha crystallins (1, 2), beta high (3), beta low 1 (4), beta low 2 (5, 6), and gamma crystallins (7). Molecular weights in Daltons were calculated based on the standard curve in Figure 5.02 on page 137 (1= > 300,000; 2=250,000; 3=105,000; 4=59,000; 5=44,000; 6=21,000; 7=14,000).

Figure 5.04 shows peaks for alpha crystallins (1, 2), beta high (3), beta low 1 (4), beta low 2 (5, 6), and gamma crystallins (7). Molecular weights in Daltons were calculated based on the standard curve in Figure 5.02 on page 137 (1= > 300,000; 2=250,000; 3=105,000; 4=64,000; 5=44,000; 6=22,000; 7=14,000).

Figure 5.05 shows peaks for alpha crystallins (1, 2), beta high (3), beta low 1 (4), beta low 2 (5, 6), and gamma crystallins (7). Molecular weights in Daltons were calculated based on the standard curve in Figure 5.02 on page 137 (1= > 300,000; 2=250,000; 3=96,000; 4=64,000; 5=41,000; 6=21,000; 7=11,000).

Molecular weights for figure 5.06 were calculated in Daltons based on the standard curve in Figure 5.02 on page 137 (1= > 300,000; 2=240,000; 3=68,000; 4=43,000; 5=21,000).

Figure 5.07 is an overlay of control sand rats (run 0, run 1, run 3), diabetic sand rats (run 2, run 4) and a normal gerbil (run 7).

FIGURE 5.03

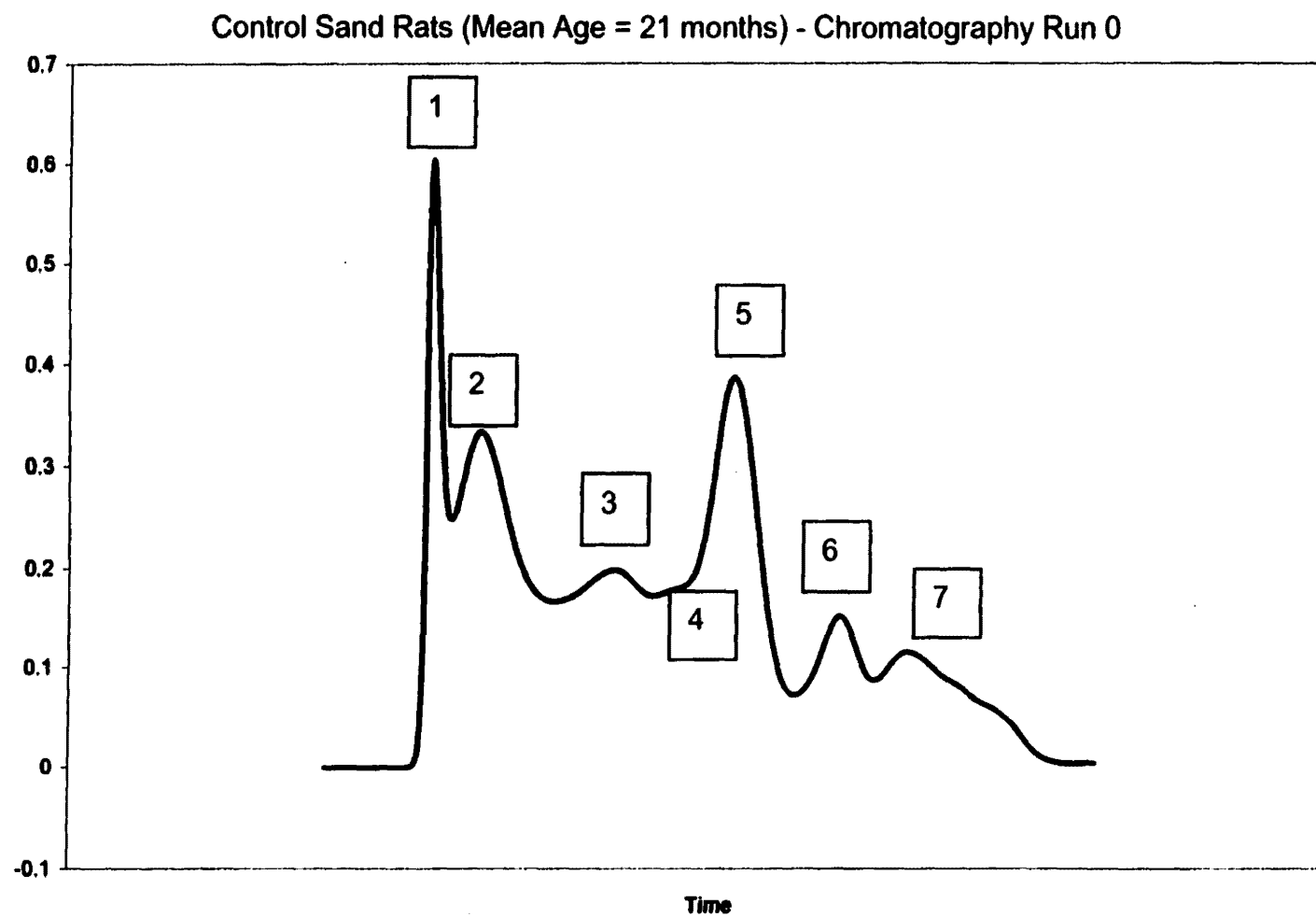


FIGURE 5.04

Control Sand Rats (Mean Age = 8.5 months) - Chromatography Run 3

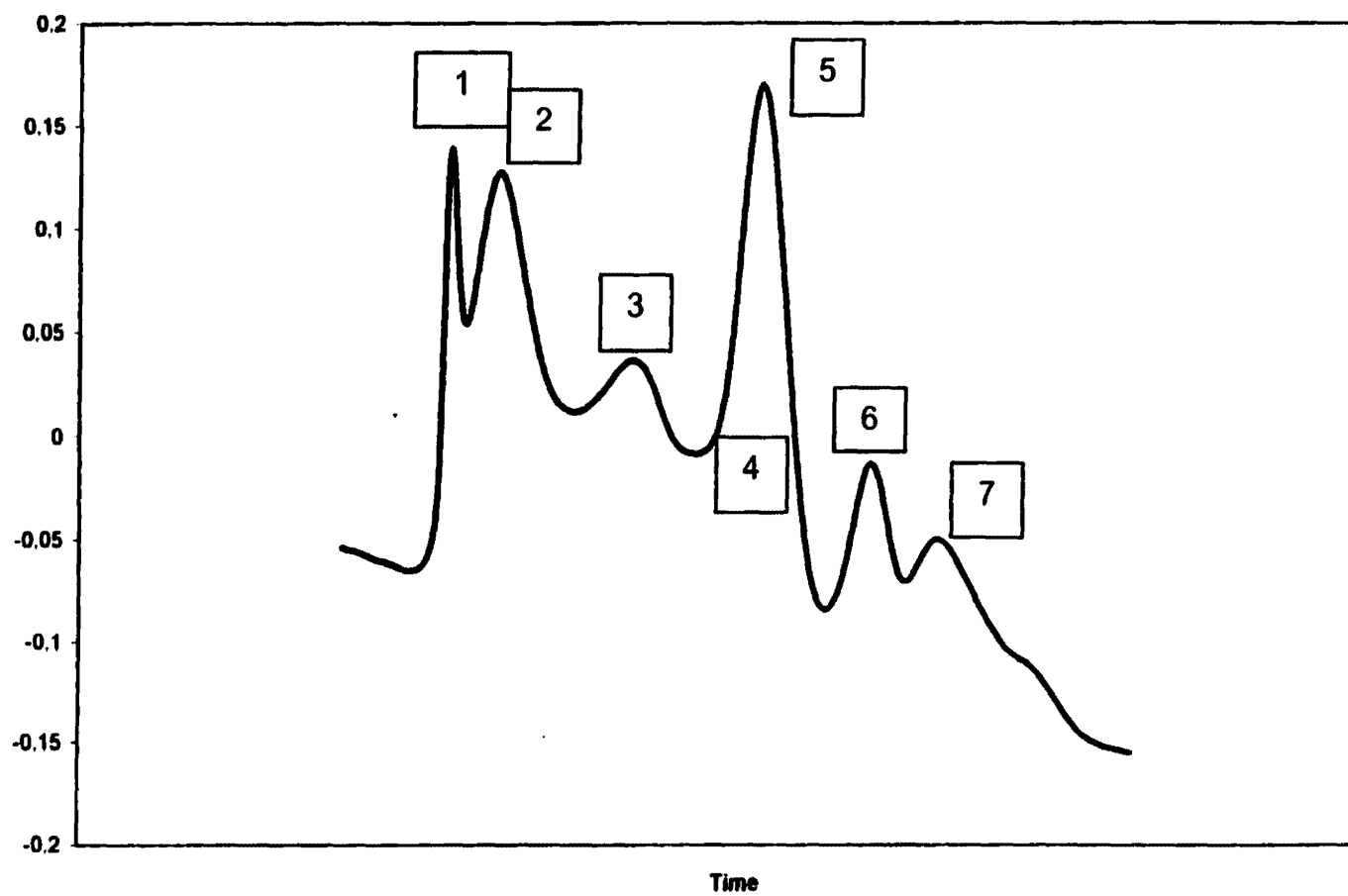


FIGURE 5.05

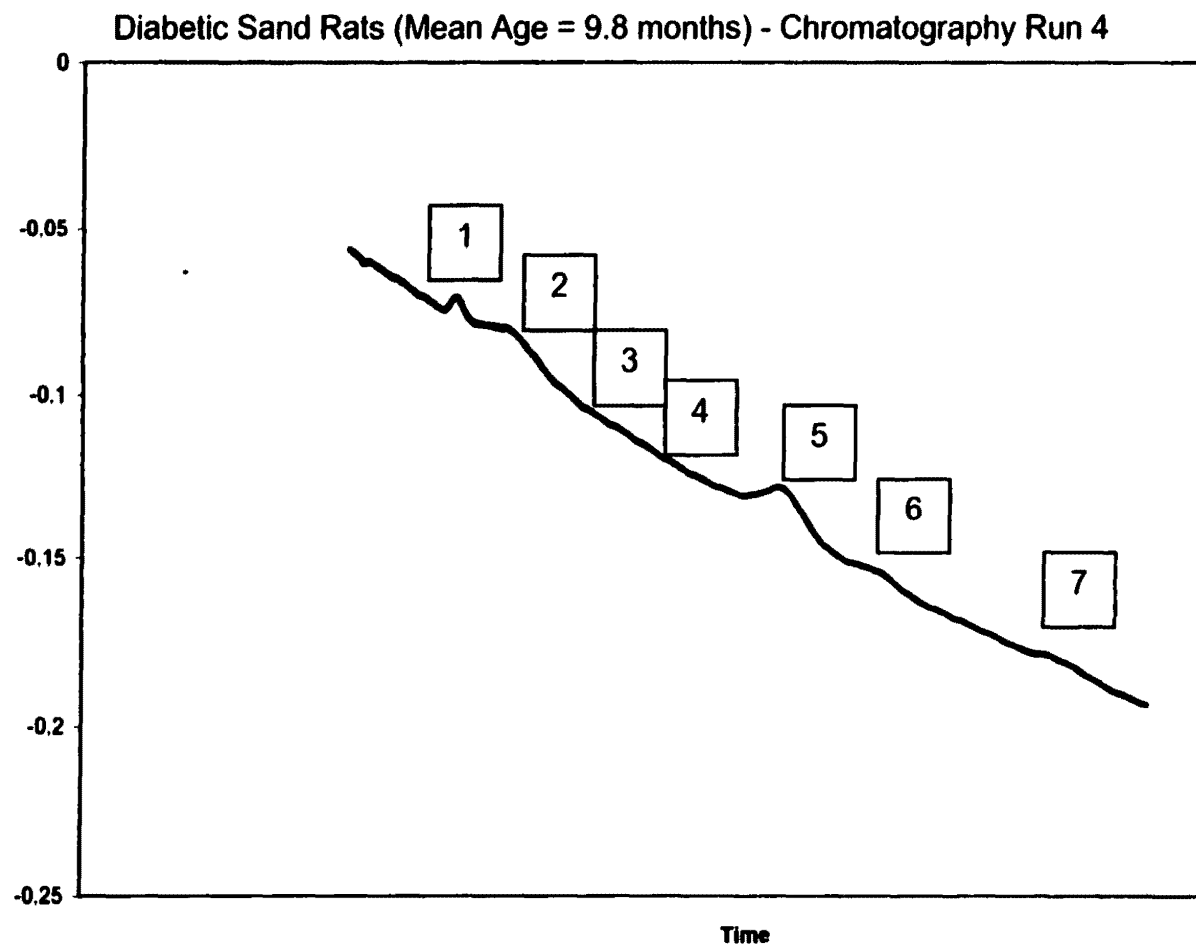


FIGURE 5.06

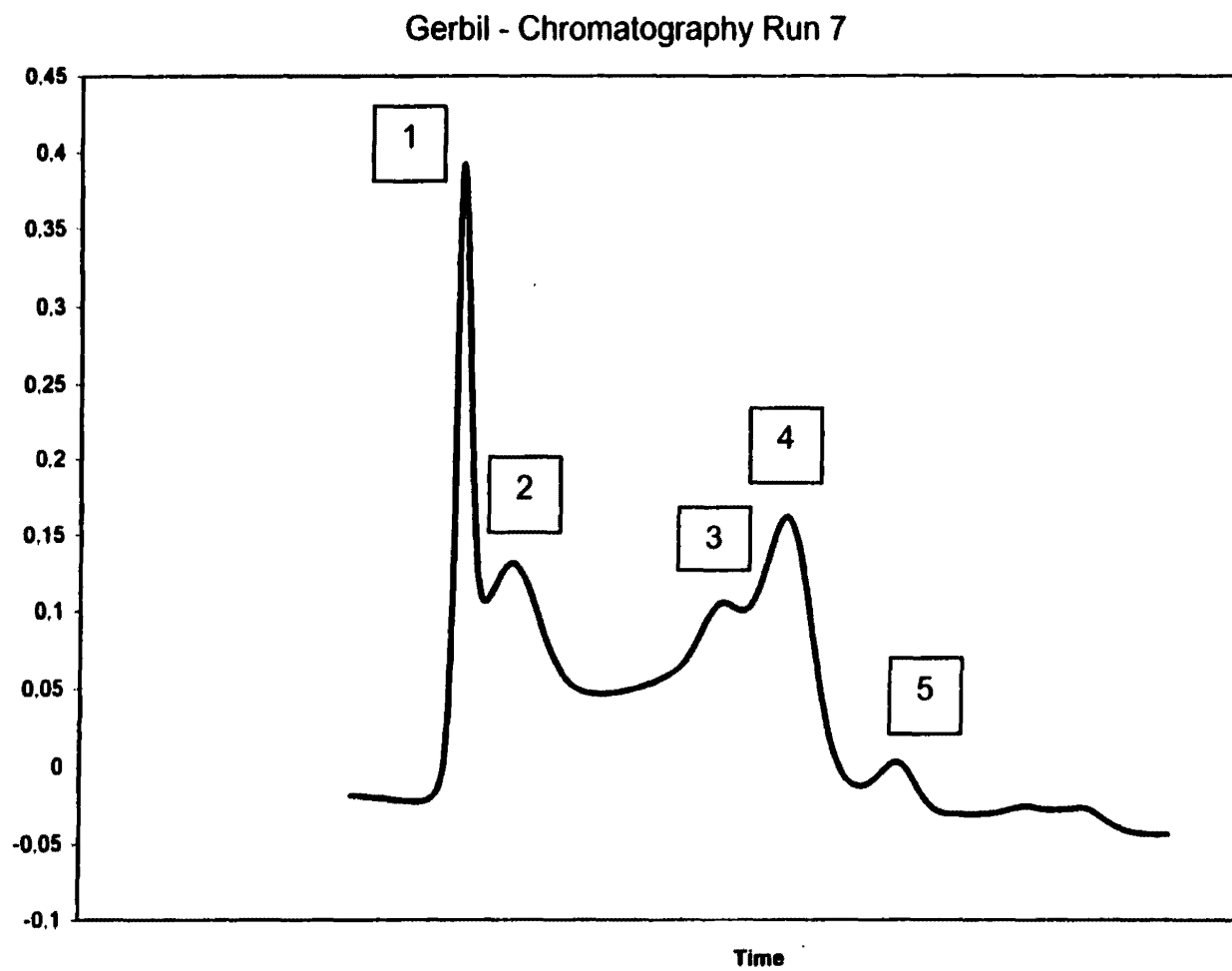


FIGURE 5.07

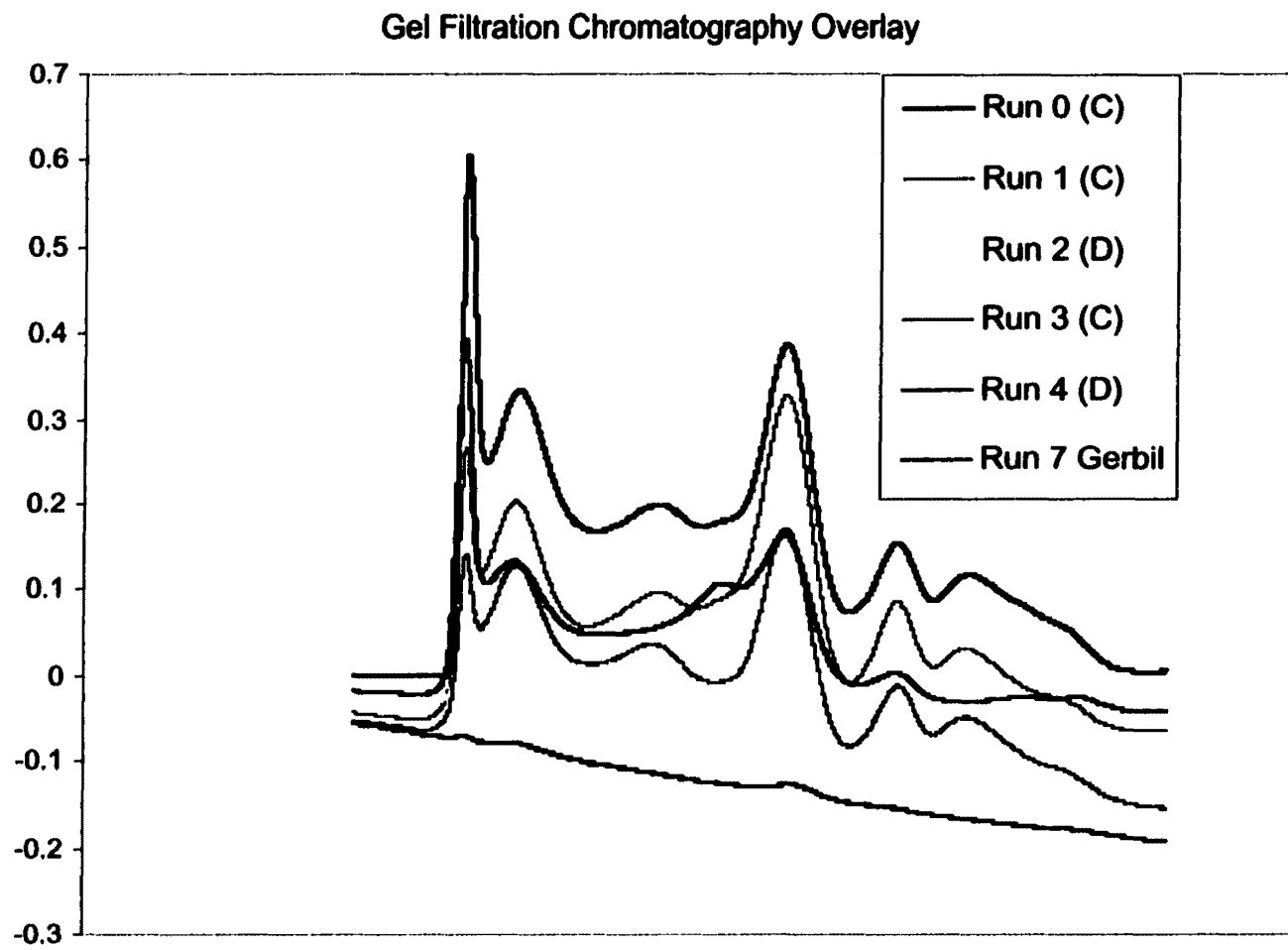


FIGURE 5.08

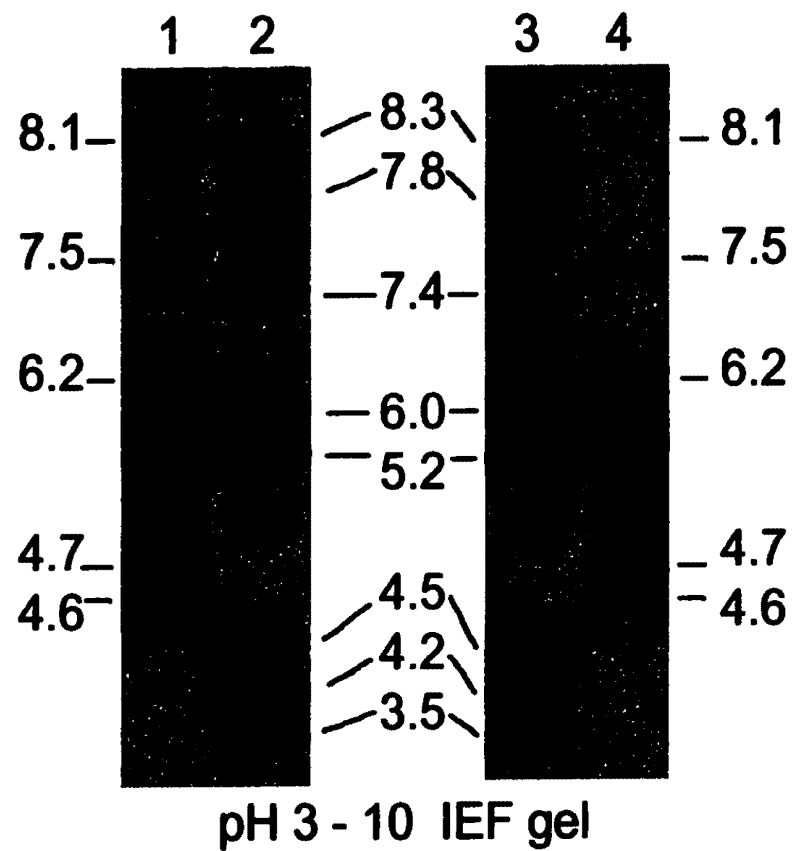


Figure 5.08 identifies the isoelectric points of proteins found in the water-soluble extract of two different control sand rats, # 156 (1) and # 165 (4). Isoelectric focusing standards are seen in lanes 2 and 3.

**FIGURE 5.09**

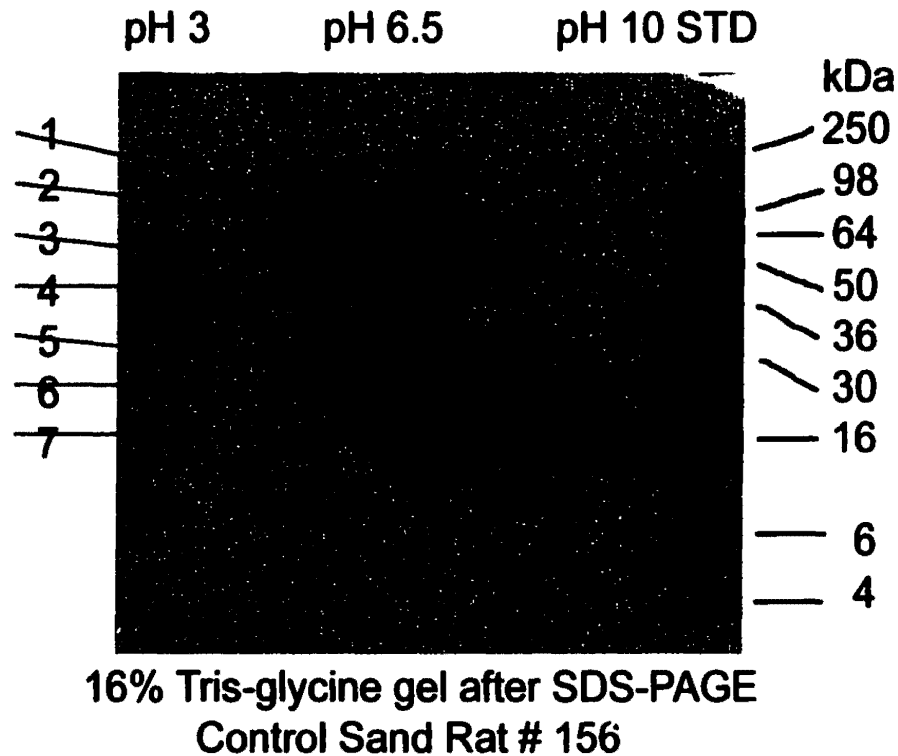
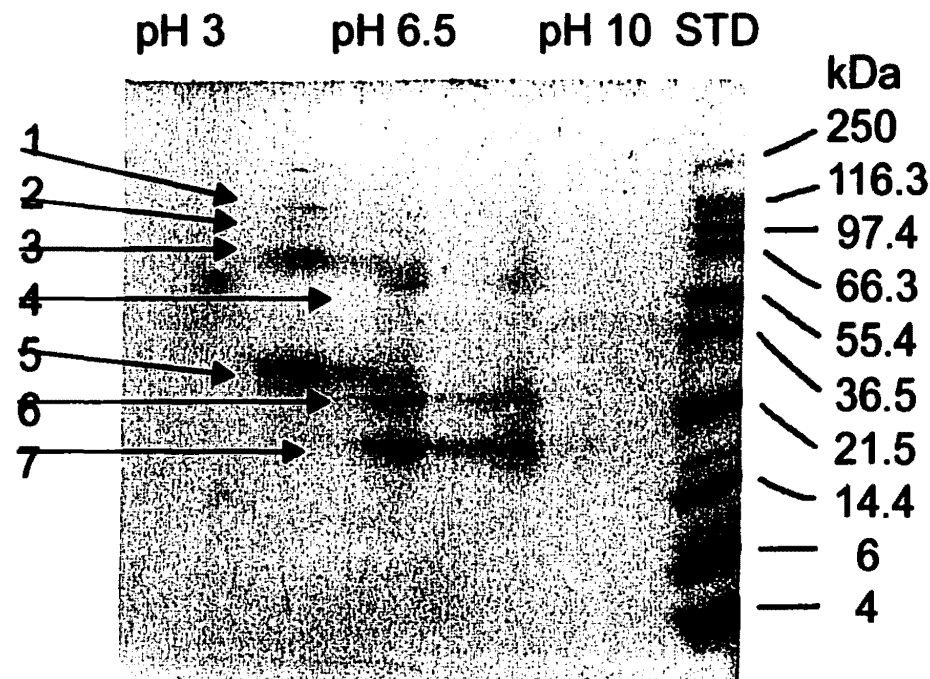


Figure 5.09 points out the proteins isolated from a lens extract of a control sand rat by 2-dimensional gel electrophoresis. The higher molecular weight proteins including 1 (pI 5.5, 175 kDa), 2 (pI 4.5 - 5.5, 100 kDa), 3 (pI 5.5, 60 kDa) and 4 (pI 6.5 - 7.0, 50 — 54 kDa) are not easily identified as being from the major crystallin classes. The major crystallin classes of beta are seen at 5 (pI 5.0 — 7.5, 28 — 32 kDa); beta and some alpha at 6 (6.0 — 7.5, 24 — 26 kDa) and gamma with some alpha at 7 (pI 6.0 — 8.0, 20 kDa). Molecular weight standards are seen in the lane to the far right (STD).

**FIGURE 5.10**



**16% Tris-glycine gel after SDS-PAGE  
Control Sand Rat # 165**

Figure 5.10 points out the proteins isolated from a lens extract of a control sand rat by 2-dimensional gel electrophoresis. The higher molecular weight proteins including 1 (pI 5.5, 175 kDa), 2 (pI 4.5 - 5.5, 100 kDa), 3 (pI 5.5, 60 kDa) and 4 (pI 6.5 - 7.0, 50 — 54 kDa) are not easily identified as being from the major crystallin classes. The major crystallin classes of beta are seen at 5 (pI 5.0 — 7.5, 28 — 32 kDa); beta and some alpha at 6 (5.0 — 7.5, 24 — 26 kDa) and gamma with some alpha at 7 (pI 6.0 — 8.0, 20 kDa). Molecular weight standards are seen in the lane to the far right (STD).

**FIGURE 5.11**

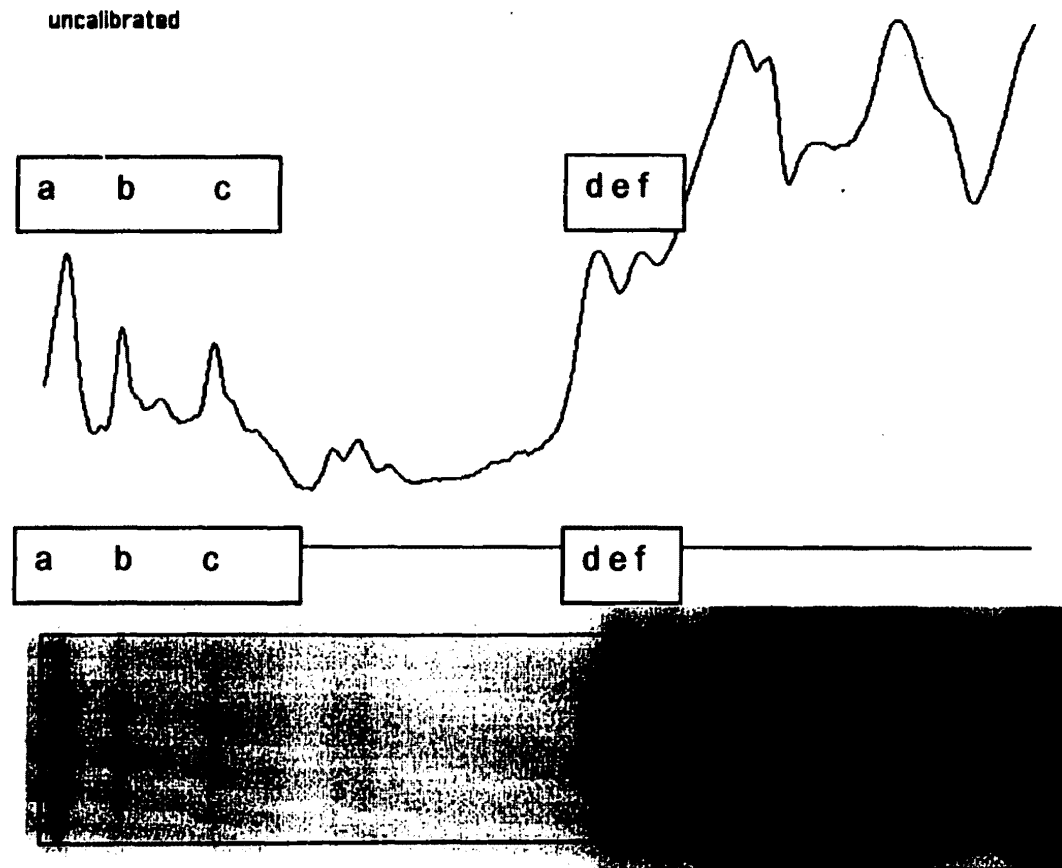


Figure 5.11 is a densitometry graph of normal lens extract (water-soluble) from the lane of an SDS-PAGE gel. Identification of retinaldehyde dehydrogenase (a),  $\alpha$ -enolase (b), phosphoglycerate kinase (c),  $\beta$ B1 (d),  $\beta$ B1/ $\beta$ B3 (e) and  $\beta$ B3/ $\beta$ B1 (f) was determined by mass spectrometry.

**FIGURE 5.12**

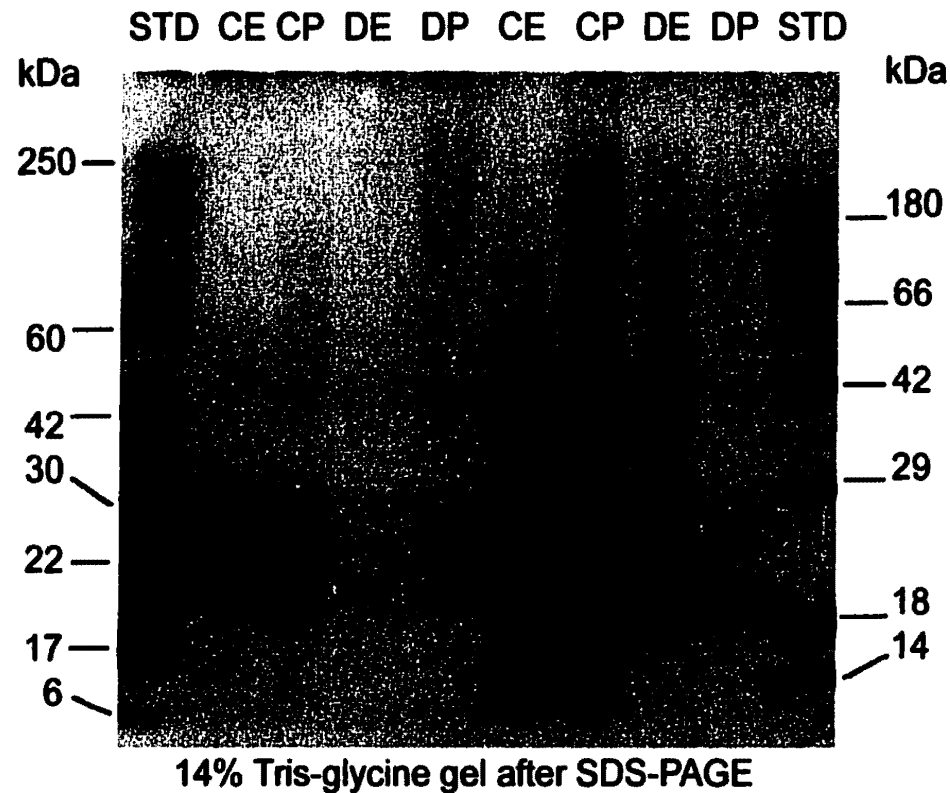


Figure 5.12 is a SDS-PAGE gel of lens extracts and pellet extracts from four sand rats (two control and two diabetic sand rats). The control sand rat lens extracts (CE) and control sand rat pellet (CP) extracts are in lanes adjacent to the diabetic sand rat lens extracts (DE) and diabetic sand rat pellet extracts (DP). Both diabetic animals had bilateral cataracts. The lanes labeled STD are MultiMark protein standards (Invitrogen, Carlsbad, CA) in the far left lane and Candy Cane protein standards (Molecular Probes, Eugene, OR) in the far right lane.

## CHAPTER 6

### Discussion

The fat sand rat is an excellent model for the study of diabetic cataracts because clinical cataract formation is rapidly induced with a simple diet change, the formation of cataracts and clinical chemistry is similar in progression to human diabetic cataracts and the sand rat is easy to breed and handle. This spontaneous model is easily converted to a diabetic state without drug injections, like alloxan or streptozocin, and without costly food additives, like a diet of 50% galactose. Simple conversion occurs in sand rat colonies that have developed diabetes prone (DP) lines. At the present time in the USUHS colony, most of the animals convert as expected but some never convert on the standard rodent chow, while others convert on the sand rat chow. It is important for this area of research that these separate lines, diabetes resistant (DR) and diabetes prone (DP), be developed in order to study early changes in diabetic cataracts. Once DP lines are established in the USUHS sand rat colony, generating diabetics for cataracts and other diabetes research will be easily and consistently accomplished.

Diabetic cataract formation in the sand rat begins with vacuole formation in the equatorial regions of the lens and progresses to involve opacity formations in the posterior subcapsular (PSC), posterior cortical, nuclear and finally the anterior cortical regions. This pattern is identical to diabetic cataract formation in the human, the dog and the rat (Albert and Jacobiec 1994). In addition, the sand rat,

like humans and dogs and unlike the rat, has the lens of a diurnal animal. The sand rat lens is convex, elliptical and more plastic than the rat lens. Rats and mice, being nocturnal species, have a hard round lens with minimal zonular attachments. Nocturnal animals do not accommodate and this accounts for the difference in lens shape and attachment.

Not only are the sand rats a more anatomically correct lens model but they are also much easier to handle. Sand rats can be readily handled without the behavioral acclimation that is required for rats and mice. Breeding parameters are also similar to rats and mice. Gestation periods are only slightly longer in sand rats, 24 days, than in rats and mice, 21 days and 20 days, respectively. Litter size is smaller in sand rats, only 3 – 6 pups per litter, whereas rats and mice commonly have litters exceeding 10 pups per litter. This difference in litter size from the mouse may be accommodated for by the longer life span of the sand rat, up to 3 years. Just based on these anatomical, biological and behavioral parameters, the sand rat is an excellent model for the study of diabetic cataracts but there are additional clinical parameters that also support this statement.

Rapid weight gain and clinical diabetes is produced in the sand rat by a simple diet change from a high protein and fiber, low digestible carbohydrate diet to a high digestible carbohydrate, low fiber diet. The body weight increases rapidly to well over 200 grams and in some cases the sand rat weights were as high as

270 grams. This body weight difference with diet change in sand rats is similar to the body weight differences seen in Mexican versus American Pima Indians (Knowler et al. 1990). The diet-induced obesity in the sand rats resulted in hyperglycemia and elevated glycated hemoglobin levels indicating a relatively high blood glucose level over time. This hyperglycemia resulted in subsequent elevated glucose in the aqueous humor and vitreous body of the eye. The elevated ocular glucose levels seen in the fat sand rats is in agreement with the literature for humans with diabetes (Daae et al. 1978), (Peclet et al. 1994), (Lundquist and Osterlin 1994) and supports the hypothesis tested in specific aim #1.

Glycated protein levels, other than hemoglobin, were difficult to determine in the sand rats. This was due to the small sample sizes, low sensitivity of the selected fructosamine test kit and small numbers of animals with a longer duration of diabetes. The sample sizes of vitreous and lens extract per animal were too small for fructosamine testing. This problem was two-fold: either the entire sample from one animal would have to be dedicated to the fructosamine test, with no opportunity to repeat the test, or a diluted sample would have to be used. The lenses were originally diluted in 1 ml of buffer but after centrifugation and utilization in several other experiments, the lens extract volumes did not allow for multiple fructosamine assays for all sand rats. The procedure of using a diluted sample was utilized with the vitreous but the test kit sensitivity was too low to report the results. Dedicating lens extract samples solely to the fructosamine

assays, utilizing a test kit with better sensitivity and pooling vitreal samples may alleviate the problems encountered with this set of experiments. Concentrating the samples may also work but this would still require sample pooling since the vitreal volumes are not adequate for the test kit. The use of more sensitive AGE testing techniques might also provide additional information on diabetic cataracts formation from other ocular samples, such as the non-water soluble lens pellet.

Since protein glycation is dependent on protein half-life and degree and duration of hyperglycemia, more diabetic sand rats, with longer diabetes duration, are also needed to compare ocular glycated protein levels to the literature. Diabetic cats with a 6-month duration of diabetes and rabbits with a 3-month duration had significantly elevated fructosamine levels in the vitreous when compared to controls (Farr et al. 1999). This elevation of glycated proteins in the vitreous has also been seen in humans with diabetes and with advanced aging (Osuna et al. 1999), (Stitt et al. 1998). Along with elevations of vitreal glycated protein levels, several reports cite glycation of the lens proteins occurring in diabetes and aging (Perry et al. 1987), (van Boekel and Hoenders 1992), (Duhaiman 1995), (van Boekel et al. 1996), (Crabbe 1998), (Shamsi et al. 1998). Since these diabetic changes are so prevalent in humans and other animals, there is every reason to believe these changes would occur and could be identified in the fat sand rat with the use of larger sample sizes, more accurate testing techniques and larger animal numbers per group. Based on the results of the research and the

discussion above of the hypothesis for specific aim #2, only the elevation in glycated hemoglobin was definitively seen.

Along with difficulty in assessing the glycated ocular protein values, there were differences with respect to the results for GLUT transporters in the sand rat eye and the literature for other species. Controversy exists over the location of each type of GLUT transporter in the eye and the primary location for glucose uptake in the lens (Kern and Ho 1973), (Goodenough et al. 1980), (Mantych et al. 1993), (Kumagai et al. 1994), (Merriman-Smith et al. 1999). The presence of GLUT-1, GLUT-3 and GLUT-4 transcript in anterior epithelial cells but lack of GLUT-1 and GLUT-3 transcripts in lens fiber cells is not definitive for the presence or absence of the GLUT transporter protein. The method used can indicate whether the message for translation into the protein is present in the anterior epithelial cells and only GLUT-4 message is present in the lens fiber cells. It is easy to hypothesize from these results that GLUT-1, GLUT-3 and GLUT-4 transport proteins would be found in anterior epithelial cells since the transcript is present. Western blot techniques could be used to test this hypothesis if antibodies to the specific glucose transporters were available and there was confidence that the antibodies would crossreact to the sand rat. It is much more difficult to extrapolate the presence of GLUT-1 and GLUT-3 transporters in lens fiber cells of sand rats unless consideration is given to the fact that the anterior epithelial cells are the stem cells for the lens fiber cells. Additional GLUT transporter research, probing for the localization of GLUT protein within specific cell types in

the lens and within designated regions of the lens, needs to be performed. This could be accomplished by in-situ fluorescent antibody testing but again only if antibodies to the glucose transporters were available and the antibodies would crossreact with the corresponding sand rat proteins. Cellular and regional localization of glucose transporters would assist in determining glucose uptake patterns in the lens and correlation to cataract formation. In conclusion, only the location of the GLUT-1 and GLUT-4 transporter transcripts was determined for specific aim #3. Since the sand rat is such an excellent diabetic cataracts model, GLUT transporters research of the lens should continue. This information is crucial for targeting GLUT transporters as a site for medical intervention in the prevention of diabetic cataracts.

Although the location of the glucose transporters could not be defined, the elevated ocular glucose levels found in the diabetic sand rats contribute to the formation of clinical diabetic cataracts. Lenticular changes that could be identified based on age and diabetic condition were determined using chromatography, gel electrophoresis, Western blotting and mass spectrometry. It was first necessary to characterize the normal lens crystallins of the fat sand rat before comparing the controls to the diabetics. Chromatography curves revealed differences in controls and diabetics and differences in animals with increasing age. As explained previously (Chapters 4 and 5), the amplitude of the first two chromatography peaks, which contained predominately alpha crystallins, shifted in the diabetic and aged animals. A trend of increased amplitude, a larger peak,

of the highest molecular weight proteins when compared to the second chromatography peak was seen. A larger peak of higher molecular weight indicates there is more aggregation of the native proteins. This shift seen in diabetic and aged sand rats may be related to alpha crystallin aggregation. This aggregation is possibly due to a post-translational modification like glycation. The literature links post-translational modifications like glycation of alpha crystallins to cataract formation in aging and diabetes (van Boekel and Hoenders 1992), (van Boekel et al. 1996), (Crabbe 1998). Chromatography also yielded biological information supporting the sand rat as a better model for human lens research than the nocturnal rat. Based on a preliminary chromatography curve from a control rat (data not shown) and the sand rat curves, a lower concentration of gamma crystallins was seen in sand rats. This preliminary data correlates to the diurnal sand rats softer lens required for accommodation. Additional chromatography studies of the lenses using larger sample volumes for diabetic lenses would help to elucidate other more subtle differences from the controls. Normalization of the chromatography curves would yield quantitative information on the major crystallin for comparison within and between rodent species.

The whole lens extracts and lens fraction samples separated by chromatography were run on SDS-PAGE. Differences were identified between diabetic and control sand rats along with three unusual high molecular weight bands seen in all sand rats. The diabetic sand rats all had a banding shift in molecular weight from 22,500 to 23,500 Daltons on Tris-Glycine gels. Some diabetics also had

additional bands whose molecular weight ranged from 35,000 to 42,000 Daltons. All sand rats tested had high molecular weight bands at 42,000, 47,000 and 51,000 Daltons. Using the Western blotting technique, the band that shifts from 22,500 to 23,500 Daltons was identified as beta crystallins. The 35,000 to 42,000 Dalton bands were identified as alpha crystallins. The high molecular weight bands seen in all sand rats were not identified as being from any of the major crystallin classes. Western blots also identified the alpha insert crystallin commonly seen in some rodents. Mass spectrometry verified the Western blot results and identified all major classes of the sand rat lens. The diabetic change to the beta crystallins is a beta B1/beta B3 shift. Beta crystallins are believed to play a role in maintaining lens transparency by regulating repulsive charges between beta complexes and preventing aggregation (Werten et al. 1999b). Changes to the N-terminal or C-terminal regions of beta A3/beta B2 (Werten et al. 1999a) and beta A3/beta A1 (Srivastava et al. 1999) from bovine lenses are seen in aging. The Philly Mouse, a Swiss-Webster strain with hereditary cataracts, has an abnormal beta B2 crystallin with a more acidic isoelectric point due to changes at the N-terminus (Russell and Chambers 1990). This alteration of the beta B2 crystallin, by itself, is believed to be responsible for the cataract in this mouse model. Post-translational changes to the N-terminal or C-terminal regions of the beta crystallins may be occurring in the sand rat with aging and diabetes, and may be related to the cataracts seen in this species.

The high molecular weight alpha crystallin bands seen in some of the diabetics are aggregates of alpha A crystallins. Since alpha crystallins have an increased association to the lens fiber cell membranes with age (Takemoto and Boyle 1998) and alpha A crystallins subunits are present in high molecular weight aggregates of senile human and bovine lenses (Takemoto et al. 1988), (Takemoto 1999), it stands to reason that in the diabetic sand rats, after continued alpha crystallin aggregation, the proteins are becoming insoluble and segregating off with the pelleted fraction. This presumably explains why extensive alpha A crystallin dimerization was not seen in diabetic sand rats of greater than 6 months of duration.

In addition, the MALDI technique identified the high molecular weight bands of the sand rat lens, 42,000 – 51,000 Daltons, as glycolytic enzymes and aldehyde dehydrogenase. These enzymes may play a role in ultraviolet light absorption and lens accommodation in this diurnal desert species. The gel electrophoresis, Western blot and mass spectrometry data support the literature on cataract formation by crystallin aggregation in diabetes and aging. Additionally, the data adds to the growing volume of information and interest in the area of taxon-specific crystallins and their function in the lens of the eye. In conclusion, the research data generally supports the specific hypotheses for specific aims # 4 and # 5, by showing that the normal sand rat does in deed have a general crystallin pattern similar to another of the gerbil species (*Meriones*) with minor

unique variations and the sand rat with diabetic cataracts does have an altered crystallin pattern.

The work presented here constitutes an initial characterization of the normal sand rat lens and paves the way for additional work on the crystallin changes seen in diabetes. Additional research on early detection of cataract formation in diabetic sand rats would prove to be interesting. This early crystallin evaluation should focus on which crystallin classes are affected first and the type of biochemical modifications occurring. It is important to determine if the beta crystallin ratio shift, which is seen in all diabetics, is the first change or if the alpha crystallin aggregation, which is seen in some diabetic animals is the primary change that results in water-soluble crystallins becoming insoluble. Perhaps the study of lens changes early in the diabetics will elucidate a mechanism for the crystallin changes seen in cataract formation. Additional evaluation by SDS-PAGE, western blot technique and mass spectrometry of lens pellets, once the pellets are made soluble, would help to identify if crystallins are lost to the pellets and if any, additional protein modifications are occurring in both the diabetic and aged animals. In conclusion, the fat sand rat provides an excellent opportunity to study the formation of cataracts in a diurnal animal that is a spontaneous model for this devastating disease.

## REFERENCES

- ADA. 1999a. Position Statement Screening for Type 2 Diabetes. *Diabetes Care* 22: S20 - S26.
- ADA. 1999b. Position Statement Tests of Glycemia in Diabetes. *Diabetes Care* 22: S70 - S73.
- Adler, J. H., R. Kalman, G. Lazarovich, H. Bar-on, and E. Ziv. 1990. Achieving Predictable Model of Type 2 Diabetes in Sand Rats. Pages 212 - 214 in E. Shafrir, ed. *Frontiers in Diabetes Research. Lessons from Animal Diabetes III*. Smith-Gordon.
- Albert, D. M., and F. A. Jacobiec. 1994. *Principles and Practice of Ophthalmology*. W.B. Saunders.
- Alberts, B., D. Bray, J. Lewis, M. Raff, K. Roberts, and J. D. Watson. 1994. *Molecular Biology of the Cell*. Garland Publishing Company.
- Andley, U. P., Z. Song, E. F. Wawrousek, and S. Bassnett. 1998. The Molecular Chaperone AlphaA-crystallin Enhances Lens Epithelial Cell Growth and resistance to UVA Stress. *Journal of Biological Chemistry* 273: 31252 - 31261.
- Araki, N., N. Ueno, B. Chakrabarti, Y. Morino, and S. Horiuchi. 1992. Immunochemical Evidence for the Presence of Advanced Glycation End products in Human Lens Proteins and Its Positive Correlation with Aging. *The Journal of Biological Chemistry* 267: 10211 - 10214.

- Baier, L. J., J. C. Sacchettini, W. C. Knowler, J. Eads, G. Paolisso, P. A. Tataranni, H. Mochizuki, P. H. Bennett, C. Bogardus, and M. Prochazka. 1995. An Amino Acid Substitution in the Human Intestinal Fatty Acid Binding Protein is Associated with Increased Fatty Acid Binding, Increased Fat Oxidation and Insulin Resistance. *Journal of Clinical Investigation* 95: 1281 - 1287.
- Barbosa, P., G. Wistow, M. Cialkowski, J. Piatigorsky, and W. E. O'Brien. 1991. Expression of Duck Lens d-Crystallin cDNAs in Yeast and Bacterial Hosts. *The Journal of Biological Chemistry* 266: 22319 - 22322.
- Bassnett, S. 1992. Mitochondrial Dynamics in Differentiating Fiber Cells of the Mammalian Lens. *Current Eye Research* 11: 1227 - 1232.
- Belpoliti, M., and G. Maraini. 1993. Sugar Alcohols in the Lens Epithelium of Age-related Cataract. *Experimental Eye Research* 56: 3-6.
- Bloemendal, H., I. Hendriks, and P. Body. 1990.  $\beta$ H - and  $\beta$ L - Crystallins are Populations of Aggregates. *Experimental Eye Research* 50: 711 - 713.
- Borras, T., H. Jornvall, A. Rodokanaki, P. Gonzalez, I. Rodriguez, and C. Hernandez-Calzadilla. 1990. The Transcripts of Zeta-Crystallin, A Lens Protein Related to the Alcohol Dehydrogenase Family, Are Altered in a Guinea-pig Hereditary Cataract. *Experimental Eye Research* 50: 729 - 735.
- Borst, D. E., and D. S. McDevitt. 1987. Eye Lens Regeneration and the Crystallins in the Adult Newt, *Notophthalmus viridescens*. *Experimental Eye Research* 45: 419 - 441.

- Bradford, M. M. 1976. A rapid and sensitive method for the quantification of microgram quantities of protein utilizing the principle of protein-dye binding. *Anal Biochem* 72: 248-54.
- Brewton, R. G., and R. Mayne. 1992. Mammalian Vitreous Humor Contains Networks of Hyaluronan Molecules: Electron Microscopic Analysis Using the Hyaluronan-binding Region (G1) of Aggrecan and Link Protein. *Experimental Cell Research* 198: 237 - 249.
- Cammarata, P. R., C. Zhou, G. Chen, I. Singh, R. E. Reeves, J. R. Kuszak, and M. L. Robinson. 1999. A Transgenic Animal Model of Osmotic Cataract. Part 1: Overexpression of Bovine Na<sup>+</sup>/Myoinositol Cotransporter in Lens Fibers. *Investigative Ophthalmology and Visual Science* 40: 1727 - 1737.
- Carroll, J. J., N. Smith, and A. L. Babson. 1970. A colorimetric serum glucose determination using hexokinase and glucose-6-phosphate dehydrogenase. *Biochem Med* 4: 171.
- Cefalau, W. T. 1988. Understanding Protein Glucosylation. *Practica Diabetologica* 7: 17 - 19.
- Charron, M. J., F. C. Brosius, S. L. Alper, and H. F. Lodish. 1989. A glucose transport protein expressed predominately in insulin-responsive tissues. *Proceedings of the National Academy of Science of the United States of America* 86: 2535-9.
- Chellan, P., and R. H. Nagaraj. 1999. Protein Crosslinking by the Maillard Reaction: Dicarbonyl-Derived Imidazolium Crosslinks in Aging and Diabetes. *Archives of Biochemistry and Biophysics* 368: 98 - 104.

- Chenault, V. M., M. N. Ediger, J. F. King, and R. R. Ansari. 1999. Dynamic Light Scattering From Space to Earth: Looking at Diabetes through the Eye. *24th Annual Technology Transfer Society Meeting*.
- Cohen, L. H., L. W. Westerhuis, W. W. De Jong, and H. Bloemendal. 1978. Rat  $\alpha$ -Crystallin A Chain with an Insertion of 22 Residues. *European Journal of Biochemistry* 89: 259-266.
- Cohen-Melamed, E., A. Nyska, A. Pollack, and Z. Madar. 1995. Aldose Reductase (EC1.1.1.21) Activity and Reduced-Glutathione Content in Lenses of Diabetic Sand Rats (*Psammomys obesus*) fed with Acarbose. *British Journal of Nutrition* 74: 607 - 615.
- Colvis, C. M., Y. Douglas-Taber, K. B. Werth, N. E. Vieira, J. A. Kowalak, A. Janjani, A. L. Yergey, and D. L. Garland. 2000. Tracking pathology with proteomics: identification of in vivo degradation products of alphaB-crystallin. *Electrophoresis* 21: 2219 - 27.
- Cooper, D. L., N. R. Isola, K. Stevenson, and E. W. Baptist. 1993. Members of the ALDH Gene Family are Lens and Corneal Crystallins. *Advances in Experimental Medicine and Biology* 328: 169 - 179.
- Cotran, R. A., V. Kumar, and T. Collins. 1999. *Robbins Pathologic Basis of Disease*. W.B. Saunders Company, Philadelphia.
- Coulter, J. B. r., J. A. Engelke, and D. K. Eaton. 1983. Insulin concentration in aqueous humor of rabbits: effects of alloxan-diabetes and insulin treatment. *Exp Eye Res* 37: 153 - 7.

- Crabbe, M. J. 1998. Cataract as a conformational disease – the Maillard reaction, alpha-crystallin and chemotherapy. *Cellular and Molecular Biology (Noisey-le-Grand)* 44: 1047-50.
- Cvekl, A., C. M. Sax, X. Li, J. B. McDermott, and J. Piatigorsky. 1995. Pax-6 and Lens-specific Transcription of the Chicken Delta 1-crystallin Gene. *Proceedings of the National Academy of Science of the United States of America* 92: 4681 - 4685.
- Daae, L. N., B. Teige, and H. Svaar. 1978. Determination of Glucose in Human Vitreous Humor. Various Analytical Methods Give Different Results. *Zeitschrift fur Rechtsmed* 80: 287 - 291.
- Das, B. K., T. X. Sun, N. J. Akhtar, L. T. Chylack, and J. Liang. 1998. Fluorescence and Immunochemical Studies of Advanced Glycation-Related Lens Pigments. *Investigative Ophthalmology and Visual Science* 39: 2058 - 2066.
- De Jong, W. W., L. H. Cohen, J. Leunissen, and A. Zweers. 1980. Internally Elongated Rodent  $\alpha$ -Crystallin A Chain: Resulting From Incomplete RNA Splicing? *Biochemical Biophysical Research Communications* 96: 648-655.
- Degenhardt, T. P., M. X. Fu, E. Voss, K. Reiff, R. Neidlein, K. Strein, S. R. Thorpe, J. W. Baynes, and R. Reiter. 1999. Aminoguanidine Inhibits Albuminuria, but not the Formation of Advanced Glycation End-products in Skin Collagen of Diabetic Rats. *Diabetes Research and Clinical Practice* 43: 81 - 89.

- Delcourt, C., B. Villatte-Cathelineau, F. Vauzelle-Kervroedan, G. Cathelineau, and L. Papoz. 1995. Visual Impairment in Type 2 Diabetic Patients. A Multicentre Study in France. CODIAB-INSERM-ZENECA Pharma Study Group. *Acta Ophthalmologica Scandinavica* 73: 293 - 298.
- Di Mattio, J., N. Altszuler, S. Ellis, and J. A. Zadunaisky. 1981. Glucose Transport Across Ocular Barriers of the Streptozotocin-diabetic Rat. *Diabetes Care* 30: 903 - 906.
- Di Mattio, J., J. A. Zadunaisky, and N. Altszuler. 1984. Onset of Changes in Glucose Transport Across Ocular Barriers in Streptozotocin-induced Diabetes. *Investigative Ophthalmology and Visual Science* 25: 820 - 826.
- DiCarlo, C. D., V. M. Chenault, and D. E. Borst. 2001. Ocular changes in a spontaneously diabetic animal model, the fat sand rat (*Psammomys obesus*). *Manuscript in preparation*.
- DiCarlo, C. D., W. P. Roach, D. A. Gagliano, S. A. Boppart, D. X. Hammer, A. B. Cox, and J. G. Fujimoto. 1999. Comparison of optical coherence tomography imaging of cataracts with histopathology. *Journal of Biomedical Optics* 4: 450 - 8.
- Duhaiman, A. S. 1995. Glycation of Human Lens proteins From Diabetic and (Nondiabetic) Senile Cataract Patients. *Glycoconjugate Journal* 12: 618 - 621.
- Farr, A. K., R. D. Braun, W. T. Cefalu, A. D. Bell-Farrow, Z. Q. Wang, and D. L. Hatchell. 1999. Increased Nonenzymatically Glycosylated Proteins in the

- Vitreous Humor of Diabetic Animals. *Laboratory Animal Science* 49: 58 - 61.
- Flegal, K. M., T. M. Ezzati, M. I. Harris, S. G. Haynes, R. Z. Juarez, W. C. Knowler, E. J. Perez-Stable, and M. P. Stern. 1991. Prevalence of diabetes in Mexican Americans, Cubans, and Puerto Ricans from the Hispanic Health Examination Survey, 1982 - 1984. *Diabetes Care* 14: 628 - 38.
- Frenkel, G., Y. Shaham, and P. F. Kraiger. 1972. Establishment of Conditions for Colony-Breeding of the Sand-Rat *Psammomys obesus*. *Laboratory Animal Science* 22: 40 - 47.
- Friedman, E. A. 1999. Advanced Glycosylated End Products and Hyperglycemia in the Pathogenesis of Diabetic Complications. *Diabetes Care* 22: B65 - 71.
- Ganea, E., and J. J. Harding. 1996. Lens proteins changes induced by sugars and pyridoxal phosphate. *Ophthalmic Research* 28: 65-8.
- Ganea, E., K. C. Rixon, and J. J. Harding. 1994. Binding of glucose, galactose and pyridoxal phosphate to lens crystallins. *Biochimica et Biophysica Acta (BBA) - Protein Structure and Molecular Enzymology* 1226: 286-90.
- Gonzalez, P., C. Hernandez-Calzadilla, P. V. Rao, I. R. Rodriguez, J. S. Zigler, and T. Borrás. 1994a. Comparative Analysis of the Zeta-crystallin/Quinone Reductase Gene in the Guinea Pig and Mouse. *Molecular Biology and Evolution* 11: 305 - 315.

- Gonzalez, P., P. V. Rao, S. B. Nunez, and J. S. Zigler, Jr. 1995. Evidence for Independent recruitment of Zeta-crystallin/Quinone Reductase (CRYZ) as a Crystallin in Camelids and Hystrichomorph Rodents. *Molecular Biology and Evolution* 12: 773 - 781.
- Gonzalez, P., P. V. Rao, and J. S. Zigler. 1994b. Organization of the Human Zeta-crystallin/quinone Reductase Gene (CRYZ). *Genomics* 21: 317 - 324.
- Goodenough, D. A., J. S. Dick, and J. E. Lyons. 1980. Lens Metabolic Cooperation: A Study of Mouse Lens Transport and Permeability Visualized with Freeze-substitution Autoradiography and Electron Microscopy. *Journal of Cellular Biology* 86: 576 - 589.
- Goodwin, S. D. 1997. The Hamster: Biology, Care, Diseases and Models. Laboratory Animal Medicine Seminar Series at USUHS, Bethesda.
- Gutman, A., A. Andreus, and J. H. Adler. 1975. Hyperinsulinemia, Insulin Resistance and Cataract Formation in Sand Rats. *Israel Journal of Medical Sciences* July 11: 714 - 722.
- Gutman, A., A. Andreus. 1976. Hyperinsulinemia, Insulin Resistance and Cataract Formation in Sand Rats. *Contemporary Topics in the Study of Diabetes and Metabolic Endocrinology*: 188 - 196.
- Hackel, D., K. Schmidt-Nielsen, H. Haines, and E. Mikat. 1965. Diabetes Mellitus in the Sand Rat (*Psammomys obesus*), Pathologic Studies. *Laboratory Investigation* 14: 200 - 207.

- Hapnes, R., and H. Bergrem. 1996. Diabetic Eye Complications in a Medium Sized Municipality in Southwest Norway. *Acta Ophthalmologica Scandinavica* 74: 497 - 500.
- Harkness, J. E., and J. E. Wagner. 1995. *The Biology and Medicine of Rabbits and Rodents*. Williams and Wilkins.
- Harris, M. I., K. M. Flegal, and C. C. Cowie. 1998. Prevalence of Diabetes, Impaired Fasting Glucose, and Impaired Glucose Tolerance in U.S. Adults: The Third National Health and Nutrition Examination Survey, 1988 - 94. *Diabetes Care* 21: 518 - 24.
- Hayman, S., M. F. Lou, L. O. Merola, and J. H. Kinoshita. 1966. Aldose Reductase Activity in the Lens and Other Tissues. *Biochimica et Biophysica Acta (BBA) - Protein Structure and Molecular Enzymology* 128: 474 - 482.
- Hendricks, W., J. Leunissen, E. Nevo, H. Bloemendal, and W. W. deJong. 1987. The Lens Protein Alpha A-crystallin of the Blind Mole Rat, *Spalax ehrenbergi*: Evolutionary Change and Functional Constraints. *Proceedings of the National Academy of Science of the United States of America* 84: 5320 - 5324.
- Hook, D. W., and J. J. Harding. 1996. Alpha-crystallin Acting as a Molecular Chaperone Protects Catalase Against Steroid-induced Inactivation. *Federation of European Biochemical Societies Letters* 382: 261-284.
- Huang, Q. L., P. Russell, S. Stone, and J. S. Zigler. 1987. Zeta crystallin, a novel lens protein from the guinea pig. *Curr Eye Res* 6: 725 - 32.

- Iida, H., and I. Yahara. 1984. A heat shock-resistant mutant of *Saccharomyces cerevisiae* shows constitutive synthesis of two heat shock proteins and altered growth. *Journal of Cell Biology* 4: 1441-50.
- Jacob, T. J. 1999. The Relationship Between Cataract, Cell Swelling and Volume Regulation. *Progress in Retinal and Eye Research* 18: 223 - 233.
- Jacot, J. L., H. Hosotani, J. P. Glover, N. Lois, and J. Robison, W. G. 1997. Diabetic-like Corneal Sensitivity Loss in Galactose-Fed Rats Ameliorated with Aldose Reductase Inhibitors. *Journal of Ocular Pharmacology and Therapeutics* 14: 169 - 180.
- Johnson, R. N., P. A. Metcalf, and J. R. Baker. 1982. Fructosamine: A new approach to the estimation of serum glycosylprotein. A index of diabetic control. *Clin Chim Acta* 127: 87.
- Johnstone, R. A. W., and M. E. Rose. 1996. *Mass Spectrometry for Chemists and Biochemists*. Cambridge University Press, Cambridge.
- Kaimbo, D. K., B. K. Kabongo, and L. Missotten. 1995. Ocular Complications in Diabetes in Zaire. *Bulletin de la Societe Belge Ophthalmol* 255: 107 - 113.
- Kaiser, N., E. M. Baillyes, B. S. Schneider, E. Cerasi, D. F. Steiner, J. C. Hutton, and D. J. Gross. 1997. Characterization of the Unusual Insulin of *Psammomys obesus*, a Rodent with Nutrition-Induced NIDDM-Like Syndrome. *Diabetes* 46: 953 - 957.
- Kalderon, B., A. Gutman, E. Shafrir, and J. Adler. 1986. Characterization of Stages in Development of Obesity-Diabetes Syndrome in Sand Rat (*Psammomys obesus*). *Diabetes Care* 35: 717 - 724.

- Kalman, R., G. Lazarovich, H. Bar-on, and E. Ziv. 1996. The Sand Rat (*Psammomys obesus*): Morphologic, Physiologic, and Biochemical Characteristics of a Model for Type II Diabetes Mellitus. *Contemporary Topics in Laboratory Animal Science* September 34: 67 - 70.
- Kern, H. L., and C. K. Ho. 1973. Localization and specificity of the transport system for sugars in the calf lens. *Exp Eye Res* 15: 751 - 65.
- Kim, R. Y., R. Glasser, and G. J. Wistow. 1992. Mu-crystallin is a Mammalian Homologue of *Agrobacterium* Ornithine Cyclodeaminase and is Expressed in Human Retina. *Proceedings of the National Academy of Science of the United States of America* 89: 9292 - 9296.
- Kim, R. Y., T. Lietman, J. Piatigorsky, and G. J. Wistow. 1991. Structure and Expression of the Duck  $\alpha$ -Enolase/t-Crystallin-encoding Gene. *Gene*. 103: 193 - 200.
- Kim, R. Y., and G. J. Wistow. 1993. Expression of the Duck  $\alpha$ -Enolase/t-Crystallin Gene in Transgenic Mice. *Federation of American Societies for Experimental Biology Journal* 7: 464 - 469.
- King, C. R., and J. Piatigorsky. 1983. Alternative RNA Splicing of the Murine A-crystallin Gene: Protein-Coding Information within an Intron. *Cell* 32: 707-712.
- Klein, B. E., R. Klein, and S. E. Moss. 1985. Prevalence of Cataracts in a Population-based Study of persons with Diabetes Mellitus. *Ophthalmology* 92: 1191 - 1196.

- Klein, B.E., R. Klein, and S.E. Moss. 1995. Incidence of Cataract Surgery in the Wisconsin Epidemiologic Study of Diabetic Retinopathy. *American Journal of Ophthalmology* 119: 295 - 300.
- Knowler, W. C., D. J. Pettitt, S. F. Mohammed, and P. H. Bennett. 1990. Diabetes Mellitus in the Pima Indians: Incidence, Risk Factors and Pathogenesis. *Diabetes/Metabolism Reviews* 6: 1 - 27.
- Krishnan, S. N., and G. G. Haddad. 1995. Cloning of glucose transporter-3 (GLUT3) cDNA from rat brain. *Life Sci* 56: 1193-9.
- Kumagai, A. K., B. J. Glasgow, and W. M. Pardridge. 1994. GLUT-1 glucose transporter expression in the diabetic and nondiabetic human eye. *Invest Ophthalmol Vis Sci* 35: 2887 - 94.
- Labrecque, J., F. Dumas, A. Lacroix, and P. V. Bhat. 1995. A novel isoenzyme of aldehyde dehydrogenase specifically involved in the biosynthesis of 9-cis and all-trans retinoic acid. *Biochem J* 305: 681-4.
- Lackner, P. A., L. Rodriguez, S. Sato, M. J. Lizak, M. Wyman, and P. F. Kador. 1997. Age-dependent Lens Changes in Galactose-Fed Dogs. *Experimental Eye Research* 64: 431-6.
- Larsen, W. J. 1997. *Human Embryology*,. Churchill Livingstone Publishers.
- Lee, A. Y., S. K. Chung, and S. S. Chung. 1995. Demonstration that Polyol Accumulation is Responsible for Diabetic Cataract by the Use of Transgenic Mice Expressing the Aldose Reductase Gene in the Lens. *Proceedings of the National Academy of Science of the United States of America* 92: 2780 - 2784.

- Lee, D. C., P. Gonzalez, P. V. Rao, J. S. Zigler, Jr., and G. J. Wistow. 1993. Carbonyl-metabolizing Enzymes and Their Relatives Recruited as Structural Proteins in the Eye Lens. *Advances in Experimental Medicine and Biology* 328: 159 - 168.
- Leske, M. C., S. Y. Wu, A. Hennis, A. M. S. Connell, L. Hyman, and A. Schachat. 1999. Diabetes, hypertension, and central obesity as cataract risk factors in a black population - The Barbados Eye Study. *Ophthalmology* 106: 35 - 41.
- Li, X., A. Cvekl, S. Bassnett, and J. Piatigorsky. 1997. Lens-preffered Activity of Chicken Delta 1- and Delta 2-crystallin Enhancers in Transgenic Mice and Evidence for Retinoic Acid-responsive Regulation of the Delta 1-crystallin Gene. *Developmental Genetics* 20: 258 - 266.
- Li, X., G. Wistow, and J. Piatigorsky. 1995. Linkage and Expression of the Argininosuccinate Lyase/Delta-crystallin Genes of the Duck: Insertion of a CR1 element in the Intergenic Spacer. *Biochimica et Biophysica Acta (BBA) - Protein Structure and Molecular Enzymology* 1261: 25 - 34.
- Lundquist, O., and S. Osterlin. 1994. Glucose Concentration in the Vitreous of Nondiabetic and Diabetic Human Eyes. *Graefes Archive for Clinical and Experimental Ophthalmology* 232: 71 - 74.
- Lyons, T. J., G. Silvestri, J. A. Dunn, D. G. Dyer, and J. W. Baynes. 1991. Role of Glycation in Modification of Lens Crystallins in Diabetic and Nondiabetic Senile Cataracts. *Diabetes* 40: 1010 - 1015.

- Ma, Z., S. R. Hanson, K. J. Lampi, L. L. David, D. L. Smith, and J. B. Smith. 1998. Age-related changes in human lens crystallins identified by HPLC and mass spectrometry. *Experimental Eye Research* 67: 21-30.
- Mantych, G. J., G. S. Hageman, and S. U. Devaskar. 1993. Characterization of glucose transporter isoforms in the adult and developing human eye. *Endocrinology* 133: 600 - 7.
- Marquie, G., J. Duhault, P. Hadjiisky, P. Petkov, and H. Bouissou. 1991. Diabetes mellitus in sand rats (*Psammomys obesus*): microangiopathy during development of the diabetic syndrome. *Cellular and Molecular Biology* 37: 651-67.
- Mathias, R. T., J. L. Rae, and G. L. Baldo. 1997. Physiological Properties of the Normal Lens. *Physiology Review* 77: 21 - 50.
- Merriman-Smith, R., P. Donaldson, and J. Kistler. 1999. Differential Expression of Facilitative Glucose Transporters GLUT1 and GLUT3 in the Lens. *Investigative Ophthalmology and Visual Science* 40: 3224 - 3230.
- Miksik, I., and Z. Deyl. 1997. Post-translational Non-enzymatic Modification of Proteins. II. Separation of Selected Protein Species After Glycation and Other Carbonyl-mediated Modifications. *J Chromatogr B Biomed Sci Appl* 699: 311 - 345.
- Miyamoto, K., Y. Ogura, H. Nishiwaki, N. Matsuda, Y. Honda, S. Kato, H. Ishida, and Y. Seino. 1996. Evaluation of Retinal Microcirculatory Alterations in the Goto-Kakizaki Rat. A Spontaneous Model of Non-Insulin-Dependent Diabetes. *Investigative Ophthalmology and Visual Science* 37: 898 - 905.

Monnier, V. M., O. Bautista, D. Kenny, D. R. Sell, J. Fogarty, W. Dahms, P. A.

Cleary, J. Lachin, and S. Genuth. 1999. Skin Collagen Glycation, Glycooxidation, and Cross-linking are Lower in Subjects with Long-Term Intensive Versus Conventional Therapy of Type 1 Diabetes: Relevance of Glycated Collagen Products versus HbA1c as Markers of Diabetic Complications. DCCT Skin Collagen Ancillary Study Group. *Diabetes Control and Complications Trial. Diabetes* 48: 870 - 880.

Monnier, V. M., and A. Cerami. 1981. Non Enzymatic Browning In Vivo: Possible Process for Aging of Long-lived Proteins. *Science* 211: 491 - 494.

Mulders, J. W., W. Hendricks, W. M. Blankesteyn, H. Bloemendal, and W. W. De Jong. 1988. Lambda crystallin, a major rabbit lens protein, is related to hydroxyacyl-coenzyme A dehydrogenases. *J Biol Chem* 263: 15462-6.

Nagaraj, R. H., and C. Sady. 1996. The Presence of a Glucose-Derived Maillard Reaction Product in the Human Lens. *Federation of European Biochemical Societies Letters* 382: 234 - 238.

Nagaraj, R. H., D. Sell, M. Prabhakaram, B. J. Ortwerth, and V. M. Monnier. 1991. High Correlation Between Pentosidine Protein Crosslinks and Pigmentation Implicates Ascorbate Oxidation in Human Lens Senescence and Cataractogenesis. *Proceedings of the National Academy of Science of the United States of America* 88: 10257 - 10261.

Nakayama, H., T. Mitshuhashi., S. Kuwajima, S. Aoki, Y. Kuroda, T. Itoh, and S. Nakagawa. 1993. Immunochemical Detection of Advanced Glycation End

- Products in Lens Crystallins From Streptozocin-Induced Diabetic Rat.  
*Diabetes* 42: 345 - 350.
- Neel, J. V. 1962. Diabetes mellitus: a "thrifty" genotype rendered detrimental by "progress?" *Am J Hum Genet* 14: 353 - 62.
- Nesher, R., D. J. Gross, M. Y. Donath, E. Cerasi, and N. Kaiser. 1999.  
Interaction Between Genetic and Dietary Factors Determines Beta-Cell  
Function in *Psammomys obesus*, An Animal Model of Type 2 Diabetes.  
*Diabetes* 48: 731 - 737.
- Nickerson, J. M., E. F. Wawrousek, J. W. Hawkins, A. S. Wakil, G. J. Wistow, G.  
Thomas, B. L. Norman, and J. Piatigorsky. 1985. The Complete Sequence  
of the Chicken Delta 1 Crystallin Gene and its 5' Flanking Region. *The  
Journal of Biological Chemistry* 260: 9100 - 9105.
- Osuna, E., A. Garcia-Villora, M. D. Perez-Carceles, J. Conejero, J. M. Abenza, P.  
Martinez, and A. Luna. 1999. Vitreous Humor Fructosamine  
Concentrations in the Autopsy Diagnosis of Diabetes Mellitus.  
*International Journal of Legal Medicine* 112: 275 - 279.
- Peclet, C., P. Picotte, and F. Jobin. 1994. The Use of Vitreous Humor Levels of  
Glucose, Lactic Acid and Blood Levels of Acetone to Establish  
Antemortem Hyperglycemia in Diabetes. *Forensic Science International*  
65: 1 - 6.
- Perry, R. E., M. S. Swamy, and E. C. Abraham. 1987. Progressive changes in  
lens crystallin glycation and high-molecular-weight aggregate formation

leading to cataract development in streptozotocin-diabetic rats.

*Experimental Eye Research* 44: 269-82.

Piatigorsky, J. 1981. Lens Differentiation in Vertebrates. A Review of Cellular and Molecular Features. *Differentiation* 19: 134 - 153.

Piatigorsky, J. 1990. Molecular Biology: Recent Studies on Enzyme/Crystallins and Alpha-crystallin Gene Expression. *Experimental Eye Research* 50: 725 - 728.

Piatigorsky, J. 1998. Gene Sharing in Lens and Cornea: Facts and Implications. *Progress in Retinal and Eye Research* 17: 145 - 174.

Piatigorsky, J., W. E. O'Brien, B. L. Norman, K. Kalumuck, G. J. Wistow, T. Borras, J. M. Nickerson, and E. F. Wawrousek. 1988. Gene Sharing by Delta-crystallin and Argininosuccinate Lyase. *Proceedings of the National Academy of Science of the United States of America* 85: 3479 - 3483.

Raman, B., T. Ramakrishna, and C. M. Rao. 1995. Temperature Dependent Chaperone-like Activity of Alpha-crystallin. *Federation of European Biochemical Societies Letters* 365: 133 - 136.

Ramanakoppa, H., R. H. Nagaraj, and C. Sady. 1996. The presence of a glucose-derived Maillard reaction product in the human lens. *FEBS Lett* 382: 234 - 8.

Rao, P. V., P. Gonzalez, B. Persson, H. Jornvall, D. Garland, and J. S. Zigler, Jr. 1997. Guinea Pig and Bovine Zeta-crystallins have Distinct Functional Characteristics Highlighting Replacements in Otherwise Similar Structures. *Biochemistry* 36: 5353 - 5362.

- Rao, P. V., J. Horwitz, and J. S. Zigler, Jr. 1994. Chaperone-like Activity of the Alpha-crystallin. The Effect of NADPH on its Interaction with Zeta-crystallin. *Journal of Biological Chemistry* 269: 13266 - 13272.
- Richardson, J., A. Cvekl, and G. Wistow. 1995. Pax-6 is essential for Lens Specific Expression of Zeta-crystallin. *Proceedings of the National Academy of Science of the United States of America* 92: 4676 - 4680.
- Robison, J., W. G. 2001. Galactosemic Animal Models. Pages 273-308 in A. A. F. Sima and E. Shafrir, eds. *Animal Models of Diabetes*. Harwood Academic Publishers, Amsterdam.
- Robison, J., W. G., N. Houlter, and J. H. Kinoshita. 1990. The Role of Lens Epithelium in Sugar Cataracts Formation. *Experimental Eye Research* 50: 641 - 646.
- Robison, J., W. G., J. L. Jacot, J. P. Glover, M. D. Basso, and T. C. Hohman. 1998. Diabetic-like Retinopathy: Early and Late Intervention Therapies in Galactose-Fed Rats. *Investigative Ophthalmology and Visual Science* 39: 1933 - 1941.
- Robison, J., W. G., N. M. Laver, J. L. Jacot, and J. P. Glover. 1995. Sorbinil Prevention of Diabetic-like Retinopathy in the Galactose-Fed Rat Model. *Investigative Ophthalmology and Visual Science* 36: 2368 - 2380.
- Roquomore, E. P., A. Dell, H. R. Morris, M. Panico, A. J. Reason, L. A. Savoy, G. J. Wistow, J. S. Zigler, Jr., B. J. Earles, and G. W. Hart. 1992. Vertebrate lens alpha-crystallins are modified by O-linked N-acetylglucosamine. *Journal of Biological Chemistry* 267: 553 - 563.

- Russell, P., and C. Chambers. 1990. Interaction of An Altered  $\beta$ -Crystallin with Other Proteins in the Philly Mouse Lens. *Experimental Eye Research* 50: 683 - 687.
- Sambrook, J., E. F. Fritsch, and T. Maniatis. 1989. *Molecular Cloning, A Laboratory Manual*. Cold Spring Harbor Laboratory.
- Sato, S., M. Kazuhiko, M. Wyman, and P. F. Kador. 1998. Dose-dependent Prevention of Sugar cataracts in Galactose-fed Dogs by the Aldose Reductase Inhibitor M79175. *Experimental Eye Research* 66: 217-22.
- Saxena, P., A. K. Saxena, X. L. Cui, M. Obrenovich, K. Gudipaty, and V. M. Monnier. 2000. Transition metal-catalyzed oxidation of ascorbate in human cataract extracts: possible role of advanced glycation end products. *Investigative Ophthalmology and Visual Science* 41: 1473-81.
- Schwab, I. R., Dawson, C.R., Hoshiwara, I., Szuter, C.F., Knowler, W.C. 1985. Incidence of Cataract Extraction in Pima Indians. Diabetes as a Risk Factor. *Archives of Ophthalmology* 103: 208 - 212.
- Sebag, J., S. Nie, K. Reiser, M. A. Charles, and N. T. Yu. 1994. Raman Spectroscopy of Human Vitreous in Proliferative Diabetic Retinopathy. *Investigative Ophthalmology and Visual Science* 35: 2976 - 2980.
- Sensi, M., F. Pricci, G. Pugliese, M. G. DeRossi, A. F. Petrucci, A. Cristina, S. Morano, G. Pozzessere, E. Valle, D. Andreani, and U. DiMario. 1995. Role of Advanced Glycation End-Products (AGE) in Late Diabetic Complications. *Diabetes Research and Clinical Practice* 28: 9 - 17.

- Shafir, E. 1996. *Lessons from Animal Diabetes VI, 75th Anniversary of the Insulin Discovery*. Birkhauser.
- Shafir, E., and A. Gutman. 1993. Psammomys obesus of the Jerusalem Colony: A Model for Nutritionally Induced, Non-Insulin-Dependent Diabetes. *Journal of Basic & Clinical Physiology & Pharmacology* 4: 83 - 95.
- Shafir, E., and A. E. Renold. 1984. *Lessons from Animal Diabetes II*. John Libbey, London and Paris.
- Shamsi, F. A., K. Lin, C. Sady, and R. H. Nagaraj. 1998. Methylglyoxal-derived modifications in lens aging and cataract formation. *Investigative Ophthalmology and Visual Science* 39: 2355-64.
- Shamsi, F. A., and R. H. Nagaraj. 1999. Immunochemical detection of the dicarbonyl-derived imidazolium protein crosslinks in human lenses. *Current Eye Research* 19: 276-84.
- Sharon-Friling, R., J. Richardson, S. Sperbeck, D. Lee, M. Rauchman, R. Maas, A. Swaroop, and G. Wistow. 1998. Lens-specific Gene Recruitment of Zeta-crystallin through Pax-6, Nrl-Maf, and Brain Suppressor Sites. *Molecular and Cellular Biology* 18: 2067 - 2076.
- Shepard, P. R., and B. B. Kahn. 1999. Glucose Transporters and Insulin Action, Implications for Insulin Resistance and Diabetes Mellitus. *New England Journal of Medicine* 341: 248 - 257.
- Shires, T. K., J. A. Faeth, and J. S. Pulido. 1990. Nonenzymatic Glycosylation of Vitreous Proteins In-vitro and in the Streptozotocin-treated Diabetic Rat. *Retina* 10: 153 - 158.

- Siuzdak, G. 1996. *Mass Spectrometry for Biotechnology*. Academic Press, San Diego.
- Slingsby, C., and L. R. Miller. 1983. Purification and Crystallization of Mammalian Lens Gamma-crystallins. *Experimental Eye Research* 37: 517 - 530.
- Srivastava, O. P., K. Srivastava, and V. Harrington. 1999. Age-Related Degradation of bA3/A1-crystallin in Human Lenses. *Biochemical and Biophysical Research Communications*. 258.
- Stapel, S. O., and W. W. De Jong. 1983. Lamprey 48-kDa lens protein represents a novel class of crystallins. *Federation of European Biochemical Societies Letters* 162: 302-9.
- Stern, M. P., S. P. Gaskill, H. P. Hazuda, L. I. Gardner, and S. M. Haffner. 1983. Does obesity explain excess prevalence of diabetes among Mexican Americans? Results of the San Antonio Heart Study. *Diabetologia* 24: 272 - 7.
- Stitt, A. W., J. E. Moore, J. A. Sharkey, G. Murphy, D. A. C. Simpson, R. Bucala, H. Vlassara, and D. B. Archer. 1998. Advanced Glycation End Products in Vitreous: Structural and Functional Implications for Diabetic Vitreopathy. *Investigative Ophthalmology and Visual Science* 39: 2517 - 2523.
- Strasser, H. 1968. A Breeding Program for Spontaneously Diabetic Experimental Animals: *Psammomys obesus* (Sand Rat) and *Acomys cahirinus* (Spiny Mouse). *Laboratory Animal Care* 18: 328 - 338.

- Swamy-Mruthinti, S., and A. L. Carter. 1999. Acetyl-L-carnitine decreases glycation of lens proteins: in vitro studies. *Experimental Eye Research* 69: 109-15.
- Takemoto, L. 1999. Increased cleavage of the c-terminal serine from alpha-A crystallin present in the high molecular weight aggregate fraction from human and bovine lenses. *Current Eye Research* 19: 450-5.
- Takemoto, L., and D. Boyle. 1998. The possible role of  $\alpha$ -crystallin in human senile cataractogenesis. *International Journal of Biological Macromolecules* 22: 331-7.
- Takemoto, L., D. Granstrom, M. Kodama, and R. Wong. 1988. Covalent change in alpha crystallin during human senile cataractogenesis. *Biochemical Biophysical Research Communications* 150: 987-95.
- Tarui, S., K. Yamada, and T. Hanafusa. 1987. Animal Models Utilized in the Research of Diabetes Mellitus - With Special Reference to Insulinitis-Associated Diabetes. Progress in Clinical and Biological Research Series. Pages 211 - 223. *Proceedings of the 6th Charles Rivers International Symposium on Laboratory Animals.*, Uyoto, Japan.
- Towbin, H., T. Staehelin, and J. Gordon. 1979. Electrophoretic transfer of proteins from polyacrylamide gels to nitrocellulose sheets: Procedures and some applications. *Proceedings of the National Academy of Science of the United States of America* 76: 4350-4.

- Turk, Z., I. Misur, and N. Turk. 1997. Temporal Association Between Lens Protein Glycation and Cataract Development in Diabetic Rats. *Acta Diabetologica* 34: 49 - 54.
- van Boekel, M. A., and H. J. Hoenders. 1992. Glycation of crystallins in lenses from aging and diabetic individuals. *Federation of European Biochemical Societies Letters* 314: 1-4.
- van Boekel, M. A., S. E. Hoogakker, J. J. Harding, and W. W. deJong. 1996. The influence of some post-translational modifications on the chaperone-like activity of alpha-crystallin. *Ophthalmic Research* 28: 32-8.
- Wadhwani, K. C., R. Fukuyama, T. Giordano, S. I. Rapoport, and K. Chandrasekaran. 1993. Quantitative reverse transcriptase-polymerase chain reaction of glucose transporter 1 mRNA levels in rat brain microvessels. *Anal Biochem* 215: 134-141.
- Waltman, S. R., C. Oestrich, T. Krupin, S. Hanish, S. Ratzan, J. Santiago, and C. Kilo. 1978. Quantitative vitreous fluorophotometry. A sensitive technique for measuring early breakdown of the blood-retinal barrier in young diabetic patients. *Diabetes* 27: 85 - 7.
- Weng, J., Q. Liang, R. R. Mohan, Q. Li, and S. E. Wilson. 1997. Hepatocyte Growth Factor, Keratinocyte Growth Factor, and other Growth Factor-Receptor Systems in the Lens. *Invest Ophthalmol Vis Sci* 38: 1543 - 54.
- Werten, P. J., R. A. Linder, J. A. Carver, and W. W. De Jong. 1999a. Formation of betaA3/betaB2-crystallin mixed complexes: involvement of N- and C-

- terminal extensions. *Biochimica et Biophysica Acta (BBA) - Protein Structure and Molecular Enzymology* 1432: 286-292.
- Werten, P. J., E. Vos, and W. W. De Jong. 1999b. Truncation of betaA3/A1-crystallin during aging of the bovine lens; possible implications for lens optical quality. *Experimental Eye Research* 68: 99-103.
- Williams, L. A., L. L. Ding, J. Horwitz, and J. Piatigorsky. 1985. Tau crystallin from the turtle lens: Purification and partial characterization. *Exp Eye Res* 40: 741 - 9.
- Wistow, G., and H. Kim. 1991. Lens Protein Expression in Mammals: Taxon-specificity and the Recruitment of Crystallins. *Journal of Molecular Evolution* 32: 262 - 269.
- Wistow, G., and J. Piatigorsky. 1987. Recruitment of enzymes as lens structural proteins. *Science* 236: 1554-6.
- Wistow, G. J. 1990. Evolution of a Protein Superfamily: Relationship between lens Crystallins and Microorganism Dormancy Proteins. *Journal of Molecular Evolution* 30: 140.
- Wistow, G. J., 1995. *Molecular Biology Intelligence Unit: Molecular Biology and Evolution of Crystallins: Gene Recruitment and Multifunctional Proteins in the Eye Lens*. R.G. Landes Company.
- Wistow, G. J., T. Lietman, L. A. Williams, S. O. Stapel, W. W. deJong, J. Horwitz, and J. Piatigorsky. 1988a. Tau-crystallin/Alpha-enolase: One Gene Encodes Both an Enzyme and a Lens Structural Protein. *Journal of Cellular Biology* 107: 2729 - 2736.

Wistow, G. J., C. Slingsby, and T. Blundell. 1981. Eye Lens Proteins: The Three Dimensional Structure of b-crystallin Predicted from Monomeric g-crystallin. *Federation of European Biochemical Societies Letters* 133: 9.

Wistow, G. J., L. Summers, and T. Blundell. 1988b. Myxococcus xanthus Spore Coat Protein S may have a Similar Structure to Vertebrate Lens bg-crystallins. *Nature* 315: 771.

Yamagata, K., N. Oda, P. J. Kaisaki, S. Menzel, H. Furuta, M. Vaxillaire, L. Southam, N. J. Cox, Y. Oda, H. Yano, M. M. LeBeau, S. Yamada, H. Nishigori, J. Takeda, S. S. Fajans, A. T. Hattersley, N. Iwasaki, T. Hansen, O. Pedersen, K. S. Polonsky, and G. I. Bell. 1996. Mutations in the Heptocyte Nuclear Factor-1 Alpha Gene in Maturity-Onset Diabetes of the Young. *Nature* 384: 455 - 458.